Arrhythmogenic remodeling of the intercalated disk

Maartje Noorman

Cover: Studio Lakmoes, Arnhem
Printed by: Proefschriftmaken.nl,
Uitgeverij BOXPress
ISBN: 9789088914751

Arrhythmogenic remodeling of the intercalated disk

Aritmogene veranderingen in de intercalairschijf

(met een samenvatting in het Nederlands)

Proefschrift

ter verkrijging van de graad van doctor aan de Universiteit Utrecht op gezag van de rector magnificus, prof.dr. G.J. van der Zwaan, ingevolge het besluit van het college voor promoties in het openbaar te verdedigen op dinsdag 23 oktober 2012 des ochtends te 10.30 uur

door

Maartje Noorman

geboren op 13 december 1983

te Veldhoven

Promotoren:
Prof.dr. R.N.W. Hauer
Prof.dr. H.V.M. van Rijen
Co-promotoren:
Dr. M.A.G. van der Heyden
Dr. A.A.B. van Veen

The research described in this thesis was supported by a grant of the Dutch Heart Foundation (DHF 2007B139) and the Interuniversity Cardiology Institute of The Netherlands (project #06901).
Financial support by the Dutch Heart Foundation and the Heart & Long Foundation Utrecht for the publication of this thesis is gratefully acknowledged.
Financial support by the Jurriaanse Stichting for the publication of this thesis is gratefully acknowledged.

Contents

CHAPTER 1

Preface

Heart failure is characterized by the inability of the heart to maintain sufficient cardiac output to optimally meet the metabolic demands of the body.[1]The progressive worsening of heart function is caused by ventricular and atrial remodeling, induced by e.g. mutations,[2] ischemic, hypertrophic or dilated cardiomyopathy.[1] Three kinds of remodeling take place during the process of heart failure: structural, contractile and electrical remodeling. Structural remodeling leads to a decreased pump function of the heart, contractile remodeling affects the excitation-contraction coupling, whereas electrical remodeling changes the electrical stability of the heart, which may increase the propensity for life-threatening arrhythmias. Stages of heart failure are subdivided into NYHA functional classes, according to severity of the symptoms (Table 1.1). Importantly, in the first two functional classes, in which patients experience only mild symptoms, about 50% of the mortality is due to fatal arrhythmias.[3] So, even in the absence of overt structural problems, electrical remodeling already plays an important role.

Table 1.1 – NYHA functional classes, stages of heart failure

Class	**Symptoms**
Class I (mild)	No limitation of physical activity. Ordinary physical activity does not cause undue fatigue, palpitation, or dyspnea.
Class II (mild)	Slight limitation of physical activity. Comfortable at rest, but ordinary physical activity results in fatigue, palpitation, or dyspnea.
Class III (moderate)	Marked limitation of physical activity. Comfortable at rest, but less than ordinary activity causes fatigue, palpitation, or dyspnea.
Class IV (severe)	Unable to carry out any physical activity without discomfort. Symptoms of cardiac insufficiency at rest. If any physical activity is undertaken, discomfort is increased.

In 1987 Philipe Coumel described three factors that are required to generate and maintain cardiac arrhythmias (Coumel's triangle). Arrhythmogeneity is dependent on: 1) the arrhythmogenic substrate, 2) triggering factors and 3) modulating factors, of which the most common is the autonomic nervous system.[4] In the line of research as de-

scribed in this thesis we have focused on development of the arrhythmogenic substrate, more specifically with regard to slow conduction related reentrant arrhythmias. Impulse propagation in the heart is dependent on three factors: 1) excitability of single myocytes, mainly determined by the cardiac sodium current which is conducted through the cardiac sodium channel $Na_V1.5$, 2) electrical communication between myocytes, determined by gap junctions of which the most important constituent in the ventricles is the protein Connexin43 (Cx43), and 3) tissue architecture; determined by collagen fibers between cardiomyocytes. In patients with heart failure a 50% reduction in $Na_V1.5$ and Cx43 and a 2-6 times increase in fibrosis has been reported.[5, 6] These changes may result in slow conduction and be in part responsible for arrhythmias in heart failure as was shown by previous studies from our lab and others. A 50% reduction in $Na_V1.5$ expression, a 50% reduction in Cx43 expression or a 5 times increase in fibrosis alone did only slightly slow ventricular conduction velocity and did not lead to enhanced arrhythmogeneity.[7, 8] Similarly, a combined reduction in Cx43 *and* $Na_V1.5$ only moderately affected conduction velocity without triggering arrhythmias.[9] When a decrease in $Na_V1.5$ was combined with increased fibrosis however, conduction was severely slowed, albeit without arrhythmias.[7] Interestingly, reduced Cx43 expression with enhanced fibrosis induced moderate, but dispersed conduction slowing which resulted in arrhythmias in about half of the mice.[10] Finally, when all factors were combined in an aged mouse model, a high incidence of arrhythmias was found.[11] These results indicate that conduction slowing and arrhythmias do not occur, at least not in the mouse heart, due to single impairments of Cx43, $Na_V1.5$ or fibrosis, but that combined changes are needed for either conduction slowing and/or arrhythmias.

$Na_V1.5$ and Cx43 are both located in the intercalated disk, a structure that is found at the longitudinal ends of the cardiomyocytes at which neighboring cardiomyocytes are mechanically and electrically connected. Electrical connection in the intercalated disk is facilitated by gap junctions, while mechanical connection is maintained by adherens junctions and desmosomes. The desmosome provides mechanical strength to the cardiomyocytes (described further in **chapter 2**). It has been shown in many studies that mutations in genes encoding for desmosomal proteins lead to loss of function in the intercalated disk: gap widening, disrupted desmosomes, and also changed gap junctional structures have been found on the ultrastructural level.[12] Furthermore, reduced Cx43 levels have been reported in patients with desmosomal mutations.[13] It has been shown, both in animal models

and in human disease, that these changes can lead to serious ventricular arrhythmias.[14-16] In a large subset of patients with Arrhythmogenic Cardiomyopathy (AC), mutations in desmosomal proteins are found. This disease is characterized by a predominant involvement of the right ventricle and patients often present with syncope, palpitations or sudden cardiac death. Prevalence is about 1:2000 - 1:5000. Many of these patients experience life threatening ventricular arrhythmias as a first symptom in the concealed phase of the disease, the phase where structural modifications are still lacking. The absence of other symptoms makes it difficult to diagnose AC in the early phase of the disease. By understanding the interactions between desmosomes and other components of the intercalated disk, we will be able in the future to detect and treat AC in an earlier stage (Figure 1.1).

Central theme in this thesis is the intercalated disk and its remodeling towards an arrhythmogenic substrate. This brings us to the main hypothesis of this thesis:

> *A large macromolecular complex is situated at the intercalated disk of the cardiomyocyte, consisting of gap junctions, sodium channels and desmosomes. Changes in expression or localization of one component will lead to changes in the others. These changes can create an arrhythmogenic substrate.*

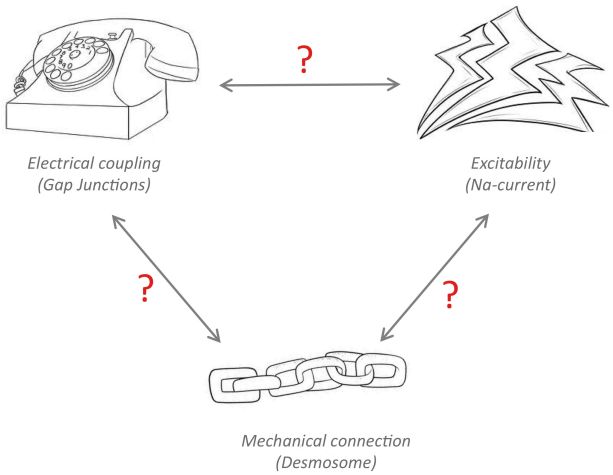

Figure 1.1 – *Model of determinants of conduction and their interaction*

This thesis starts in **chapter 2** with an overview of the components at the intercalated disk that maintain mechanical and electrical coupling of cardiomyocytes. Furthermore, several disease and mouse models are reviewed in which one of the components ensuring mechanical or electrical coupling is affected, leading to disturbances in the other junctions. In **chapter 3** we study the interaction between Cx43 and $Na_V1.5$ using a mouse model, which expresses only 5% of the normal Cx43 amount. Conduction is severely impaired in these animals, leading to a 50% arrhythmia incidence. We compared animals susceptible to arrhythmias to animals that were non-susceptible, and analyzed the heterogeneous downregulation of Cx43 and decreased $Na_V1.5$ expression. In **chapter 4** we compare a number of studies on the prevalence of mutations in desmosomal protein encoding genes in relation to the geographic distribution of the study population. In **chapter 5** the case of an AC patient with a *PKP2* mutation is described. The patient had to undergo a heart transplant, which provided the opportunity to study the heart extensively and to perform histological, immunohistochemical, and ultrastructural analyses on this heart. In this chapter we have studied, among others, the effect of the defective PKP2 on Cx43 expression and distribution. In **chapter 6 and 7** we studied biopsies of the right ventricular septum and post-mortem material from a group of AC patients. First, we compare distribution of several intercalated disk proteins in these tissue samples: PKP2, Cx43 and $Na_V1.5$ are all studied. Secondly, a more technical issue is addressed: immunohistochemistry on cryo-material is compared to immunohistochemistry on formalin-fixed, paraffin-embedded material. **Chapter 8** describes a study on mice heterozygous for the desmosomal protein Plakophilin-2. We characterized the structural consequences of the reduction in PKP2 in these mice, and also studied the relation between PKP2 abundance and sodium channel function. Finally, the results of all studies are put into perspective in **chapter 9**.

References

1. Nattel S, Maguy A, Le Bouter S, Yeh YH. Arrhythmogenic ion-channel remodeling in the heart: Heart failure, myocardial infarction, and atrial fibrillation. *Physiol Rev.* 2007;87:425-456
2. Sen-Chowdhry S, Syrris P, McKenna WJ. Genetics of right ventricular cardiomyopathy. *J Cardiovasc Electrophysiol.* 2005;16:927-935
3. Kjekshus J. Arrhythmias and mortality in congestive heart failure. *Am J Cardiol.* 1990;65:42I-48I
4. Coumel P. The management of clinical arrhythmias. An overview on invasive versus non-invasive electrophysiology. *Eur Heart J.* 1987;8:92-99
5. Peters NS. New insights into myocardial arrhythmogenesis: Distribution of gap-junctional coupling in normal, ischaemic and hypertrophied human hearts. *Clin Sci (Lond).* 1996;90:447-452
6. Kostin S, Rieger M, Dammer S, Hein S, Richter M, Klovekorn WP, Bauer EP, Schaper J. Gap junction remodeling and altered connexin43 expression in the failing human heart. *Mol Cell Biochem.* 2003;242:135-144
7. van Veen TA, Stein M, Royer A, Le Quang K, Charpentier F, Colledge WH, Huang CL, Wilders R, Grace AA, Escande D, de Bakker JM, van Rijen HV. Impaired impulse propagation in scn5a-knockout mice: Combined contribution of excitability, connexin expression, and tissue architecture in relation to aging. *Circulation.* 2005;112:1927-1935
8. van Rijen HV, Eckardt D, Degen J, Theis M, Ott T, Willecke K, Jongsma HJ, Opthof T, de Bakker JM. Slow conduction and enhanced anisotropy increase the propensity for ventricular tachyarrhythmias in adult mice with induced deletion of connexin43. *Circulation.* 2004;109:-1048-1055
9. Stein M, van Veen TA, Remme CA, Boulaksil M, Noorman M, van Stuijvenberg L, van der Nagel R, Bezzina CR, Hauer RN, de Bakker JM, van Rijen HV. Combined reduction of intercellular coupling and membrane excitability differentially affects transverse and longitudinal cardiac conduction. *Cardiovasc Res.* 2009;83:52-60
10. Jansen JA, van Veen TA, de Jong S, van der Nagel R, van Stuijvenberg L, Driessen H, Labzowski R, Oefner CM, Bosch AA, Nguyen TQ, Goldschmeding R, Vos MA, de Bakker JM, van Rijen HV. Reduced cx43 expression triggers increased fibrosis due to enhanced fibroblast activity. *Circ Arrhythm Electrophysiol.* 2012
11. Stein M, Noorman M, van Veen TA, Herold E, Engelen MA, Boulaksil M, Antoons G, Jansen JA, van Oosterhout MF, Hauer RN, de Bakker JM, van Rijen HV. Dominant arrhythmia vulnerability of the right ventricle in senescent mice. *Heart Rhythm.* 2008;5:438-448
12. Basso C, Czarnowska E, Della Barbera M, Bauce B, Beffagna G, Wlodarska EK, Pilichou K, Ramondo A, Lorenzon A, Wozniek O, Corrado D, Daliento L, Danieli GA, Valente M, Nava A, Thiene G, Rampazzo A.

Ultrastructural evidence of intercalated disk remodelling in arrhythmogenic right ventricular cardiomyopathy: An electron microscopy investigation on endomyocardial biopsies. *Eur Heart J*. 2006;27:1847-1854

13. Asimaki A, Tandri H, Huang H, Halushka MK, Gautam S, Basso C, Thiene G, Tsatsopoulou A, Protonotarios N, McKenna WJ, Calkins H, Saffitz JE. A new diagnostic test for arrhythmogenic right ventricular cardiomyopathy. *N Engl J Med*. 2009;360:1075-1084
14. Li D, Liu Y, Maruyama M, Zhu W, Chen H, Zhang W, Reuter S, Lin SF, Haneline LS, Field LJ, Chen PS, Shou W. Restrictive loss of plakoglobin in cardiomyocytes leads to arrhythmogenic cardiomyopathy. *Hum Mol Genet*. 2011;20:4582-4596
15. Kirchhof P, Fabritz L, Zwiener M, Witt H, Schafers M, Zellerhoff S, Paul M, Athai T, Hiller KH, Baba HA, Breithardt G, Ruiz P, Wichter T, Levkau B. Age- and training-dependent development of arrhythmogenic right ventricular cardiomyopathy in heterozygous plakoglobin-deficient mice. *Circulation*. 2006;114:1799-1806
16. Pilichou K, Remme CA, Basso C, Campian ME, Rizzo S, Barnett P, Scicluna BP, Bauce B, van den Hoff MJ, de Bakker JM, Tan HL, Valente M, Nava A, Wilde AA, Moorman AF, Thiene G, Bezzina CR. Myocyte necrosis underlies progressive myocardial dystrophy in mouse dsg2-related arrhythmogenic right ventricular cardiomyopathy. *J Exp Med*. 2009;206:1787-1802

CHAPTER 2

Cardiac cell-cell junctions in health and disease: electrical versus mechanical coupling

Maartje Noorman[1,2], Marcel AG van der Heyden[1], Toon AB van Veen[1], Moniek GPJ Cox[2,3], Richard NW Hauer[2,3], Jacques MT de Bakker[2], Harold VM van Rijen[1]

1. Department of Medical Physiology, Division Heart & Lungs, University Medical Center Utrecht, Utrecht, The Netherlands
2. Interuniversity Cardiology Institute of The Netherlands, Utrecht, The Netherlands
3. Department of Cardiology, Division Heart & Lungs, University Medical Center Utrecht, Utrecht, The Netherlands

Journal of Molecular and Cellular Cardiology 2009

Abstract

Intercalated disks are the membrane sites where individual cardiomyocytes are connected to each other. Adherens-, desmosomal-, and gap junctions are situated in the intercalated disk and ensure mechanical coupling between cells and enable propagation of electrical impulses throughout the heart. A number of cardiac disorders, for example arrhythmogenic right ventricular dysplasia/cardiomyopathy, have been described in which an impaired mechanical coupling leads to electrical dysfunction, with occurrence of fatal arrhythmias.

In this article the interaction between electrical and mechanical coupling is explored by reviewing studies performed in patients, animals, and *in vitro*. In these studies the effect of changes in protein composition of a mechanical junction on the electrical junction, and vice versa were investigated. It is shown that impaired electrical coupling does not change mechanical coupling. However, impaired mechanical coupling largely affects electrical coupling.

Introduction

The fascinating phenomenon of excitation contraction coupling is subjected to all the individual cardiomyocytes that compose the heart. Up scaling of this manifestation to the well coordinated excitation and contractile performance of the total organ demands our attention to a tiny but very ingeniously orchestrated part of cardiomyocytes: the intercalated disk (ID). Already in the nineteenth century, Engelmann brought forward the concept that the heart was a functional syncytium.[1] Much later, Weidmann suggested, based on Engelmann's concept, that cardiac cells had to be connected by low cell-to-cell resistances[2]. However, it became evident that cardiac cells are not only connected, but also separated by IDs.[3, 4] This apparent lack of cytoplasmic continuity was refuted by Barr and coworkers, who were the first to define the gap junctions in the IDs as the molecular substrate that facilitated the low resistance intercellular pathway.[5]

The IDs between individual cardiomyocytes therefore have at least two syncytial functions: 1) to ensure mechanical coupling and 2) to enable fast propagation of electrical impulses throughout the heart. Improper mechanical coupling between myocytes leads to a deteriorated cardiac pump function, while improper electrical coupling may lead to abnormal conduction of the electrical impulse and subsequent development of cardiac arrhythmias.

The ID is a complex and highly orchestrated structure, where multiple proteins interact and form large complexes. In the past years, a number of cardiac disorders have been described, in which defective *mechanical* coupling between cardiomyocytes leads to degenerative cardiomyopathies that are besides contractile impairment, also characterized by *electrical* disorders with occurrence of fatal arrhythmias. An example of such complex disorders is arrhythmogenic right ventricular dysplasia/cardiomyopathy (ARVD/C).[6, 7] Disturbance of the delicate interplay between mechanical and electrical coupling at the ID seems to be the key feature of these disorders, and has been the subject of multiple human, animal and *in vitro* studies in the past few years. This review will focus on cardiac cell-cell junctions in health and disease and explores the interaction between electrical and mechanical coupling.

Cardiac junctions

The main site of myocyte interconnection is the ID, situated at the long ends of the cell[3, 4]. In the ID three different protein complexes are apparent that provide mechanical strength and electrical coupling: adherens-, desmosomal-, and gap junctions.

Adherens junctions (AJ) provide a strong mechanical connection of cardiomyocytes via linkage to the actin cytoskeleton, which provides a uniform mechanical strength to the heart.[8] They keep the cells tightly together as the heart expands and contracts. AJs are also the anchor-point where myofibrils are attached, enabling transmission of contractile force from one cell to another.[9] AJs are constructed from cadherins and catenins (Figure 2.1). Cadherins, in cardiomyocytes N-cadherin is the main isoform, are transmembrane proteins that zip together adjacent cells in a homophilic manner over a distance of 0.2-0.5 mm. At the AJ the apposing membranes become separated by ~20 nm. The transmembrane cadherins form complexes with cytosolic α-, β-, γ-(plakoglobin), and p120 catenin, thereby establishing the connection to the actin cytoskeleton.[10]

Desmosomes, also called desmosomal junctions, provide structural support between myocytes via interaction with intermediate filaments. Desmosomes are dense, robust structures that are primarily abundant in tissues that are subject to strong contractile stress or abrasive forces, like cardiac muscle and epithelia.[11-13] Desmosomes consist of an inter- and an intracellular part (Figure 2.2). The intercellular part is formed by the desmosomal cadherins desmocollin and desmoglein, which interact in a heterophilic manner in the extracellular space to connect adjacent cells. The intracellular part of the desmosome consists of the proteins plakoglobin (γ-catenin), plakophilin, and desmoplakin, the latter one being the molecule that connects the desmosome to the intermediate filaments. Desmosomes are less than 0.5 μm in diameter. The space between apposing cells at the site of desmosomes is 20-35 nm.[14] Gap junctions (GJs) mediate direct communication between adjacent cells. These intercellular channels connect the cytoplasm of neighboring cells, enabling passive diffusion of various compounds, like metabolites, water and ions, up to a molecular mass of 1000 Da.[15] Thereby they warrant electrical and metabolic communication between cells.[16] GJs are present in nearly all tissues and cells throughout the entire body.[17] In cardiac muscle GJs ensure a proper propagation of the electrical impulse which triggers sequential and coordinated contraction of the cardiomyocytes.[18] A GJ channel consists of twelve connexin proteins,

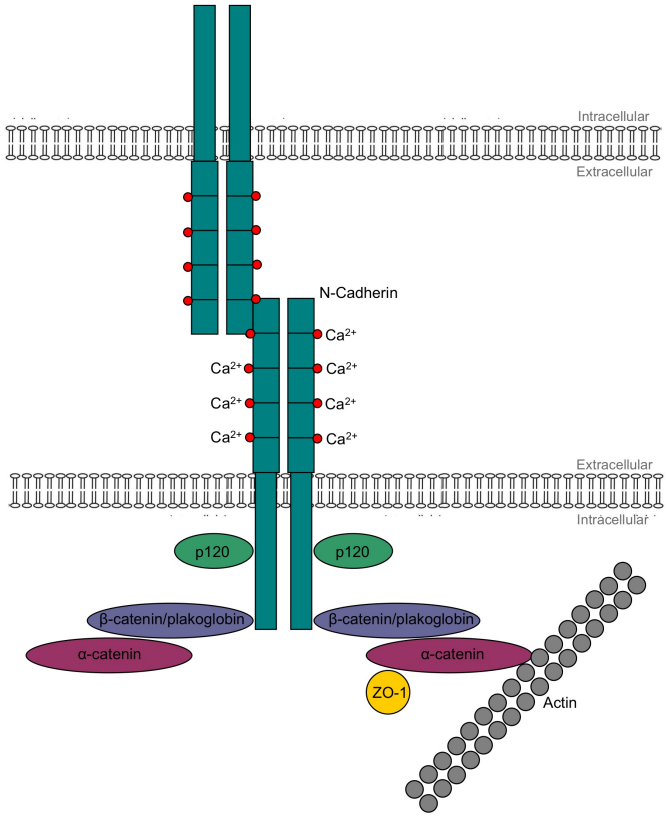

Figure 2.1 – *Adherens junction.* AJs connect adjoining cells in a homophilic way to each other through N-Cadherin. At the intracellular part the AJ consist of α- and β-catenin, plakoglobin, p120 catenin, and ZO-1. Via these proteins the AJ connects to the actin cytoskeleton.

six of which are contributed by each cell (Figure 2.3). The six connexin subunits form a hemi-channel in the plasma membrane, which is called a connexon.[19, 20] A connexon docks to another connexon in the intercellular space to create a complete GJ channel.[21] The intercellular space between adjacent cells at the site of a GJ is 3.5 nm.[22] Connexins form a large protein family of highly related though functionally distinct connexins.[17] In the ventricular myocardium the most important connexin isoform is Connexin43 (Cx43).[23-25]

Figure 2.4 shows the distinct morphological association between mechanical and electrical junctions in the ID. Electron microscopy revealed that GJ plaques in the ID alternate with AJ.[26, 27] AJs are situated in the zones of the ID perpendicular to the long axis of the

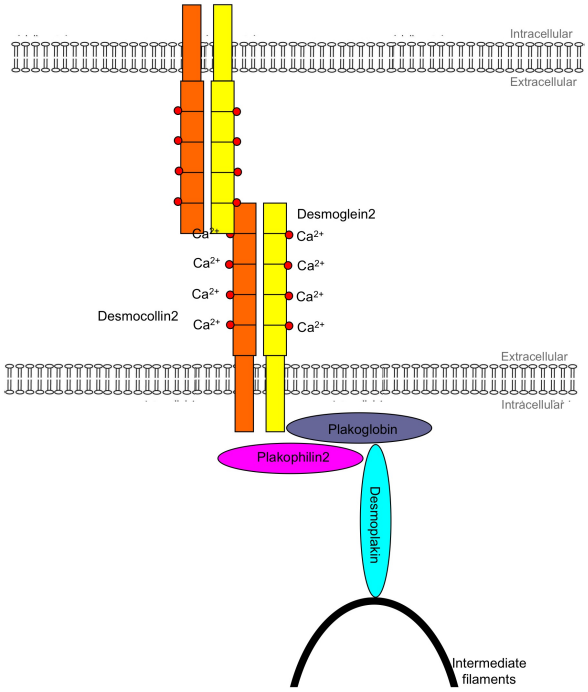

Figure 2.2 – *Desmosome.* Desmosomes connect neighboring cells to each other in a heterophilic manner. The extracellular part consists of two desmosomal cadherins: Desmoglein2 and Desmocollin2. Intracellularly are plakoglobin, plakophilin2 and desmoplakin the proteins that connect the cadherins to the intermediate filaments.

myocyte (plicate), to be able to transmit mechanical forces from one cell to another. GJs are predominantly located in the zones parallel to the long axis of the cell (interplicate). Desmosomes are usually found in the longitudinal zones, adjoining the GJs, but they are also located adjacent to AJs indicating clustering of the three junction structures. The high degree of structural organization within the ID suggests a tight interplay and framework for both mechanical and electrical interaction between myocytes. The ultrastructural organization of the ID has been described in detail in several enlightening studies by Severs.[28]

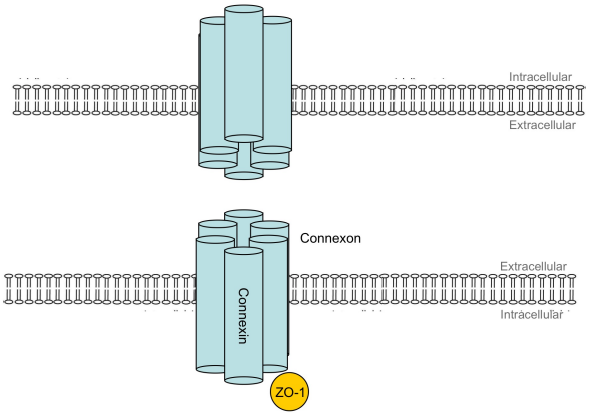

Figure 2.3 – *Gap junction.* GJ consist of two hemichannels, called connexons, one of each delivered by each cell. Connexons are build up from six connexins.

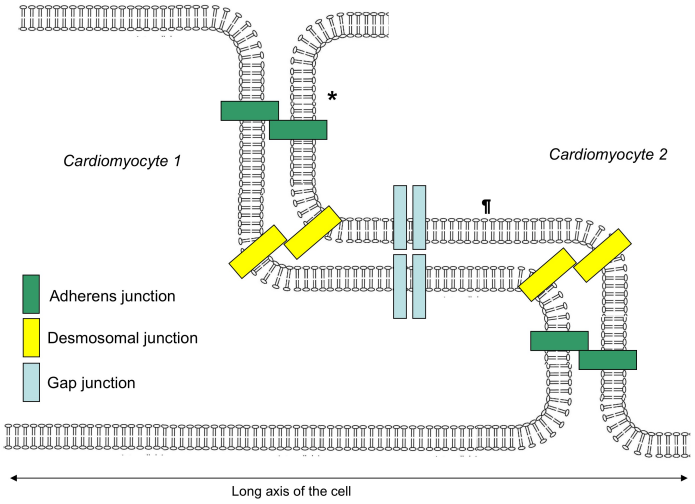

Figure 2.4 – *Intercalated disk.* AJs are situated in the ID at the sites perpendicular to the long axis of the cell, whereas GJs are mainly located at sites parallel to the long axis. Desmosomes are found adjoining both the AJ and GJ. A plicate region is depicted by *. An interplicate region is depicted by ¶.

Cardiac disorders caused by changes in mechanical junctions

ARVD/C is a progressive disease that can lead to arrhythmias, heart failure and sudden cardiac death. The prevalence of this disease has been estimated to be approximately 1 in 5000.[29] However, in some regions like e.g. northern Italy, prevalence is much higher, and approaches 1 in 2000. The exact prevalence remains unknown, because diagnosing ARVD/C is difficult, with many cases going un- or misdiagnosed. About 50% of the confirmed cases is familial, based on genetic modifications with an autosomal dominant inheritance. Usually, first symptoms of ARVD/C occur between the second and fourth decade of life. Dramatically, for a large cohort of patients, the first presentation of the disease is sudden death.

The first clinical and pathological examinations of ARVD/C patients have been described by Marcus, Nava, and Thiene more than 20 years ago.[6, 30, 31] ARVD/C typically is characterized by a progressive loss of right ventricular myocardium, which is gradually replaced by adipose and fibrous tissue. This degeneration of the right ventricle may extend to the left ventricle and, less often, to the interventricular septum. Clinical manifestations in patients include sudden cardiac death, syncope, or palpitations due to nonsustained or sustained ventricular arrhythmias originating primarily from the right ventricle. Intriguingly, some carriers of pathogenic mutations are asymptomatic or only have minor abnormalities, which suggests that additional factors are necessary to develop the phenotype.

ARVD/C is considered a desmosomal disease, since it has been shown that mutations in desmosomal genes are associated with development of the ARVD/C phenotype. The mutations may affect number and integrity of desmosomes, but importantly, it has been shown that this also may influence the amount and distribution of other ID proteins, including GJ proteins and cardiac ion channels. As a result this may deregulate intercellular conductance and as such enhance arrhythmogeneity. Several loci of inherited mutations have been mapped, and five causal genes have been identified, encoding the desmosomal proteins desmoplakin,[32] plakoglobin,[33] plakophilin 2,[34, 35] desmocollin 2[36, 37] and desmoglein 2.[38]

Plakophilin2 (PKP2) mutations have been found to be the most common genetic cause of ARVD/C. About 70% of the familial cases of ARVD/C is caused by a pathogenic PKP2 mutation.[35] Immunohisto-

chemistry in an ARVD/C patient with PKP2 mutation not only showed a reduction of PKP2 in the heart, but also a reduction of plakoglobin, desmoplakin and Cx43. N-Cadherin expression remained normal.[39] In a study by Fidler *et al*, endomyocardial biopsies of ARVD/C patients with a PKP2 mutation were studied with immunofluorescence.[40] In these biopsies, Cx43 expression was decreased, regardless of the type of mutation. This reduction in Cx43 expression in ARVD/C patients is in compliance with the PKP2 siRNA experiments in a mouse cardiomyocyte cell line.[40]

A canine model of spontaneous ARVD/C recapitulates major manifestations seen in patients.[41, 42] These dogs showed histological abnormalities, like severe right ventricular loss of cardiomyocytes and fibrofatty replacement, classical observations in ARVD/C. Immunofluorescence microscopy was used to study the ID composition of affected dogs. A slight reduction in N-Cadherin and PKP2 expression levels was observed, while larger reductions in desmoplakin, plakoglobin and Cx43 expression levels were identified. In most of the affected dogs the changes in ID organization could be linked to induction of ventricular arrhythmias, suggesting that the alterations had created an arrhythmogenic substrate.[41, 42]

Effects of changes in mechanical junctions on electrical junctions

Spatiotemporal distribution of AJ and GJ

During cardiomyocyte maturation, large changes in the spatiotemporal distribution of GJs and AJs occur. As shown in a study by Angst et al[43] GJs and AJs are uniformly distributed along the plasma membrane of rat cardiomyocytes at postnatal day 1. At postnatal day 20 GJs are still distributed along the entire plasma membrane, while in contrast AJs concentrate at the developing ID. At postnatal day 90 all three types of cardiac junctions are located primarily at the ID. This process was also confirmed in dogs[43] and these findings suggest that AJs first ensure a 'protected environment' before GJs migrate to the ID.

This spatiotemporal relation of subcellular localization of AJs and GJs has also been described *in vitro* using isolated adult rat cardiomyocytes. In this study it was found that when isolated myocytes are allowed to make contact, first AJs assemble at the ID, subsequently followed by GJs.[44] However, in developing human ventricular myocardium,

the process of spatiotemporal migration of GJs and AJs to the ID has been found to occur simultaneously.[45] Furthermore, in a study in which the border zone of myocardial infarcts was investigated in rats, it was found that after infarction GJs virtually disappear, whereas the expression of desmosomal protein desmoplakin and AJ protein cadherin decreased, but remained present.[46] Later in the healing phase of post-infarct remodeling, the number of all three junction types increased again, but they located intracellularly in invaginations of cells, suggesting that GJ remodeling after myocardial infarction is closely linked to the remodeling of AJs.[46]

Interestingly, pulsatile stretch experiments mimicking the mechanical performance of coupled cardiomyocytes also revealed a correlation between neoformation of AJs and GJs in cardiomyocytes. Many of the responses to mechanical pulsatile stretch by isolated neonatal rat cardiomyocytes seem to recapitulate characteristics of hypertrophic response, hence pulsatile stretch experiments seem to be a representative *in vitro* model of cardiac responses to hypertrophy *in vivo*. Studies by Zhuang *et al.*[47] and Yamada *et al.*[48] showed that the amount of N-Cadherin, desmoplakin, plakoglobin and Cx43 protein was largely increased upon pulsatile stretch. Also, on top of an increase in amount of junctional proteins, the cell-cell junctions were larger, more abundant, and more mature after pulsatile stretch.

Role of N-Cadherin in modulation of GJ

Cadherins are single pass transmembrane proteins, which have one transmembrane domain, a cytoplasmic domain, and five extracellular domains,[49] that can be divided into repeated subdomains on basis of their amino acid sequence (Figure 2.1). The recognition sites between cadherin molecules consist of a HAV motif (single-letter code for amino acids) and are localized to the adhesion dimer interface. Ca^{2+} is involved in linking the five subdomains to create the rod-shape morphology of cadherins. The extracellular domain forms a dimer in which two monomers are arranged in parallel at the plasma membrane. The dimers are arranged like a zipper in the intercellular space[50] where apposing cells bind as homodimers to form a junction in a calcium-dependent manner.[51]

To determine the function of cardiac AJs and of its most important protein N-cadherin (N-Cad), several studies have been performed in animal models in which the coding gene has been deleted, either entirely or partially. Complete knockout of N-Cad in a mouse model

showed that this protein plays a critical role in embryonic development of the heart and other organs and tissues since knockout embryos died at E10.[52] Myocardial tissue had been formed at this stage, but myocytes dissociated and the heart tube failed to develop properly, due to adhesion problems. Myocytes isolated from these mutant embryos showed that the cells could aggregate and weakly contract, suggesting that N-Cad is not exclusively required for cell adhesion or electrical coupling in the embryonic stage.[52]

To reveal the function of N-Cad in the adult heart, a conditional knockout mouse model was created.[53] Cardiac N-Cad was specifically deleted in 6 to 10 week old transgenic animals, which caused the mice to die after approximately 2 months. Hearts showed a dilated cardiomyopathy and impaired left ventricular function, while spontaneous ventricular tachyarrhythmias and abnormal conduction patterns were observed. As an underlying cause for this phenotype it appeared that depletion of N-Cad caused a reduction in Cx43 expression levels, which correlated to the decrease in conduction velocity and increased propensity to arrhythmias. Next to the reduction in Cx43 protein levels, also the amount of other ID proteins like plakoglobin, α-, β-, and p120 catenin appeared reduced. In contrast, the amount of desmoplakin remained unchanged.[53, 54] In another study, mice heterozygous for both N-Cad and Cx43 were examined.[55] Mice with combined haploinsufficiency were more susceptible to arrhythmias than mice heterozygous for only one of the proteins. In the N-Cad/Cx43 heterozygous animals, GJ plaques were reduced in size even more than in mice only heterozygous for Cx43. This demonstrated that there is an intimate relationship between Cx43 and N-Cad in the heart and that N-Cad is needed to maintain GJ complexes at the cell membrane in the adult heart.[55]

Role of PKP2 in modulation of GJ

The armadillo protein plakophilin is an intracellular component of desmosomes, which provides lateral association of desmosomal cadherins. Plakophilins consist of nine armadillo repeats. They have a large N-terminal domain (~275-380 residues, depending on the isoform), and a very short C-terminus. The N-terminal domain binds to several other components in the desmosome. In plakophilin the armadillo repeats do not bind other proteins, as is shown for other armadillo proteins, like plakoglobin and β-catenin.[56] In the heart the main isoform of plakophilin is PKP2. PKP2 was found to be essential

for embryonic heart development.[57] PKP2 knockout mice show lethal abnormalities in heart morphogenesis, like rupture of the cardiac walls and blood leakage into the pericardiac cavity. In PKP2 deficient mice, N-Cad, β-catenin, plakoglobin, and desmoglein protein content was decreased, illustrating the importance of PKP2 for organization of the ID and maintenance of desmosomal function.[57] Using siRNA to silence the expression of PKP2 in cultured rat cardiomyocytes, it was shown that the number of cell-cell contacts was decreased and that Cx43 content of these cells was decreased and redistributed to the intracellular space.[58, 59] Apparently, PKP2 is an important component of the desmosome, being a linker protein between the inter- and intracellular part of the desmosome.

Role of plakoglobin (γ-catenin) in modulation of GJ

Plakoglobin (PG) is an armadillo protein that is present in the intracellular part of both desmosomes and AJs. It is essential for cardiac development, as illustrated in mice with targeted deletion of PG.[60, 61] Such mice die around day 12 of embryogenesis from severe heart defects, like burst ventricles and blood in the pericardium. In PG deficient mice, desmosomes are absent and are replaced by extended AJs, containing desmosomal proteins.[60, 61] Heterozygous PG-deficient mice show increased right ventricular volume, reduced right ventricular function and spontaneous ventricular ectopic activity.[62] Surprisingly, left ventricular size and function were not affected and structure of desmosomes and AJs was not altered. It was also found that endurance training of the animals accelerated development of cardiac dysfunction and increased arrhythmia vulnerability.[62] The predominant right ventricular involvement in this model is in concordance with the general right ventricular phenotype observed in ARVD/C patients.

An autosomal recessive cardiocutaneous subtype of ARVD/C, known as Naxos disease, is caused by a mutation in PG. This syndrome was first described by Protonotarios *et al.* in 1986[63] and is associated with a high incidence of sudden cardiac death. Naxos disease is characterized by woolly hair, palmoplantar keratoderma and heart disease. The PG mutation causes a decrease of the binding capacity of PG to other proteins in the desmosome and AJ. Interestingly, the phenotype of this disease is restricted to the heart, skin and hear, while PG expression is much more general. Apparently, PG abnormalities are only evident in structures subjected to constant mechanical stress, as a result of which PG defects present mainly in these tissues.

In a study by Kaplan *et al.* myocardial expression of intercellular junction proteins was characterized in four patients with Naxos disease.[64] They showed that the amount of PG was markedly decreased at the IDs in both left and right ventricle. Immunoblotting showed that a truncated form of PG was expressed in the myocardium, but that it failed to localize at the intercellular junctions. N-Cad, desmocollin-2, desmoplakin-1, α-, β-catenins and PKP2 were localized normally in the cell junctions. The amount of Cx43 protein was reduced in both the left and right ventricle of Naxos patients with the highest reduction found at the right side. The authors concluded that in Naxos disease, loss of mechanical coupling leads to impairment of electrical coupling, which in turn may lead to slowing of impulse conduction, explaining the high incidence of arrhythmias in this disease.[64]

Role of desmoplakin in modulation of GJ

Desmoplakin (DP) is one of the major components of desmosomes. It connects the desmosomal complex to the intermediate filaments of the cell and also plays an important role in lateral clustering of the desmosomal cadherins. DP is a very large protein, with N- and C-terminal domains of almost 1000 amino acids. Between the C- and N-terminal, an α-helix of almost of the same size is found. The molecule is approximately 180 nm long, with a central rod of ~130 nm which connects two globular heads. DP and PKP2 interact with each other at their N-terminal domains.[56]

In transgenic mice with cardiac-restricted overexpression of a C-terminal mutant form of DP, cardiomyocyte apoptosis, fibrosis, lipid accumulation, cardiac dysfunction and ventricular enlargement were found, indicating severe pathophysiological alterations. Histological examination of the mutant hearts showed that GJs and AJs were normally present, but desmosomes were not apparent in mutant hearts, suggesting that DP is required for maintenance of cardiac tissue integrity.[65]

Carvajal syndrome, a variant of Naxos disease, is also a cardiocutaneous syndrome characterized by woolly hair, palmoplantar keratoderma and cardiac disease. Unlike the underlying cause of Naxos disease (mutation of PG), this disease is caused by a mutation in DP and is phenotypically presented in the heart as a generalized dilated cardiomyopathy rather than ARVD/C. Kaplan *et al* showed that this cardiomyopathy is characterized by ventricular hypertrophy and dilatation, focal ventricular aneurysms, and distinct ultrastructural abnormalities of the IDs.[66] No fibrofatty infiltration or replacement of the

myocardium was apparent. It was shown that DP is virtually undetectable in a Carvajal syndrome heart and also PG, desmin and Cx43 protein levels are reduced. The amounts of N-Cad and desmocollin protein are normal.[66]

The mutation in DP may interfere with molecular interactions among DP, PG, and the desmosomal cadherins. Comparable to Naxos disease, the abnormal protein-protein interactions at the intercellular junctions are likely to cause the contractile and electrical dysfunction in the Carvajal syndrome.[66]

DP is apparent in the outer dense plaque of the desmosome. It has been hypothesized that mutations in proteins in this region, causing a disturbed binding to desmin, may give rise to an ARVD/C phenotype with left ventricular involvement. This, in contrast to mutations in desmosomal proteins situated in the inner dense plaque, causing disturbed binding between cells, which may explain a more right ventricular phenotype.[67]

Desmin

In cardiomyocytes, intermediate filaments are composed of desmin. Mice with a null mutation in desmin develop normally, indicating that this protein is not essential for cardiac development *per se*. However, it was shown that adult mice displayed concentric hypertrophy, ventricular dilatation and compromised systolic function, demonstrating that desmin is an important factor required for normal cardiac function.[68, 69] Transgenic mice with a mutation in desmin that impaired linkage between desmin and DP showed conduction slowing and a severe remodeling of the ID. The amounts of Cx43, DP, desmocollin, N-Cad and PG protein in the ID were largely reduced; however, total cellular protein content of these proteins was not decreased, indicating that the reduction was not caused by insufficient protein synthesis rather than an obstructed distribution.[70]

Role of ZO-1 in modulation of GJ

Scaffolding protein zonula occludens-1 (ZO-1) is a member of the membrane-associated guanylate kinase (MAGUK) protein family. Proteins from this family contain among others at least three different protein binding domains, including a PDZ domain. ZO-1 interacts with its PDZ domain with the last 20 amino acids of the C-terminus of Cx43. The interaction between ZO-1 and Cx43 has been shown *in vitro* in a

cellular system.[71] This study proposed that the linkage between ZO-1 and Cx43 is responsible for the localization of Cx43 at the ID, thereby generating functional GJ.[71] In the healthy human heart ZO-1 can be found in the ID, in contrast to the failing heart, where ZO-1 is almost completely abolished.[72]

In addition to the interaction with Cx43, ZO-1 can bind directly to α-catenin, which associates with N-Cad. The co-distribution of ZO-1, Cx43 and N-Cad is described in adult rat ventricle.[73] Within the ID a high level of colocalization of ZO-1 and N-Cad was seen, in contrast to a low colocalization of Cx43 and ZO-1. However, the association level of Cx43 and ZO-1 increased significantly after induction of GJ endocytosis. This indicates that ZO-1 plays a role in GJ turnover during cardiac remodeling, due to development or disease processes.[73]

Effects of changes in electrical junctions on mechanical junctions

Gap junctions

As indicated in the previous part of this review, changes in the expression patterns of desmosomal or AJ proteins have a strong effect on the formation or stability of GJs. In this paragraph we will summarize the effects of changes in GJ protein expression on proteins in the desmosome and AJ. In a study by Saffitz *et al.*[74] the effect of diminished expression of Cx43 on GJ number and size is described. In mice heterogeneous for Cx43 especially the number of GJ plaques was decreased and not their individual sizes. Furthermore, the amount of N-Cad was not changed in these heterozygous mice. Interestingly, a study by Gutstein *et al.*[75] showed that AJ proteins as well as their associated catenins are regulated independently of GJ in the ID. In this study a mouse model with cardiac specific conditional knockout of Cx43 was used. Cx43 knockout mice were compared to control mice by immunofluorescence microscopy and western blotting. AJs as well as desmosomes were structurally unchanged in the absence of Cx43 protein. In the absence of Cx43, not only N-Cad and DP were localized normally in the IDs, but this was also shown for the distribution of catenins and ZO-1. From this study it can be concluded that Cx43 is not necessary for the organization of mechanical cell junctions at the ID.[75]

In humans, a number of mutations in the Cx43 coding gene have

been linked to oculodentodigital dysplasia (ODDD). In some cases, ODDD patients present hair and skin abnormalities as found in a number of desmosomal diseases.[76-78] Some mutations have been associated with cardiac developmental defects and one family presented cardiac rhythm disturbances.[76] In an ODDD mouse model, disturbed Cx43 trafficking was observed in the heart resulting in a decreased number of Cx43 based GJs[79] but not beyond levels that would affect normal cardiac conduction. Overall, as deduced from this experimental evidence, it appears that dysfunctional cardiac Cx43 per se is not a primary inducer of mechanical or electrical coupling defects associated with ventricular arrhythmia.

In a study on dilated cardiomyopathy, mimicked by a knockout mouse for muscle LIM protein, which showed enlargement of the ventricular chambers, wall thinning and reduced left ventricular function, changes in the ID were observed. Components of AJ, like N-Cad, α-catenin, β-catenin, and PG were upregulated, whereas GJ Cx43 protein was downregulated. Desmosomal proteins like DP and desmoglein were equally expressed in knockout and control mice.[80] These data could partially be confirmed in a guinea pig model of chronic pressure overload, since N-Cad expression levels remained unchanged, β-catenin increased, and Cx43 levels decreased largely.[81]

Effect of heart failure on electrical and mechanical junctions

Changes in GJ expression and distribution are a common feature during cardiac remodeling and heart failure. Typically, Cx43 expression levels are reduced and Cx43 migrates from the ID to the lateral sides of the cell. A detailed description of GJ remodeling during heart failure is beyond the scope of this review, and has already thoroughly been reviewed by others.[82-84]

While in models in which no genetic modifications have been made to induce heart failure the effects of heart failure on Cx43 are well described, information on the fate of mechanical junctions is far more scarce. In a number of these studies, using either rabbit and dog models of, or patients with non-congenital forms of heart failure, a downregulation and redistribution of Cx43 was observed, while N-Cad expression levels and distribution were unaffected.[85-87] In a dog model of chronic heart failure, however, N-Cad was clearly downregulated in the borderzone of micro-infarctions.[88] In a rat model of MI, N-Cad and DP were downregulated in the borderzone, though to a moderate extent

when compared to downregulation of Cx43.[46] In rats with hypertrophied right ventricles resulting from monocrotaline-induced pulmonary hypertension, again a redistribution of Cx43 to the lateral side of the cell was observed, while DP remained exclusively present in the ID.[89] Reports on remodeling of ZO-1 are more contradictive. Some studies report a downregulation of ZO-1 in human dilated and ischemic cardiomyopathy,[72, 90] while others claim an upregulation[73] and an increased association with Cx43.[91]

In comparison, studies on genetic modifications targeting mechanical junctions show disturbances of these junctions concomitant with severely affected GJ expression. In non-genetic models of heart failure, GJ expression and subcellular distribution also seem to be affected, while desmosomes and AJ composition remain unaltered or are only mildly affected.

Concluding remarks

This review summarized data on cardiac cell-cell junctions in health and disease and explored the interaction between electrical and mechanical coupling. Data show that changes in electrical junction expression and distribution do not directly influence the composition of mechanical junctions in the heart, both AJ and desmosomes.

However, alterations in the composition of the AJ had large effects on GJ expression and function. Studies using animal models with affected components of AJ showed that fully functional AJ are not only necessary for embryonic development, but also for normal cardiac function and integrity in adulthood.[52, 53] GJ organization appeared very sensitive to changes in N-Cad levels in the heart.[55] Possibly, the molecular linkage between Cx43 and the AJ via ZO-1 is an important factor in this process. There is little or no knowledge about human cardiac diseases based on loss of function mutations in N-Cadherin, presumably because such mutations are lethal *in utero*.

Desmosomal mutations, however, are frequently observed in patients with arrhythmogenic cardiomyopathies, suggesting that these mutations result in a milder phenotype than mutations in components of the AJ. However, as was shown in cases of ARVD/C, desmosomal mutations frequently cause problems at later age. A very common finding is that changes in the function of desmosomal proteins lead to abnormal expression and distribution of GJ, which may, at least in part, underlie the arrhythmogenic vulnerability of these patients.

Summarizing, there is a clear interaction between the three types of junctions in the ID. Changes in electrical junctions do not affect mechanical interaction in the ID. However, functional changes in mechanical junctions severely affect GJ function. This explains why an impaired *mechanical* coupling in several cardiomyopathies leads to *electrical* dysfunction with increased arrhythmogeneity, explaining the phenotype of ARVD/C.

At current, it is however largely unknown which molecular interactions or abnormalities therein are directly involved in the translation from mutations in mechanical junctions to electrical abnormalities. Further studies are needed to increase our understanding of ID development and function.

References

1. Engelmann TW. Über die leitung der erregung im herzmuskel. *Pflugers Arch*. 1875;11:465-480
2. Weidmann S. The electrical constants of purkinje fibers. *Journal of Physiology*. 1952;118:348-360
3. Söstrand FS, Andersson E. Electron microscopy of the intercalated disk of cardiac muscle. *Experientia*. 1954;10:369-370
4. van Breemen VL. Intercalated disks in heart muscle studied with the electron microscope. *Anat Rec*. 1953;117:49-63
5. Barr L, Dewey MM, Berger W. Propagation of action potentials and the structure of the nexus in cardiac muscle. *Journal of General Physiology*. 1965;48:797-823
6. Thiene G, Nava A, Corrado D, Rossi L, Pennelli N. Right ventricular cardiomyopathy and sudden death in young people. *N Engl J Med*. 1988;318:129-133
7. Corrado D, Basso C, Thiene G, McKenna WJ, Davies MJ, Fontaliran F, Nava A, Silvestri F, Blomstrom-Lundqvist C, Wlodarska EK, Fontaine G, Camerini F. Spectrum of clinicopathologic manifestations of arrhythmogenic right ventricular cardiomyopathy/dysplasia: A multicenter study. *J Am Coll Cardiol*. 1997;30:1512-1520
8. Tepass U, Truong K, Godt D, Ikura M, Peifer M. Cadherins in embryonic and neural morphogenesis. *Nat Rev Mol Cell Biol*. 2000;1:91-100
9. Ferreira-Cornwell MC, Luo Y, Narula N, Lenox JM, Lieberman M, Radice GL. Remodeling the intercalated disk leads to cardiomyopathy in mice misexpressing cadherins in the heart. *J Cell Sci*. 2002;115:1623-1634
10. Niessen CM. Tight junctions/adherens junctions: Basic structure and function. *J Invest Dermatol*. 2007;127:2525-2532
11. Farquhar MG, Palade GE. Junctional complexes in various epithelia. *J Cell Biol*. 1963;17:375-412
12. Odland GF. The fine structure of the interrelationship of cells in the human epidermis. *J Biophys Biochem Cytol*. 1958;4:529-538
13. Rayns DG, Simpson FO, Ledingham JM. Ultrastructure of desmosomes in mammalian intercalated disk; appearances after lanthanum treatment. *J Cell Biol*. 1969;42:322-326
14. Garrod D, Chidgey M. Desmosome structure, composition and function. *Biochim Biophys Acta*. 2008;1778:572-587
15. Elfgang C, Eckert R, Lichtenberg-Fraté H, Butterweck A, Traub O, Klein RA, Hülser DF, Willecke K. Specific permeability and selective formation of gap junction channels in connexin-transfected hela cells. *Journal of Cell Biology*. 1995;129:805-817
16. Kumar NM, Gilula NB. The gap junction communication channel. *Cell*. 1996;84:381-388
17. Willecke K, Eiberger J, Degen J, Eckardt D, Romualdi A, Guldenagel M, Deutsch U, Sohl G. Structural and functional diversity of connexin

genes in the mouse and human genome. *Biol Chem.* 2002;383:725-737
18. Bernstein SA, Morley GE. Gap junctions and propagation of the cardiac action potential. *Adv Cardiol.* 2006;42:71-85
19. Unwin PNT, Ennis PD. Two configurations of a channel-forming membrane protein. *Nature.* 1984;307:609-612
20. Makowski L, Caspar DL, Phillips WC, Goodenough DA. Gap junction structures. Ii. Analysis of the x-ray diffraction data. *J Cell Biol.* 1977;74:629-645
21. Sohl G, Willecke K. Gap junctions and the connexin protein family. *Cardiovasc Res.* 2004;62:228-232
22. Perkins G, Goodenough D, Sosinsky G. Three-dimensional structure of the gap junction connexon. *Biophys J.* 1997;72:533-544
23. Beyer EC, Paul DL, Goodenough DA. Connexin43: A protein from rat heart homologous to a gap junction protein from liver. *Journal of Cell Biology.* 1987;105:2621-2629
24. Yancey SB, John SA, Lal R, Austin BJ, Revel JP. The 43-kd polypeptide of heart gap juctions: Immunolocalization (i), topology (ii), and functional domains (iii). *Journal of Cell Biology.* 1989;108:2241-2254
25. Van Kempen MJA, Vermeulen JLM, Moorman AFM, Gros D, Paul DL, Lamers WH. Developmental changes of connexin40 and connexin43 mrna distribution patterns in the rat heart. *cardiovascular research.* 1996;32:886-900
26. Hoyt RH, Cohen ML, Saffitz JE. Distribution and three-dimensional structure of intercellular junctions in canine myocardium. *Circ Res.* 1989;64:563-574
27. Severs NJ. The cardiac gap junction and intercalated disk. *Int J Cardiol.* 1990;26:137-173
28. Severs NJ. Gap junction shape and orientation at the cardiac intercalated disk. *Circ Res.* 1989;65:1458-1462
29. Thiene G, Corrado D, Basso C. Arrhythmogenic right ventricular cardiomyopathy/dysplasia. *Orphanet J Rare Dis.* 2007;2:45
30. Marcus FI, Fontaine GH, Guiraudon G, Frank R, Laurenceau JL, Malergue C, Grosgogeat Y. Right ventricular dysplasia: A report of 24 adult cases. *Circulation.* 1982;65:384-398
31. Nava A, Thiene G, Canciani B, Scognamiglio R, Daliento L, Buja G, Martini B, Stritoni P, Fasoli G. Familial occurrence of right ventricular dysplasia: A study involving nine families. *J Am Coll Cardiol.* 1988;12:1222-1228
32. Rampazzo A, Nava A, Malacrida S, Beffagna G, Bauce B, Rossi V, Zimbello R, Simionati B, Basso C, Thiene G, Towbin JA, Danieli GA. Mutation in human desmoplakin domain binding to plakoglobin causes a dominant form of arrhythmogenic right ventricular cardiomyopathy. *Am J Hum Genet.* 2002;71:1200-1206
33. Asimaki A, Syrris P, Wichter T, Matthias P, Saffitz JE, McKenna WJ. A novel dominant mutation in plakoglobin causes arrhythmogenic right ventricular cardiomyopathy. *Am J Hum Genet.* 2007;81:964-973

34. Gerull B, Heuser A, Wichter T, Paul M, Basson CT, McDermott DA, Lerman BB, Markowitz SM, Ellinor PT, MacRae CA, Peters S, Grossmann KS, Drenckhahn J, Michely B, Sasse-Klaassen S, Birchmeier W, Dietz R, Breithardt G, Schulze-Bahr E, Thierfelder L. Mutations in the desmosomal protein plakophilin-2 are common in arrhythmogenic right ventricular cardiomyopathy. *Nat Genet*. 2004;36:1162-1164
35. van Tintelen JP, Entius MM, Bhuiyan ZA, Jongbloed R, Wiesfeld AC, Wilde AA, van der Smagt J, Boven LG, Mannens MM, van Langen IM, Hofstra RM, Otterspoor LC, Doevendans PA, Rodriguez LM, van Gelder IC, Hauer RN. Plakophilin-2 mutations are the major determinant of familial arrhythmogenic right ventricular dysplasia/cardiomyopathy. *Circulation*. 2006;113:1650-1658
36. Heuser A, Plovie ER, Ellinor PT, Grossmann KS, Shin JT, Wichter T, Basson CT, Lerman BB, Sasse-Klaassen S, Thierfelder L, MacRae CA, Gerull B. Mutant desmocollin-2 causes arrhythmogenic right ventricular cardiomyopathy. *Am J Hum Genet*. 2006;79:1081-1088
37. Syrris P, Ward D, Evans A, Asimaki A, Gandjbakhch E, Sen-Chowdhry S, McKenna WJ. Arrhythmogenic right ventricular dysplasia/cardiomyopathy associated with mutations in the desmosomal gene desmocollin-2. *Am J Hum Genet*. 2006;79:978-984
38. Pilichou K, Nava A, Basso C, Beffagna G, Bauce B, Lorenzon A, Frigo G, Vettori A, Valente M, Towbin J, Thiene G, Danieli GA, Rampazzo A. Mutations in desmoglein-2 gene are associated with arrhythmogenic right ventricular cardiomyopathy. *Circulation*. 2006;113:1171-1179
39. Tandri H, Asimaki A, Dalal D, Saffitz JE, Halushka MK, Calkins H. Gap junction remodeling in a case of arrhythmogenic right ventricular dysplasia due to plakophilin-2 mutation. *J Cardiovasc Electrophysiol*. 2008
40. Fidler LM, Wilson GJ, Liu F, Cui X, Scherer SW, Taylor GP, Hamilton RM. Abnormal connexin43 in arrhythmogenic right ventricular cardiomyopathy caused by plakophilin-2 mutations. *J Cell Mol Med*. 2008
41. Oxford EM, Everitt M, Coombs W, Fox PR, Kraus M, Gelzer AR, Saffitz J, Taffet SM, Moise NS, Delmar M. Molecular composition of the intercalated disk in a spontaneous canine animal model of arrhythmogenic right ventricular dysplasia/cardiomyopathy. *Heart Rhythm*. 2007;4:1196-1205
42. Basso C, Fox PR, Meurs KM, Towbin JA, Spier AW, Calabrese F, Maron BJ, Thiene G. Arrhythmogenic right ventricular cardiomyopathy causing sudden cardiac death in boxer dogs: A new animal model of human disease. *Circulation*. 2004;109:1180-1185
43. Angst BD, Khan LU, Severs NJ, Whitely K, Rothery S, Thompson RP, Magee AI, Gourdie RG. Dissociated spatial patterning of gap junctions and cell adhesion junctions during postnatal differentiation of ventricular myocardium. *Circ Res*. 1997;80:88-94
44. Kostin S, Hein S, Bauer EP, Schaper J. Spatiotemporal development

and distribution of intercellular junctions in adult rat cardiomyocytes in culture. *Circ Res.* 1999;85:154-167

45. Peters NS, Severs NJ, Rothery SM, Lincoln C, Yacoub MH, Green CR. Spatiotemporal relation between gap junctions and fascia adherens junctions during postnatal development of human ventricular myocardium. *Circulation.* 1994;90:713-725
46. Matsushita T, Oyamada M, Fujimoto K, Yasuda Y, Masuda S, Wada Y, Oka T, Takamatsu T. Remodeling of cell-cell and cell-extracellular matrix interactions at the border zone of rat myocardial infarcts. *Circ Res.* 1999;85:1046-1055
47. Zhuang J, Yamada KA, Saffitz JE, Kleber AG. Pulsatile stretch remodels cell-to-cell communication in cultured myocytes. *Circ Res.* 2000;87:316-322
48. Yamada K, Green KG, Samarel AM, Saffitz JE. Distinct pathways regulate expression of cardiac electrical and mechanical junction proteins in response to stretch. *Circ Res.* 2005;97:346-353
49. Li J, Patel VV, Radice GL. Dysregulation of cell adhesion proteins and cardiac arrhythmogenesis. *Clin Med Res.* 2006;4:42-52
50. Takeichi M. Morphogenetic roles of classic cadherins. *Curr Opin Cell Biol.* 1995;7:619-627
51. Giepmans BN. Gap junctions and connexin-interacting proteins. *Cardiovasc Res.* 2004;62:233-245
52. Radice GL, Rayburn H, Matsunami H, Knudsen KA, Takeichi M, Hynes RO. Developmental defects in mouse embryos lacking n-cadherin. *Dev Biol.* 1997;181:64-78
53. Li J, Patel VV, Kostetskii I, Xiong Y, Chu AF, Jacobson JT, Yu C, Morley GE, Molkentin JD, Radice GL. Cardiac-specific loss of n-cadherin leads to alteration in connexins with conduction slowing and arrhythmogenesis. *Circ Res.* 2005;97:474-481
54. Kostetskii I, Li J, Xiong Y, Zhou R, Ferrari VA, Patel VV, Molkentin JD, Radice GL. Induced deletion of the n-cadherin gene in the heart leads to dissolution of the intercalated disk structure. *Circ Res.* 2005;-96:346-354
55. Li J, Levin MD, Xiong Y, Petrenko N, Patel VV, Radice GL. N-cadherin haploinsufficiency affects cardiac gap junctions and arrhythmic susceptibility. *J Mol Cell Cardiol.* 2008;44:597-606
56. Stokes DL. Desmosomes from a structural perspective. *Curr Opin Cell Biol.* 2007;19:565-571
57. Grossmann KS, Grund C, Huelsken J, Behrend M, Erdmann B, Franke WW, Birchmeier W. Requirement of plakophilin 2 for heart morphogenesis and cardiac junction formation. *J Cell Biol.* 2004;167:149-160
58. Pieperhoff S, Schumacher H, Franke WW. The area composita of adhering junctions connecting heart muscle cells of vertebrates. V. The importance of plakophilin-2 demonstrated by small interference rna-mediated knockdown in cultured rat cardiomyocytes. *Eur J Cell Biol.* 2008;87:399-411

59. Oxford EM, Musa H, Maass K, Coombs W, Taffet SM, Delmar M. Connexin43 remodeling caused by inhibition of plakophilin-2 expression in cardiac cells. *Circ Res.* 2007;101:703-711
60. Bierkamp C, McLaughlin KJ, Schwarz H, Huber O, Kemler R. Embryonic heart and skin defects in mice lacking plakoglobin. *Dev Biol.* 1996;180:780-785
61. Ruiz P, Brinkmann V, Ledermann B, Behrend M, Grund C, Thalhammer C, Vogel F, Birchmeier C, Gunthert U, Franke WW, Birchmeier W. Targeted mutation of plakoglobin in mice reveals essential functions of desmosomes in the embryonic heart. *J Cell Biol.* 1996;135:215-225
62. Kirchhof P, Fabritz L, Zwiener M, Witt H, Schafers M, Zellerhoff S, Paul M, Athai T, Hiller KH, Baba HA, Breithardt G, Ruiz P, Wichter T, Levkau B. Age- and training-dependent development of arrhythmogenic right ventricular cardiomyopathy in heterozygous plakoglobin-deficient mice. *Circulation.* 2006;114:1799-1806
63. Protonotarios N, Tsatsopoulou A, Patsourakos P, Alexopoulos D, Gezerlis P, Simitsis S, Scampardonis G. Cardiac abnormalities in familial palmoplantar keratosis. *Br Heart J.* 1986;56:321-326
64. Kaplan SR, Gard JJ, Protonotarios N, Tsatsopoulou A, Spiliopoulou C, Anastasakis A, Squarcioni CP, McKenna WJ, Thiene G, Basso C, Brousse N, Fontaine G, Saffitz JE. Remodeling of myocyte gap junctions in arrhythmogenic right ventricular cardiomyopathy due to a deletion in plakoglobin (naxos disease). *Heart Rhythm.* 2004;1:3-11
65. Yang Z, Bowles NE, Scherer SE, Taylor MD, Kearney DL, Ge S, Nadvoretskiy VV, DeFreitas G, Carabello B, Brandon LI, Godsel LM, Green KJ, Saffitz JE, Li H, Danieli GA, Calkins H, Marcus F, Towbin JA. Desmosomal dysfunction due to mutations in desmoplakin causes arrhythmogenic right ventricular dysplasia/cardiomyopathy. *Circ Res.* 2006;99:646-655
66. Kaplan SR, Gard JJ, Carvajal-Huerta L, Ruiz-Cabezas JC, Thiene G, Saffitz JE. Structural and molecular pathology of the heart in carvajal syndrome. *Cardiovasc Pathol.* 2004;13:26-32
67. Tsatsopoulou AA, Protonotarios NI, McKenna WJ. Arrhythmogenic right ventricular dysplasia, a cell adhesion cardiomyopathy: Insights into disease pathogenesis from preliminary genotype–phenotype assessment. *Heart.* 2006;92:1720-1723
68. Thornell L, Carlsson L, Li Z, Mericskay M, Paulin D. Null mutation in the desmin gene gives rise to a cardiomyopathy. *J Mol Cell Cardiol.* 1997;29:2107-2124
69. Milner DJ, Taffet GE, Wang X, Pham T, Tamura T, Hartley C, Gerdes AM, Capetanaki Y. The absence of desmin leads to cardiomyocyte hypertrophy and cardiac dilation with compromised systolic function. *J Mol Cell Cardiol.* 1999;31:2063-2076
70. Gard JJ, Yamada K, Green KG, Eloff BC, Rosenbaum DS, Wang X, Robbins J, Schuessler RB, Yamada KA, Saffitz JE. Remodeling of gap junctions and slow conduction in a mouse model of desmin-related car-

diomyopathy. *Cardiovasc Res.* 2005;67:539-547
71. Toyofuku T, Yabuki M, Otsu K, Kuzuya T, Hori M, Tada M. Direct association of the gap junction protein connexin-43 with zo-1 in cardiac myocytes. *J Biol Chem.* 1998;273:12725-12731
72. Laing JG, Saffitz JE, Steinberg TH, Yamada KA. Diminished zonula occludens-1 expression in the failing human heart. *Cardiovasc Pathol.* 2007;16:159-164
73. Barker RJ, Price RL, Gourdie RG. Increased association of zo-1 with connexin43 during remodeling of cardiac gap junctions. *Circ Res.* 2002;90:317-324
74. Saffitz JE, Green KG, Kraft WJ, Schechtman KB, Yamada KA. Effects of diminished expression of connexin43 on gap junction number and size in ventricular myocardium. *Am J Physiol Heart Circ Physiol.* 2000;278:H1662-1670
75. Gutstein DE, Liu FY, Meyers MB, Choo A, Fishman GI. The organization of adherens junctions and desmosomes at the cardiac intercalated disk is independent of gap junctions. *J Cell Sci.* 2003;116:875-885
76. Paznekas WA, Boyadjiev SA, Shapiro RE, Daniels O, Wollnik B, Keegan CE, Innis JW, Dinulos MB, Christian C, Hannibal MC, Jabs EW. Connexin 43 (gja1) mutations cause the pleiotropic phenotype of oculodentodigital dysplasia. *Am J Hum Genet.* 2003;72:408-418
77. van Steensel MA, Spruijt L, van der Burgt I, Bladergroen RS, Vermeer M, Steijlen PM, van Geel M. A 2-bp deletion in the gja1 gene is associated with oculo-dento-digital dysplasia with palmoplantar keratoderma. *Am J Med Genet A.* 2005;132A:171-174
78. Kelly SC, Ratajczak P, Keller M, Purcell SM, Griffin T, Richard G. A novel gja 1 mutation in oculo-dento-digital dysplasia with curly hair and hyperkeratosis. *Eur J Dermatol.* 2006;16:241-245
79. Manias JL, Plante I, Gong XQ, Shao Q, Churko J, Bai D, Laird DW. Fate of connexin43 in cardiac tissue harbouring a disease-linked connexin43 mutant. *Cardiovasc Res.* 2008;80:385-395
80. Ehler E, Horowits R, Zuppinger C, Price RL, Perriard E, Leu M, Caroni P, Sussman M, Eppenberger HM, Perriard JC. Alterations at the intercalated disk associated with the absence of muscle lim protein. *J Cell Biol.* 2001;153:763-772
81. Wang X, Gerdes AM. Chronic pressure overload cardiac hypertrophy and failure in guinea pigs: Iii. Intercalated disk remodeling. *J Mol Cell Cardiol.* 1999;31:333-343
82. Severs NJ, Bruce AF, Dupont E, Rothery S. Remodelling of gap junctions and connexin expression in diseased myocardium. *Cardiovasc Res.* 2008;80:9-19
83. Kanno S, Saffitz JE. The role of myocardial gap junctions in electrical conduction and arrhythmogenesis. *Cardiovasc Pathol.* 2001;10:169-177
84. Saffitz JE, Kleber AG. Effects of mechanical forces and mediators of hypertrophy on remodeling of gap junctions in the heart. *Circ Res.* 2004;94:585-591

85. Wiegerinck RF, van Veen TA, Belterman CN, Schumacher CA, Noorman M, de Bakker JM, Coronel R. Transmural dispersion of refractoriness and conduction velocity is associated with heterogeneously reduced connexin43 in a rabbit model of heart failure. *Heart Rhythm.* 2008;5:1178-1185
86. Akar FG, Spragg DD, Tunin RS, Kass DA, Tomaselli GF. Mechanisms underlying conduction slowing and arrhythmogenesis in nonischemic dilated cardiomyopathy. *Circ Res.* 2004;95:717-725
87. Kostin S, Dammer S, Hein S, Klovekorn WP, Bauer EP, Schaper J. Connexin 43 expression and distribution in compensated and decompensated cardiac hypertrophy in patients with aortic stenosis. *Cardiovasc Res.* 2004;62:426-436
88. Sharov VG, Todor AV, Sabbah HN. Left ventricular histomorphometric findings in dogs with heart failure treated with the acorn cardiac support device. *Heart Fail Rev.* 2005;10:141-147
89. Uzzaman M, Honjo H, Takagishi Y, Emdad L, Magee AI, Severs NJ, Kodama I. Remodeling of gap junctional coupling in hypertrophied right ventricles of rats with monocrotaline-induced pulmonary hypertension. *Circ Res.* 2000;86:871-878
90. Kostin S. Zonula occludens-1 and connexin 43 expression in the failing human heart. *J Cell Mol Med.* 2007;11:892-895
91. Bruce AF, Rothery S, Dupont E, Severs NJ. Gap junction remodelling in human heart failure is associated with increased interaction of connexin43 with zo-1. *Cardiovasc Res.* 2008;77:757-765

CHAPTER 3

Reduced heterogeneous expression of Cx43 results in decreased $Na_V1.5$ expression and reduced sodium current which accounts for arrhythmia vulnerability in conditional Cx43 knockout mice

John A Jansen[1*], Maartje Noorman[1,2*], Hassan Musa[3], Mèra Stein[4], Sanne de Jong[1], Roel van der Nagel[1], Thomas J Hund[5], Peter J Mohler[6], Marc A Vos[1], Toon AB van Veen[1], Jacques MT de Bakker[2], Mario Delmar[7], Harold VM van Rijen[1]

1. Department of Medical Physiology, University Medical Center Utrecht, Utrecht, The Netherlands
2. Interuniversity Cardiology Institute of The Netherlands, Utrecht, The Netherlands
3. Center for Arrhythmia Research, Department of Internal Medicine, University of Michigan, Ann Arbor, MI, USA
4. Department of Cardiology, University Medical Center Utrecht, Utrecht, The Netherlands
5. Dorothy M. Davis Heart and Lung Research Institute, Departments of Biomedical Engineering and Internal Medicine, Ohio State University Medical Center, Columbus, OH, USA
6. Dorothy M. Davis Heart and Lung Research Institute, Departments of Internal Medicine and Physiology, Ohio State University Medical Center, Columbus, OH, USA
7. The Leon H Charney Division of Cardiology, New York University School of Medicine, New York, NY, USA

* *These authors contributed equally to this work*

Heart Rhythm 2012

Abstract

Background - Reduced Connexin43 (Cx43), sodium channel ($Na_V1.5$) expression and increased collagen expression (fibrosis) are important determinants of impulse conduction in the heart.
Objective - To study the importance and interaction of these factors at very low Cx43 expression, inducible Cx43 KO mice with and without inducible ventricular tachycardia (VT) were compared by electrophysiology and immunohistochemistry.
Methods - $Cx43^{CreER(T)/fl}$ mice were induced with Tamoxifen and sacrificed after 2 weeks. Epicardial activation mapping was performed on Langendorff-perfused hearts, and arrhythmia vulnerability was tested. Mice were subdivided in VT+ (n=13) and VT- (n=10) and heart tissue was analyzed for Cx43, $Na_V1.5$ and fibrosis.
Results - VT+ mice had decreased Cx43 expression with increased global, but not local, heterogeneity of Cx43, compared to VT- mice. $Na_V1.5$-immunoreactive protein expression was reduced in VT+ versus VT- mice, specifically at sites devoid of Cx43. Levels of fibrosis were similar between VT- and VT+ mice. QRS-duration was increased and epicardial activation was more dispersed in VT+ mice than in VT- mice. The effective refractory period (ERP) was similar between both groups. Premature stimulation resulted in a more severe conduction slowing in VT+ compared to VT- hearts in the right ventricle. Separate patch clamp experiments in isolated rat ventricular myocytes confirmed that loss of Cx43 expression correlated with decreased sodium current amplitude.
Conclusions - Global heterogeneity in Cx43 expression and concomitant heterogeneous downregulation of sodium channel protein expression and sodium current leads to slowed and dispersed conduction, which sensitizes the heart for ventricular arrhythmias.

Introduction

A reduced expression of the main ventricular gap junction protein in the heart, Connexin43 (Cx43), is commonly found in a variety of cardiac pathologies, such as ischemia, hypertrophy and heart failure.[1, 2] The loss of Cx43, together with increased collagen deposition[3, 4] and a decreased expression of the cardiac sodium channel $Na_V1.5$,[5, 6] are thought to impair proper conduction of the electrical impulse, increasing the risk for fatal ventricular arrhythmias.[7] Besides a decreased expression, a more inhomogeneous distribution of Cx43 has been found in remodeled hearts, resulting in a more dispersed conduction, which is also correlated with an increased susceptibility for arrhythmias.[8-11]

Previous studies have shown that a 50% reduction in Cx43 expression mice did not affect impulse conduction.[12, 13] However, further reduced Cx43 levels by conditional deletion of the Cx43 gene to <5%, resulted in a high vulnerability for arrhythmias due to slowed and dispersed conduction.[13, 14] It was then proposed,[13] as shown in a genetic model of heterogeneous Cx43 expression,[8] that decreased and heterogeneous expression of Cx43 protein levels allowed for the occurrence of ventricular arrhythmias.

Despite the fact that genetic tools allow for specific down-regulation of Cx43, recent studies have shown that the intercalated disk is a highly dynamic structure with interaction between the different proteins that are located at the disk and that determine impulse conduction. A regulatory mechanism for $Na_V1.5$ was shown to be localized at the intercalated disk, and $Na_V1.5$ and Cx43 can be co-immunoprecipitated, suggesting an interaction at the level of the intercalated disk.[15, 16] Furthermore, in vitro experiments on cultured cardiomyocytes have shown that loss of Plakophilin-2 results in both Cx43 remodeling and decreased sodium current (I_{Na}).[17-19] These studies point to a close relationship between Cx43 and $Na_V1.5$, suggesting that proper expression and functioning of one protein is essential for the other.

In the present study, we focused on the factors that are responsible for the vulnerability to arrhythmias in mice with very low (<5%) Cx43 expression. We hypothesized that specifically in arrhythmogenic animals, extremely low expression levels of Cx43 can be found, with regions completely devoid of Cx43, resulting in slow and dispersed conduction. Secondly, given the interactions between Cx43 and the voltage gated sodium channel complex,[19] we speculated that diminished Cx43 protein levels may affect the abundance, distribution and/or function of $Na_V1.5$ in these animals, further contributing to conduc-

tion disturbances. For this purpose, we subdivided Tamoxifen-induced $Cx43^{Cre\text{-}ER(T)/fl}$ mice into arrhythmogenic (VT+) and non-arrhythmogenic (VT-) animals, and compared conduction parameters and tissue characteristics. Our data show that VT+ mice have a more severe reduction in Cx43 protein levels compared to VT- mice, which is accompanied by a global, but not local, heterogeneity in Cx43 expression. Furthermore, the abundance of the $Na_V1.5$-immunoreactive protein was reduced in VT+ compared to VT- mice, whereas collagen content was similar. Separate studies showed that loss of Cx43 expression led to a decrease in the amplitude of I_{Na} in adult rat ventricular myocytes. Together, these combined changes resulted in dispersed conduction and severe conduction slowing during premature stimulation, making the heart highly prone to arrhythmias.

Materials and Methods

Animals

$Cx43^{Cre\text{-}ER(T)/fl}$ (n=17) mice were generated as described previously[13] and injected intraperitonally with 3-4mg Tamoxifen (Sigma), dissolved in 100μl plant oil for 5 consecutive days. Electrophysiological experiments were performed 13-15 days after the first injection. Extended analysis of previous data (n=15) on similar Tamoxifen-induced $Cx43^{Cre\text{-}ER(T)/fl}$ mice, were included in this study.[13] Animal experiments were performed in accordance with institutional guidelines for animal use in research.

Preparation of the Hearts and Ventricular Conduction

Mice were anesthetized by 2.5% isoflurane in oxygen. A 3-lead electrocardiogram was recorded and analyzed off-line as described previously.[20] Afterwards, the heart was excised, prepared and connected to a Langendorff perfusion setup as described previously.[21-23] The hearts were continuously perfused with carbogen-gassed buffer of 37°C, composed of (in mmol/L): NaCl 116, KCl 5, $MgSO_4$ 1.1, NaH_2PO_4 0.35, $NaHCO_3$ 27, glucose 10, mannitol 16 and $CaCl_2$ 1.8.

Extracellular electrograms were recorded using a 247-point multiterminal electrode (19x13 grid, 0.3-mm spacing) of both the left and right ventricle of the heart as described previously.[21] Recordings were made during stimulation (1ms pulse duration, 2x diastolic stimulation threshold) from the center of the grid at a basic cycle length (BCL) of

120ms. The effective refractory period (ERP), the longest coupling interval of the premature stimulus that failed to activate the entire heart, was determined for each ventricle separately as described previously.[24] If spontaneous arrhythmias were absent, susceptibility for arrhythmias was provoked by programmed stimulation in the following sequence. First, 16 basic stimuli followed by 1 or 3 premature stimuli 5ms longer than the locally determined ERP were applied. Next, if 1 or 3 premature stimuli failed to induce arrhythmias, 2-second burst pacing at the shortest possible cycle length was applied. Arrhythmias in mice were classified as sustained (>15 complexes followed stimulation), according to Lambeth Conventions.[25]

Data Analysis

The moment of maximal negative dV/dt in the unipolar electrograms was selected as the time of local activation and determined with custom written software based on MatLab (2006, The MathWorks Inc., Natrick, MA).[26] Activation times were used to construct activation maps. Conduction velocities parallel (CV_L) and perpendicular (CV_T) to fiber orientation were determined from activation maps generated from BCL-pacing. Activation times of at least 4 consecutive electrode terminals along lines perpendicular to intersecting isochronal lines were used to calculate CVs. Anisotropic ratio was defined as CV_L/CV_T. Dispersion of conduction was assessed for both LV and RV using the method described by Lammers et al.[27]

Statistics

Two-group comparisons were performed using an unpaired t-test. A Fisher exact test was performed to compare gender-distribution. Ranked pictures of $Na_V1.5$ expression were compared using a Wilcoxon Rank Sum test. Values are given as mean±SEM. $P \leq 0.05$ was considered as statistically significant. Data were analyzed using SPSS 17.0 (2008, SPSS Inc, Chicago, IL) software.

Immunohistochemistry and Histology

After electrophysiological measurements, hearts were rapidly frozen in liquid nitrogen and stored at -80ºC. Coronal (4-chamber view) sections with a thickness of 10ìm were taken from different levels of the hearts. Sections were double immuno-labeled with a rabbit polyclonal antibody against Cx43 (1:250, Zymed, Invitrogen) or $Na_V1.5$ (1:100;

see [28]) and a mouse monoclonal antibody against N-cadherin (1:800, Sigma, Aldrich). Afterwards, sections were incubated with FITC-conjugated anti rabbit whole IgG and Texas Red-conjugated anti mouse whole IgG, mounted in Vectashield (Vector Laboratories) and examined with a classic light microscope with epifluorescence equipment (Nikon Optiphot-2). To evaluate the presence of fibrosis, sections were fixed with 4% paraformaldehyde (in PBS, 30 minutes at room temperature), stained with Picrosirius Red and examined by light microscopy.

The amount of fibrosis and Cx43 immuno-signals were determined in at least 5 hearts of each group. At least 8 randomly chosen pictures of both LV and RV of each heart were analyzed at 200x magnification. Blinded operators calculated Cx43 expression as percentage of the total tissue using Image J 1.43u (2010, NIH, Bethesda, MD). Photomicrographs were transformed into RGB (i.e. Red Green Blue) stack, and true Cx43 pixels were defined in the 256-leveled green channel using a minimal cut-off level of 50. For fibrosis quantification, a comparable procedure was used, but now the range between 90 and 190 in the red channel was defined as true fibrotic tissue.

Heterogeneity of Cx43 expression was determined using MatLab. Photographs were transformed into 8-bit white (Cx43) and black (background) pictures and a background subtraction with a rolling ball radius of 250 was performed. Each picture was subdivided in 140 equal squares and total intensity of the white-signal was measured for each square. Afterwards, the mean intensity of the squares and the standard deviation of the intensity among the squares were determined for each photograph separately. Micro heterogeneity, a relative value for the local heterogeneity in Cx43 expression, was defined as the standard deviation divided by the mean. An average value of all pictures of one ventricle of a heart was calculated.

To determine global heterogeneity of Cx43 expression, we determined the intensity of the total picture and measured the average intensity and the standard deviation among these intensities of all pictures of each ventricle of the heart. This macro heterogeneity was defined as this standard deviation divided by the average intensity of the pictures.

For $Na_V1.5$ quantification, at least 5 hearts of both groups were used. Of each heart, 3-5 randomly taken pictures were analyzed. Three blinded observers individually ranked all 45 pictures from high to low expression. Statistical analysis was performed on every ranking separately.

Determination of sodium current properties in Cx43-knockdown (Cx43-KD) cells.

Adult rat ventricular myocytes were isolated and cultured using standard procedures.[18] siRNA for Cx43, or a non-targeting construct, were transfected into isolated myocytes using a commercially available kit (Dharmafect; see [19]). Efficiency rof Cx43-KD was determined for each experiment by comparing Cx43 abundance (by Western blot) in cells isolated and cultured in parallel to those used for the patch clamp studies. I_{Na} was recorded by conventional single-electrode patch clamp in the whole-cell configuration. All recordings were obtained three days after the cells were presented to the siRNA (or control) constructs. Protocols for Cx43 immunoblot, and for determination of I_{Na}, were as previously published.[18, 19]

Results

Arrhythmogeneity

We analyzed 32 Tamoxifen-induced $Cx43^{Cre\text{-}ER(T)/fl}$ mice, of which 9 died within 2 weeks after induction. Of the remaining 23 mice, 13 mice were susceptible to arrhythmias during Langendorff perfusion (57%). Five mice showed spontaneous arrhythmias and in 8 other hearts, arrhythmias were induced by either premature stimulation or burst pacing (Figure 3.1C). The majority of arrhythmias (10 out of 13) were sustained (>15 complexes followed stimulation). The other arrhythmias were non-sustained (~8 complexes followed stimulation, 1 heart) or premature beats (2 hearts). In the remaining 10 Tamoxifen-induced $Cx43^{Cre\text{-}ER(T)/fl}$ mice, no arrhythmias could be induced.

Figure 3.1A shows a typical example of a spontaneous started polymorphic ventricular tachycardia. The activation maps of this pVT (lower panels) show irregular activation patterns. In contrast, epicardial electrograms of an induced arrhythmia in another heart showed a monomorphic ventricular tachycardia, with comparable activation patterns of consecutive beats (Figure 3.1B).

Ventricular conduction

Mice were divided in arrhythmogenic (13 mice, VT+) and non-arrhythmogenic (10 mice, VT-) animals to determine factors that are associated with the susceptibility for arrhythmias. No differences in

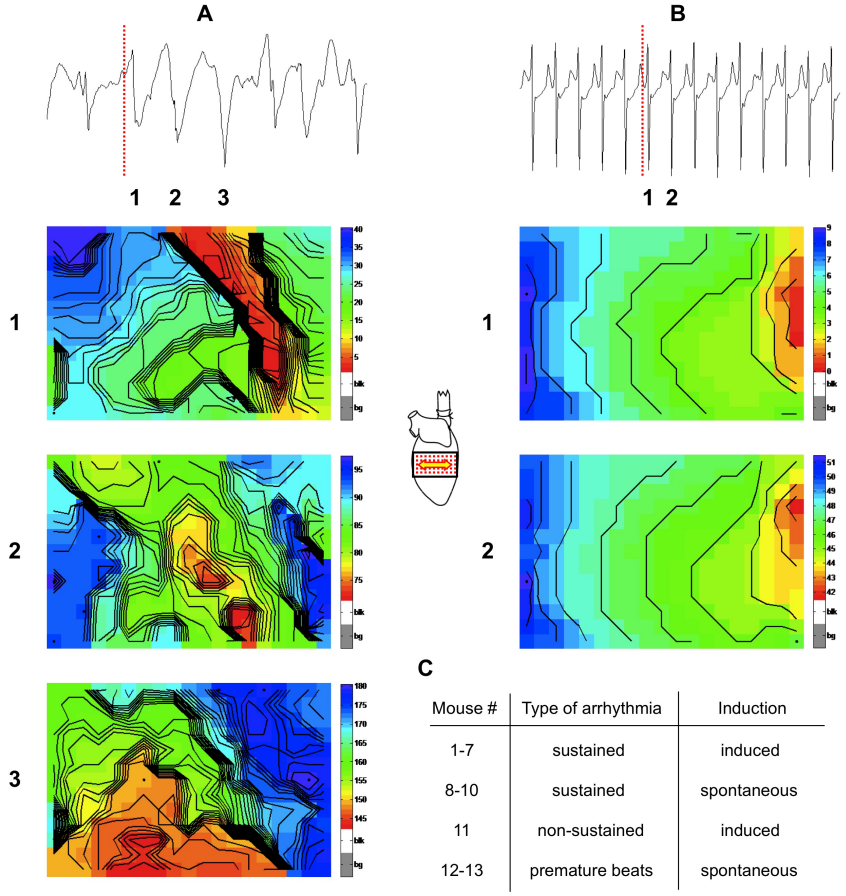

Mouse #	Type of arrhythmia	Induction
1-7	sustained	induced
8-10	sustained	spontaneous
11	non-sustained	induced
12-13	premature beats	spontaneous

Figure 3.1 – *Ventricular tachycardias.* Panel A shows an epicardial electrogram (upper panel) of a sustained polymorphic tachycardia. The corresponding activation maps of the 3 numbered consecutive beats are presented below, showing irregular activation patterns. The upper panel in B shows an epicardial electrogram of a sustained monomorphic tachycardia, with comparable activation maps of 2 consecutive beats (lower panels). The yellow arrow in the schematics of the heart indicates fiber direction. Colors indicate areas activated within the same time interval and are similar for each map of one arrhythmia. Lines are isochronal lines at distances of 1ms. The red dotted lines correspond to t=0 in the activation maps. Panel C overviews the induction and type of arrhythmia of individual susceptible mice.

induction-time, heart weight / body weight (HW/BW) ratio or gender distribution were found between the two groups (Table 3.1).

QRS-duration was higher in VT+ compared to VT- mice (15.4±1.1

Table 3.1 – Induction-time, heart weight / body weight ratio, gender and electrophysiology

	VT– (n = 10)	VT+ (n = 13)
Induction-time (days)	13.8 ± 0.6	13.5 ± 0.3
HW/BW (%)	0.72 ± 0.03	0.77 ± 0.14
Male (%)	60	38
Arrhythmias (%)	0	100
LV CVL (cm/s)	54.6 ± 4.3	45.7 ± 7.1
RV CVL (cm/s)	47.2 ± 4.2	40.9±6.2
LV CVT (cm/s)	26.1 ± 2.1	21.1±1.6
RV CVT (cm/s)	27.7 ± 1.6	22.5 ± 2.8
LV AR (CVL/CVT)	2.11 ± 0.08	2.23 ± 0.22
RV AR (CVL/CVT)	1.72 ± 0.13	1.82 ± 0.15
LV CV Disp Index	1.41 ± 0.15	1.90 ± 0.19
RV CV Disp Index	1.41 ± 0.17	2.31 ± 0.36 *
LV ERP (ms)	70.0 ± 10.1	75.6 ± 7.3
RV ERP (ms)	47.0 ± 3.4	46.1 ± 4.1
QRS-duration (ms)	12.1 ± 0.3	15.4 ± 1.1 *
LV CVL extra (cm/s)	41.0 ± 4.4	34.4 ± 6.7
RV CVL extra (cm/s)	39.1 ± 6.2	22.2 ± 2.1 *
LV CVT extra (cm/s)	22.0 ± 2.5	17.1 ± 2.1
RV CVT extra (cm/s)	21.6 ± 2.4	13.4 ± 1.1 *
LV AR extra	1.88 ± 0.06	1.92 ± 0.20
RV AR extra	1.75 ± 0.18	1.64 ± 0.05

VT–, Cx43Cre-ER(T)/fl mice without arrhythmias; VT+, Cx43Cre-ER(T)/fl mice with arrhythmias; induction-time, time from start Tamoxifen-induction to Langendorff experiments; HW/BW, heart weight / body weight ratio; LV, left ventricle; RV, right ventricle; CVL, longitudinal conduction velocity; CVT, transversal conduction velocity; AR, anisotropic ratio; CV Disp, dispersion of conduction velocity; ERP, effective refractory period. Values are ± SEM.
* $p<0.05$ vs VT–.

ms vs 12.1±0.3 ms respectively, Table 3.1). The left panel in Figure 3.2 shows representative epicardial activation maps of $Cx43^{Cre\text{-}ER(T)/fl}$ VT- and VT+ hearts of both LV and RV during stimulation at a BCL of 120ms. Stimulation from the center of the grid resulted in anisotropic activation patterns determined by the fiber direction. No significant differences in impulse conduction velocity longitudinal (CV_L) and trans-

verse (CV_T) to the fiber orientation were found between the groups, although conduction was generally somewhat slowed in VT+ compared to VT-. Concomitantly, the anisotropic ratio (CV_L/CV_T) in LV and RV were not different between both groups (Table 3.1). However, VT+ hearts showed regions with crowding of isochrones, indicative of local conduction slowing. Therefore, we determined the dispersion of conduction index.[27] We found higher values of dispersion in VT+ compared to VT- mice, which was significant in RV with a near-significant similar trend in LV (p=0.058).

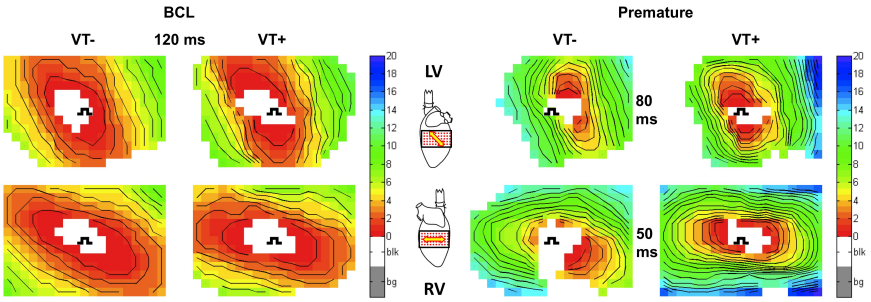

Figure 3.2 – *Activation maps.* Typical epicardial activation patterns of LV (upper panels) and RV (lower panels) of $Cx43^{Cre\text{-}ER(T)/fl}$ mice without (VT-) and with (VT+) arrhythmias during BCL (120ms, left panels) or premature stimulation (ERP+5ms, right panels). The pacing site is shown in the center of each activation map, resulting in anisotropic conduction. The yellow arrows in the schematics of the heart indicate fiber direction. Colors indicate areas activated within the same time interval and are similar for each map. Lines are isochronal lines at distances of 1ms.

The right panel in Figure 3.2 shows epicardial activation after premature stimulation (ERP+5ms). Conduction slowing both longitudinal and transverse to the fiber direction was more prominent in VT+ compared to VT- hearts, which was significant for CV_L and CV_T in RV (Table 3.1). The effective refractory period (ERP) was similar in both LV and RV for $Cx43^{Cre\text{-}ER(T)/fl}$ hearts VT- and VT+ (Table 3.1).

Cx43 expression and heterogeneity

Figure 3.3 shows typical examples of Cx43-immunolabeled sections of Tamoxifen-induced $Cx43^{Cre\text{-}ER(T)/fl}$ VT- and VT+ hearts. As expected, Tamoxifen-induction resulted in a very low Cx43 expression in both LV and RV, while N-cadherin (a highly stable component of the adherens

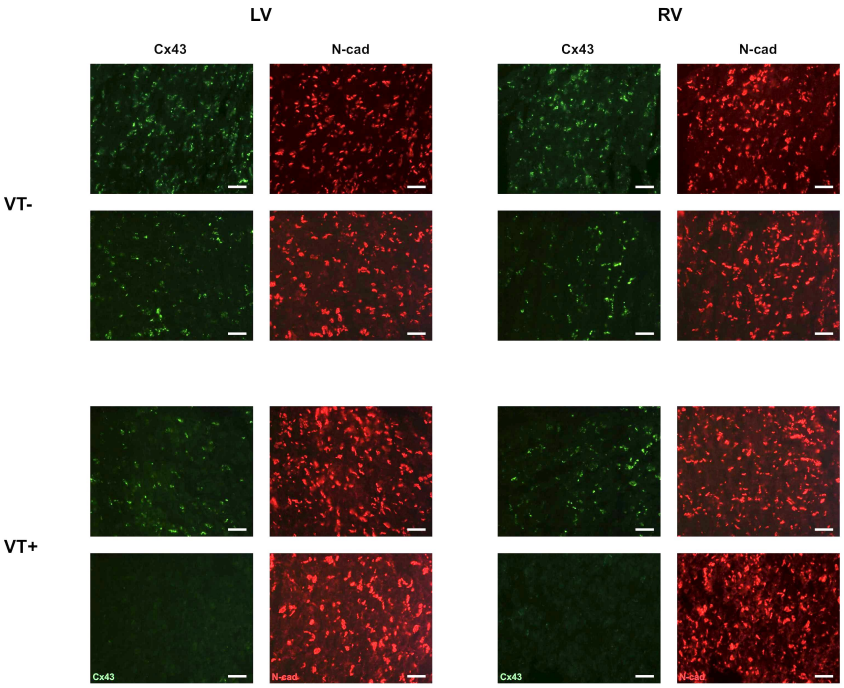

Figure 3.3 – *Cx43 expression and heterogeneity.* Typical pictures of Cx43 expression with corresponding N-cadherin staining of LV (left panels) and RV (right panels) of $Cx43^{Cre\text{-}ER(T)/fl}$ mice without (VT-) and with (VT+) arrhythmias. Whereas Cx43 expression is present throughout the hearts of VT- mice, regions completely devoid of Cx43 can be found in VT+ hearts (lower panels). Bars represent 50μm.

junction in the ID) was still abundantly present at the intercalated disks. Whereas Cx43 was detectible throughout the ventricles in VT- mice, large areas in VT+ hearts showed a complete depletion of Cx43 expression (lower panels VT+ in Figure 3.3), with some local spots, positive for Cx43 (upper panels VT+ in Figure 3.3). As a result, total Cx43-immunosignal was decreased in VT+ compared to VT- hearts in both LV and RV (Table 3.2).

Next, we checked whether expression of Cx43 was more inhomogeneous in VT+ compared to VT- hearts. We first analyzed local Cx43 heterogeneity by quantifying intensity differences in Cx43 expression within pictures. Table 3.2 shows that this micro heterogeneity of Cx43 expression was similar between VT+ and VT- hearts in both LV and RV. However, macro heterogeneity of Cx43 expression, which quanti-

Table 3.2 – Tissue characteristics

	VT–	VT+
Cx43-exp LV (%)	0.25 ± 0.06	0.05 ± 0.04 *
Cx43-exp RV (%)	0.22 ± 0.07	0.03 ± 0.02 *
Cx43-het micro LV	0.39 ± 0.02	0.38 ± 0.03
Cx43-het micro RV	0.43 ± 0.03	0.43 ± 0.03
Cx43-het macro LV	0.22 ± 0.03	0.34 ± 0.03 *
Cx43-het macro RV	0.22 ± 0.03	0.34 ± 0.03 *
Nav1.5-exp (rank obs. #1)	15.48	30.86 **
Nav1.5-exp (rank obs. #2)	15.96	30.36 **
Nav1.5-exp (rank obs. #3)	15.70	30.64 **
Fibrosis LV (%)	0.48 ± 0.12	0.51 ± 0.13
Fibrosis RV (%)	0.54 ± 0.09	0.49 ± 0.04

Cx43-exp, Cx43 expression; Cx43-het, Cx43 heterogeneity; Nav1.5-exp, Nav1.5 expression; rank obs. #1, average rank of observer 1; VT–, Cx43Cre-ER(T)/fl mice without arrhythmias; VT+, Cx43Cre-ER(T)/fl mice with arrhythmias. Values are ± SEM.
* $p<0.05$ vs VT–
** $p<0.005$ vs VT–

fies the differences among regions of one complete ventricle of a heart, was significantly increased in both LV and RV in VT+ compared to VT- hearts (Table 3.2).

$Na_V1.5$ expression and fibrosis

We further analyzed the cardiac tissue on other determinants of conduction, and stained for the cardiac sodium channel $Na_V1.5$. As can be appreciated from Figure 3.4A, the intensity of the $Na_V1.5$ immmunoreactive signal was reduced in VT+ compared to VT- hearts, while N-cadherin staining was comparable. To quantify these differences, three blinded observers ranked all pictures from high to low expression, and three independent Wilcoxon Rank Sum tests were performed. Table 3.2 shows that the average rank of pictures of VT- hearts was significantly higher compared to pictures of VT+ hearts for all observers ($p<0.001$ for each individual ranking, average ranking of the three observers was 15.71±0.14 vs 30.62±0.14, respectively), showing quantitatively that $Na_V1.5$ expression was decreased in VT+ compared to VT- hearts.

To identify the possible correlation between heterogeneous Cx43

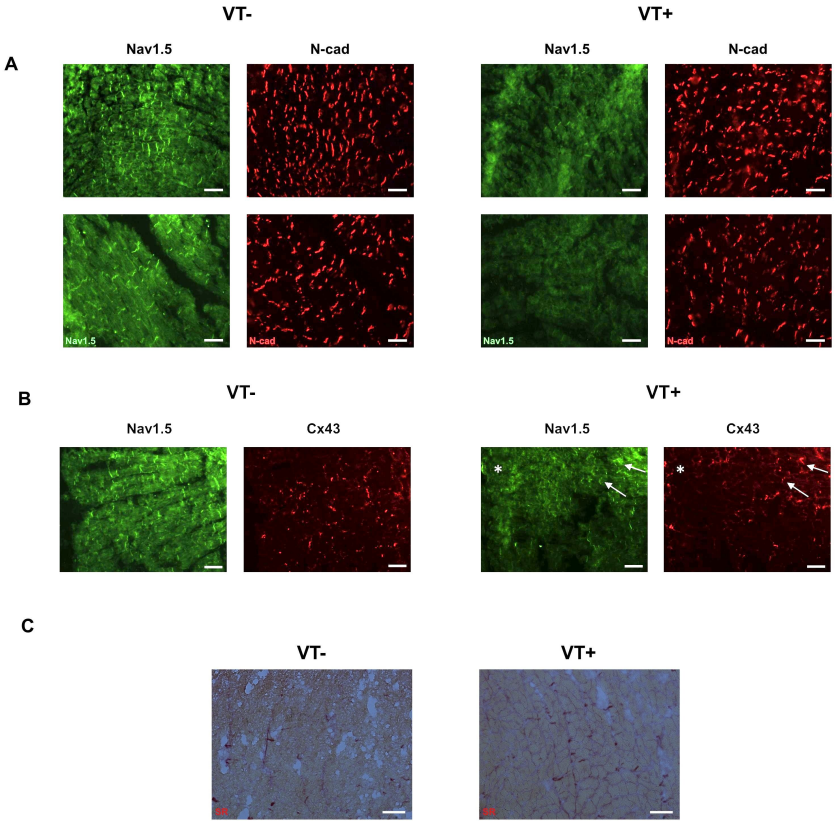

Figure 3.4 – *$Na_V1.5$ expression and fibrosis.* Panel A shows typical pictures of $Na_V1.5$ expression with corresponding N-cadherin staining of $Cx43^{Cre\text{-}ER(T)/fl}$ mice without (VT-) and with (VT+) arrhythmias. Panel B shows a double labeling for both Cx43 and $Na_V1.5$ of $Cx43^{Cre\text{-}ER(T)/fl}$ mice without (VT-) and with (VT+) arrhythmias. The arrows in the pictures of VT+ mice indicate regions of co-localization of Cx43 and $Na_V1.5$, whereas the asterisk points to a region of co-decrease. Typical pictures of Picrosirius Red staining of $Cx43^{Cre\text{-}ER(T)/fl}$ mice without (VT-) and with (VT+) arrhythmias are shown in panel C. Bars represent 50μm.

and $Na_V1.5$ expression, we performed a double labeling for both proteins. As shown in Figure 3.4B, staining for both Cx43 and $Na_V1.5$ was quite homogeneous in VT-, whereas in VT+ hearts, heterogeneous expression of Cx43 colocalized with heterogeneous expression of $Na_V1.5$. In regions positive for Cx43 expression, $Na_V1.5$ expression was present as well (arrows), while in regions devoid of Cx43, $Na_V1.5$ expression

was also absent (asterisk).

Finally, we determined the presence of fibrosis by histochemical analysis with Picrosirius Red staining. Figure 3.4C shows low amounts of interstitial collagen in both VT- and VT+ hearts. Quantification revealed no significant differences in collagen content between VT- and VT+ hearts (Table 3.2).

Sodium current in Cx43-deficient cardiac ventricular myocytes

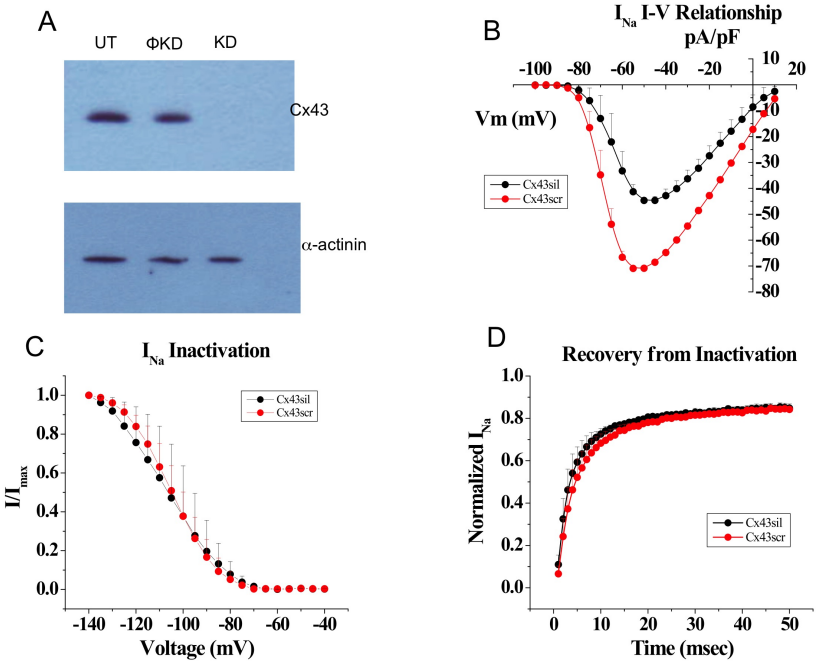

Figure 3.5 – *Decreased Cx43 expression and I_{Na} in isolated adult rat ventricular myocytes.* Panel A: Western blot for Cx43 in cells that were untreated (UNT), treated with an oligonucleotide targeting Cx43 expression (KD) or a non-targeting construct ϕKD. Sodium current parameters were measured in the latter two cell populations, using standard single-electrode patch clamp methods. Panel B: Peak sodium current density was decreased in cells lacking Cx43 (black dots and lines; labeled "Cx43sil") when compared to cells treated with the non-targeting construct (red lines and symbols; labeled "Cx43scr"). Panels C and D: Loss of Cx43 expression did not affect steady-state inactivation (C) or recovery from inactivation (D) kinetics.

The experiments described above led us to characterize sodium cur-

rent properties in Cx43-deficient cells. Isolated, adult rat ventricular myocytes were exposed to siRNA for Cx43 (Cx43-KD) or to a non-silencing construct (Cx43-ϕKD). As shown in Figure 3.5A, siRNA treatment caused a decrease in Cx43 abundance to near zero levels. As shown in Figure 3.5B, loss of Cx43 expression led to a significant decrease in the average peak sodium current density. Yet, voltage dependence of inactivation (Figure 3.5C), and time course of reactivation (Figure 3.5D), were not affected by the loss of Cx43 expression. Overall, these results support the notion of a cross-talk between Cx43 expression, and the level of functional sodium current in cardiac myocytes.

Discussion

The main finding of this study is that in the background of very low (~5%) Cx43 levels, differences in tissue characteristics determine arrhythmia susceptibility in individual mice: severely reduced Cx43 protein levels with large regions of total depletion of Cx43, leading to global, but not local, heterogeneity of Cx43 expression. In regions devoid of Cx43 expression, the expression of $Na_V1.5$ was absent as well. Separate experiments showed that loss of Cx43 expression leads to a decrease in the amplitude of I_{Na}, recorded from isolated ventricular myocytes. These data suggest that heterogeneous and combined downregulation of Cx43 and $Na_V1.5$ lead to slowed and dispersed conduction which results in an increased propensity to ventricular arrhythmias.

Cx43 expression and heterogeneity

The very low Cx43 expression levels in $Cx43^{CreER(T)/fl}$ mice after Tamoxifen-induction are in agreement with previous studies.[13, 29] Here we showed that VT+ mice have decreased Cx43 protein levels compared to VT- mice, indicating that the actual reduction in Cx43 expression is an important arrhythmogenic factor. With regard to conduction reserve, which is defined as 'the ability of the heart to maintain near normal impulse conduction velocity in the background of moderate changes in tissue characteristics (up to a ~50% reduction in Cx43 or $Na_V1.5$, or a small increase in collagen content (~3 times increase))', this might have important implications.[30] Several studies have shown that when this conduction reserve is reduced, the heart becomes susceptible for arrhythmias.[24, 31] Although conduction was considerably slowed in VT- mice compared to mice with normal Cx43 expression

($Cx43^{fl/fl}$ mice) arrhythmias were absent.[13] Noteworthy, we found that the further reduction in Cx43 expression in VT+ mice was accompanied by an increased heterogeneity of Cx43. From our data we cannot determine whether the extremely low total Cx43 expression levels, or the global heterogeneity, with regions of total depletion of Cx43, is the main arrhythmogenic factor. Concerning this vulnerability to arrhythmias, it is likely that also the concomitantly decreased expression of the cardiac sodium channel $Na_V1.5$ plays a role. Interestingly, we previously showed that a combined 50% decrease of both Cx43 and $Na_V1.5$ did not increase arrhythmia susceptibility.[32] Apparently, a moderate reduction in both proteins did not exceed conduction reserve. However, a reduced $Na_V1.5$ expression combined with the extremely low levels of Cx43 as found in VT+ mice in this study, presumably makes the heart highly vulnerable to arrhythmias.

In remodeled hearts, reduced Cx43 levels are generally accompanied by an increased heterogeneity of Cx43 expression.[1, 2] We and others have shown that arrhythmogeneity is highly associated with a heterogeneous distribution of Cx43, both in mice and in patients.[8-11] Therefore, we thoroughly analyzed Cx43 heterogeneity in this study by distinguishing local from global inhomogeneity. We calculated micro heterogeneity as a measure for local heterogeneity of Cx43 expression, which quantified differences in Cx43 intensity within a small region of the heart. Interestingly, we found no differences in this micro heterogeneity between VT- and VT+ mice. In contrast, macro heterogeneity calculated variations in Cx43 intensities among different regions of the heart, which was significantly increased in VT+ compared to VT- mice. This indicates that in our study, global, rather than local, heterogeneity is associated with arrhythmia vulnerability. This implies that the large areas in which Cx43 is totally depleted (lowest pictures Figure 3.3) significantly contribute to the formation of an arrhythmogenic substrate.

$Na_V1.5$ expression and fibrosis

Besides gap junctional coupling between cardiomyocytes, impulse conduction in the heart is also dependent on the expression and function of the cardiac sodium channel $Na_V1.5$, and the tissue architecture, mainly determined by the amount of collagen. Therefore, we stained for $Na_V1.5$ and found a reduced expression in VT+ compared to VT- mice. This raised the important question whether this reduction in $Na_V1.5$ is a direct consequence of the very low Cx43 protein levels. This question was addressed by co-labeling Cx43 and $Na_V1.5$ and showed that regions

devoid of Cx43 were characterized by absence of $Na_V1.5$, while regions with Cx43 labeling also showed $Na_V1.5$ labeling. This indicates that reduction of Cx43 is connected to reduction of $Na_V1.5$ expression. Previous studies have shown that Cx43 and $Na_V1.5$ are both present in the intercalated disk, and that destabilization of the desmosome by a loss of Plakophillin-2 results in Cx43 remodeling as well as a decreased functioning of $Na_V1.5$.[15, 17, 18] We have also shown that stressing mice with reduced or mutated $Na_V1.5$ by aging or pressure overload resulted in a decreased expression of Cx43.[33, 34] These studies show a close relation between those proteins, which suggest that the depletion of Cx43, as found in large areas throughout the hearts of VT+ mice, may directly affect the function and/or abundance of $Na_V1.5$. On the other hand, Johnson et al showed that in isolated neonatal cardiomyocytes from Cx43 null mice, $Na_V1.5$ expression and function was unaffected[35]. We have directly shown in this study that downregulation of Cx43 leads to reduction of sodium current. However, the consequences of Cx43 depletion in isolated cells may differ from the effects in an intact heart i.e. by stretch on the cardiomyocytes. Besides, the effects of silencing of Cx43 in a developmentally established system, as described in this study, may differ from the implications of Cx43-depletion during development. Additional research is required to prove a direct link between the decreased Cx43 and $Na_V1.5$ levels in VT+ mice.

Because fibrosis is an important parameter for impulse conduction, we checked whether extremely low levels of Cx43 would also increase fibroblast activity, leading to increased collagen deposition. However, we found only low levels of interstitial fibrosis, which was similar in VT- and VT+ mice, indicating that fibrosis did not play a role in determining arrhythmia vulnerability in this study.

Impulse conduction

ECG analysis and epicardial activation mapping was performed on VT+ and VT- hearts to determine the electrical effects of the heterogeneous reduction in Cx43 and decreased $Na_V1.5$ expression. We found a significant increased QRS-duration in VT+ compared to VT- mice, although epicardial conduction during Langendorff-perfusion was not significantly slowed during S1S1 pacing. However, we showed that conduction was more dispersed (only significant for RV) in VT+ compared to VT- mice. It is likely that the global heterogeneity of Cx43 expression is mainly responsible for this dispersed conduction: conduction is slowed in the regions of Cx43-depletion, whereas it is relatively nor-

mal in parts that express Cx43. Challenging the hearts by premature stimulation resulted in a more severe conduction slowing in VT+ than in VT- hearts (only significant for RV). The decreased $Na_V1.5$ availability in VT+ mice could play a fundamental role, since the upstroke velocity of the action potential is restricted by the number of active $Na_V1.5$ channels, which is particularly crucial during premature stimulation. The slow impulse conduction during premature stimulation in VT+ mice enables the induction of ventricular tachycardias. Interestingly, we found no differences in ERP between VT- and VT+ mice, indicating that arrhythmia vulnerability was not caused by alterations in refractoriness.

Study limitations

In this study we used different methods to quantify Cx43 and $Na_V1.5$ expression. Because of the relatively high background staining in $Na_V1.5$ labeled sections, we could not apply a standardized method by Image J. Therefore, pictures were ranked by 3 blinded observers and statistically analyzed by a Wilcoxon Ranked Sum Test. The variance among the observers was very low, and statistical analysis of all 3 individual tests showed a significant difference between VT+ and VT- mice, indicating a very high reliability of this quantification.

Conclusion

In conclusion we have shown that in the background of very low Cx43 levels, arrhythmogenic mice have a more severe reduction in Cx43 with global, but not local, heterogeneity of Cx43 expression. In regions with depletion of Cx43, $Na_V1.5$ expression was also absent, which is presumably caused by direct interaction at the intercalated disk and leads to reduction of sodium current. This results in slowed and dispersed conduction, which allows for the occurrence of ventricular arrhythmias.

References

1. Peters NS. New insights into myocardial arrhythmogenesis: Distribution of gap-junctional coupling in normal, ischaemic and hypertrophied human hearts. *Clin Sci (Lond).* 1996;90:447-452
2. Kostin S, Rieger M, Dammer S, Hein S, Richter M, Klovekorn WP, Bauer EP, Schaper J. Gap junction remodeling and altered connexin43 expression in the failing human heart. *Mol Cell Biochem.* 2003;242:135-144
3. La Vecchia L, Ometto R, Bedogni F, Finocchi G, Mosele GM, Bozzola L, Bevilacqua P, Vincenzi M. Ventricular late potentials, interstitial fibrosis, and right ventricular function in patients with ventricular tachycardia and normal left ventricular function. *Am J Cardiol.* 1998;81:790-792
4. Kawara T, Derksen R, de Groot JR, Coronel R, Tasseron S, Linnenbank AC, Hauer RN, Kirkels H, Janse MJ, de Bakker JM. Activation delay after premature stimulation in chronically diseased human myocardium relates to the architecture of interstitial fibrosis. *Circulation.* 2001;104:3069-3075
5. Borlak J, Thum T. Hallmarks of ion channel gene expression in end-stage heart failure. *FASEB J.* 2003;17:1592-1608
6. Valdivia CR, Chu WW, Pu J, Foell JD, Haworth RA, Wolff MR, Kamp TJ, Makielski JC. Increased late sodium current in myocytes from a canine heart failure model and from failing human heart. *J Mol Cell Cardiol.* 2005;38:475-483
7. Kleber AG, Rudy Y. Basic mechanisms of cardiac impulse propagation and associated arrhythmias. *Physiol Rev.* 2004;84:431-488
8. Gutstein DE, Morley GE, Vaidya D, Liu F, Chen FL, Stuhlmann H, Fishman GI. Heterogeneous expression of gap junction channels in the heart leads to conduction defects and ventricular dysfunction. *Circulation.* 2001;104:1194-1199
9. Kitamura H, Ohnishi Y, Yoshida A, Okajima K, Azumi H, Ishida A, Galeano EJ, Kubo S, Hayashi Y, Itoh H, Yokoyama M. Heterogeneous loss of connexin43 protein in nonischemic dilated cardiomyopathy with ventricular tachycardia. *J Cardiovasc Electrophysiol.* 2002;13:865-870
10. Cabo C, Yao J, Boyden PA, Chen S, Hussain W, Duffy HS, Ciaccio EJ, Peters NS, Wit AL. Heterogeneous gap junction remodeling in reentrant circuits in the epicardial border zone of the healing canine infarct. *Cardiovasc Res.* 2006;72:241-249
11. Boulaksil M, Winckels SK, Engelen MA, Stein M, van Veen TA, Jansen JA, Linnenbank AC, Bierhuizen MF, Groenewegen WA, van Oosterhout MF, Kirkels JH, de Jonge N, Varro A, Vos MA, de Bakker JM, van Rijen HV. Heterogeneous connexin43 distribution in heart failure is associated with dispersed conduction and enhanced susceptibility to ventricular arrhythmias. *Eur J Heart Fail.* 2010;12:913-921

12. Morley GE, Vaidya D, Samie FH, Lo C, Delmar M, Jalife J. Characterization of conduction in the ventricles of normal and heterozygous cx43 knockout mice using optical mapping. *J Cardiovasc Electrophysiol*. 1999;10:1361-1375
13. van Rijen HV, Eckardt D, Degen J, Theis M, Ott T, Willecke K, Jongsma HJ, Opthof T, de Bakker JM. Slow conduction and enhanced anisotropy increase the opensity for ventricular tachyarrhythmias in adult mice with induced deletion of connexin43. *Circulation*. 2004;109:-1048-1055
14. Gutstein DE, Morley GE, Tamaddon H, Vaidya D, Schneider MD, Chen J, Chien KR, Stuhlmann H, Fishman GI. Conduction slowing and sudden arrhythmic death in mice with cardiac-restricted inactivation of connexin43. *Circ Res*. 2001;88:333-339
15. Petitprez S, Zmoos AF, Ogrodnik J, Balse E, Raad N, El-Haou S, Albesa M, Bittihn P, Luther S, Lehnart SE, Hatem SN, Coulombe A, Abriel H. Sap97 and dystrophin macromolecular complexes determine two pools of cardiac sodium channels $Na_v1.5$ in cardiomyocytes. *Circ Res*. 2011;108:294-304
16. Malhotra JD, Thyagarajan V, Chen C, Isom LL. Tyrosine-phosphorylated and nonphosphorylated sodium channel beta1 subunits are differentially localized in cardiac myocytes. *J Biol Chem*. 2004;279:40748-40754
17. Oxford EM, Musa H, Maass K, Coombs W, Taffet SM, Delmar M. Connexin43 remodeling caused by inhibition of plakophilin-2 expression in cardiac cells. *Circ Res*. 2007;101:703-711
18. Sato PY, Musa H, Coombs W, Guerrero-Serna G, Patino GA, Taffet SM, Isom LL, Delmar M. Loss of plakophilin-2 expression leads to decreased sodium current and slower conduction velocity in cultured cardiac myocytes. *Circ Res*. 2009;105:523-526
19. Sato PY, Coombs W, Lin X, Nekrasova O, Green KJ, Isom LL, Taffet SM, Delmar M. Interactions between ankyrin-g, plakophilin-2, and connexin43 at the cardiac intercalated disk. *Circ Res*. 2011;109:193-201
20. Royer A, van Veen TA, Le Bouter S, Marionneau C, Griol-Charhbili V, Leoni AL, Steenman M, van Rijen HV, Demolombe S, Goddard CA, Richer C, Escoubet B, Jarry-Guichard T, Colledge WH, Gros D, de Bakker JM, Grace AA, Escande D, Charpentier F. Mouse model of scn5a-linked hereditary lenegre's disease: Age-related conduction slowing and myocardial fibrosis. *Circulation*. 2005;111:1738-1746
21. van Rijen HV, van Veen TA, van Kempen MJ, Wilms-Schopman FJ, Potse M, Krueger O, Willecke K, Opthof T, Jongsma HJ, de Bakker JM. Impaired conduction in the bundle branches of mouse hearts lacking the gap junction protein connexin40. *Circulation*. 2001;103:1591-1598
22. van Veen TA, van Rijen HV, Wiegerinck RF, Opthof T, Colbert MC, Clement S, de Bakker JM, Jongsma HJ. Remodeling of gap junctions in mouse hearts hypertrophied by forced retinoic acid signaling. *J Mol Cell Cardiol*. 2002;34:1411-1423

23. Alcolea S, Jarry-Guichard T, de Bakker J, Gonzalez D, Lamers W, Coppen S, Barrio L, Jongsma H, Gros D, van Rijen H. Replacement of connexin40 by connexin45 in the mouse: Impact on cardiac electrical conduction. *Circ Res.* 2004;94:100-109
24. Stein M, Noorman M, van Veen TA, Herold E, Engelen MA, Boulaksil M, Antoons G, Jansen JA, van Oosterhout MF, Hauer RN, de Bakker JM, van Rijen HV. Dominant arrhythmia vulnerability of the right ventricle in senescent mice. *Heart Rhythm.* 2008;5:438-448
25. Huggins CE, Bell JR, Pepe S, Delbridge LM. Benchmarking ventricular arrhythmias in the mouse–revisiting the 'lambeth conventions' 20 years on. *Heart Lung Circ.* 2008;17:445-450
26. Potse M, Linnenbank AC, Grimbergen CA. Software design for analysis of multichannel intracardial and body surface electrocardiograms. *Comput Methods Programs Biomed.* 2002;69:225-236
27. Lammers WJ, Schalij MJ, Kirchhof CJ, Allessie MA. Quantification of spatial inhomogeneity in conduction and initiation of reentrant atrial arrhythmias. *Am J Physiol.* 1990;259:H1254-1263
28. Hund TJ, Koval OM, Li J, Wright PJ, Qian L, Snyder JS, Gudmundsson H, Kline CF, Davidson NP, Cardona N, Rasband MN, Anderson ME, Mohler PJ. A beta(iv)-spectrin/camkii signaling complex is essential for membrane excitability in mice. *J Clin Invest.* 2010;120:3508-3519
29. Eckardt D, Theis M, Degen J, Ott T, van Rijen HV, Kirchhoff S, Kim JS, de Bakker JM, Willecke K. Functional role of connexin43 gap junction channels in adult mouse heart assessed by inducible gene deletion. *J Mol Cell Cardiol.* 2004;36:101-110
30. de Bakker JM, van Rijen HM. Continuous and discontinuous propagation in heart muscle. *J Cardiovasc Electrophysiol.* 2006;17:567-573
31. Noorman M, van Rijen HV, van Veen TA, de Bakker JM, Stein M. Differences in distribution of fibrosis in the ventricles underlie dominant arrhythmia vulnerability of the right ventricle in senescent mice. *Neth Heart J.* 2008;16:356-358
32. Stein M, van Veen TA, Remme CA, Boulaksil M, Noorman M, van Stuijvenberg L, van der Nagel R, Bezzina CR, Hauer RN, de Bakker JM, van Rijen HV. Combined reduction of intercellular coupling and membrane excitability differentially affects transverse and longitudinal cardiac conduction. *Cardiovasc Res.* 2009;83:52-60
33. van Veen TA, Stein M, Royer A, Le Quang K, Charpentier F, Colledge WH, Huang CL, Wilders R, Grace AA, Escande D, de Bakker JM, van Rijen HV. Impaired impulse propagation in scn5a-knockout mice: Combined contribution of excitability, connexin expression, and tissue architecture in relation to aging. *Circulation.* 2005;112:1927-1935
34. Jansen JA, van Veen TA, de Jong S, van der Nagel R, van Stuijvenberg L, Driessen H, Labzowski R, Oefner CM, Bosch AA, Nguyen TQ, Goldschmeding R, Vos MA, de Bakker JM, van Rijen HV. Reduced cx43 expression triggers increased fibrosis due to enhanced fibroblast activity. *Circ Arrhythm Electrophysiol.* 2012

35. Johnson CM, Green KG, Kanter EM, Bou-Abboud E, Saffitz JE, Yamada KA. Voltage-gated na+ channel activity and connexin expression in cx43-deficient cardiac myocytes. *J Cardiovasc Electrophysiol*. 1999;10:1390-1401

CHAPTER 4

Geographical distribution of Plakophilin-2 mutation prevalence in patients with arrhythmogenic cardiomyopathy

Kirolos A Jacob[1,2,*], Maartje Noorman[1,3,*], Moniek GPJ Cox[2,3], Judith A Groeneweg[2,3], Richard NW Hauer[2,3], Marcel AG van der Heyden[1]

1. Department of Medical Physiology, Division Heart & Lungs, University Medical Center Utrecht, Utrecht, The Netherlands
2. Department of Cardiology, Division Heart & Lungs, University Medical Center Utrecht, Utrecht, The Netherlands
3. Interuniversity Cardiology Institute of The Netherlands, Utrecht, The Netherlands

* *These authors contributed equally to this work*

Netherlands Heart Journal 2012

Abstract

Arrhythmogenic cardiomyopathy (AC) is characterised by myocardial fibrofatty tissue infiltration and presents with palpitations, ventricular arrhythmias, syncope and sudden cardiac death. AC is associated with mutations in genes encoding the desmosomal proteins plakophilin-2 (*PKP2*), desmoplakin (*DSP*), desmoglein-2 (*DSG2*), desmocollin-2 (*DSC2*) and junctional plakoglobin (*JUP*).

In the present study we compared 28 studies (2004-2011) on the prevalence of mutations in desmosomal protein encoding genes in relation to geographic distribution of the study population. In most populations, mutations in *PKP2* showed the highest prevalence. Mutation prevalence in *DSP*, *DSG2* and *DSC2* varied among the different geographic regions. Mutations in *JUP* were rarely found, except in Denmark and the Greece/Cyprus region.

Introduction

Arrhythmogenic cardiomyopathy (AC), previously known as arrhythmogenic right ventricular cardiomyopathy or dysplasia (ARVC/D), is a myocardial disease usually with autosomal dominant inheritance and an estimated prevalence of 1:2000 to 1:5000 in the Western world.[1, 2] Based on clinical symptomology, the disease affects men more commonly than women (3:1) and usually becomes manifest between the second and the fourth decade of life. In clinical practice, patients with AC generally manifest with ventricular arrhythmias, palpitations, syncope related to physical exertion, and in a late-stage congestive heart failure. Unfortunately, sudden cardiac death during various daily life activities is the first presentation in 7-23% of affected patients.[3] Histopathologically, the heart of patients with AC shows myocardial cell death and progressive fibrofatty tissue substitution primarily of the right ventricular myocardium, preceding ventricular dilatation.

Cardiac tissue has to withstand high pressures to enable ejection and therefore individual cardiomyocytes are interconnected robustly by desmosomes in the intercalated disks (IDs). IDs, which consist of three multiprotein complexes, *i.e.* adherens junctions, desmosomes and gap junctions, provide mechanical and electrical coupling between cells, and serve as an anchoring site for ion channels.[4, 5] Loss-of-function mutations in five different desmosomal protein encoding genes, plakophilin-2 (*PKP2*), desmoplakin (*DSP*), desmoglein-2 (*DSG2*), desmocollin-2 (*DSC2*) and junctional plakoglobin (*JUP*), have been identified in AC.[6] The prevalence of these mutations might be related to ethnicity, founder mutations or founder populations[7-9] and therefore may be different in geographically distinct populations. For example, as shown by Van der Zwaag et al.[9] 12 index patients carrying the same *PKP2* mutation shared the same haplotype, indicative for a common founder. Geographical distribution of the index patients suggested that the mutation originated in the northern part of The Netherlands.[9] In the present study we describe results from literature on the geographical distribution of mutation prevalence of diagnosed AC patients. Our analysis demonstrates that approximately 46% of AC cases can be correlated with mutations in one or more desmosomal genes. Furthermore, mutations within the *PKP2* gene have the strongest prevalence within the AC population. Finally, some large differences between populations of distinct geographical locations exist.

Table 4.1 – Number of mutations in five desmosomal genes in genetic studies on AC patients of different geographical regions

Geographical region Author/year [ref.#]	Total patients	*PKP2* (%)	*DSP* (%)	*DSG2* (%)	*DSC2* (%)	*JUP* (%)	Patients with mutation (%)
USA							
Dalal et al/2006 [28]	58	25 (43)	n.d.	n.d.	n.d.	n.d.	25 (43)
Awad et al/2006 [21]	33[a]	0 (0)	0 (0)	4 (12)	n.d.	n.d.	4 (12)
Yang et al/2006 [29]	66	n.d.	4 (6)	n.d.	n.d.	n.d.	4 (6)
Den Haan et al/2009 [22]	82	37 (45)	1 (1)	7 (9)	0 (0)	1 (1)	43 (52)
USA/Netherlands							
Kapplinger et al. 2011 [12]	175	88(50)	2(1)	16(9)	4(2)	1(1)	102 (58)
USA/Canada							
Marcus et al/2009 [30]	100[b]	22 (22)					22 (22)
Canada							
Barahona-Dussault et al/2010 [23]	23[c]	7 (30)	1 (4)	1 (4)	3 (13)	0 (0)	10 (43)
Germany/USA							
Gerull et al/2004 [6]	120	32 (27)	n.d.	n.d.	n.d.	n.d.	32 (27)
Heuser et al/2006 [31]	88[d]	0 (0)	n.d.	0 (0)	1 (1)	n.d.	1 (1)
United Kingdom							
Syrris et al/2006 [32]	77[e]	0 (0)	0 (0)	0 (0)	4 (5)	0 (0)	4 (5)
Syrris et al/2006 [33]	100[f]	11 (11)	0 (0)	n.d.	n.d.	0 (0)	11 (11)
Sen-Chowdhry et al/2007 [19]	156	10 (6)	17 (11)	10 (6)	2 (1)	0 (0)	39 (25)
Sen Chowdhry et al/2007 [24]	69	6 (9)	7 (10)	5 (7)	2 (3)	0 (0)	20 (30)
Syrris et al/2007 [34]	86[g]	0 (0)	0 (0)	9 (10)	n.d.	0 (0)	9 (10)
The Netherlands							
Basso et al/2006 [37]	21	3 (14)	3 (14)	4 (19)	n.d.	n.d.	10 (48)
Italy							
Pilichou et al/2006 [20]	80[h]	11 (14)	13 (16)	8 (10)	n.d.	n.d.	32 (40)
Bauce et al/2010 [26]	42	7 (17)	5 (12)	4 (10)	2 (5)	0 (0)	18 (43)
France/Switzerland							
Fressart et al/2010 [17]	135	42 (31)	6 (5)	14 (10)	2 (2)	0 (0)	62 (46)
Greece/Cyprus							
Antoniades et al/2006 [38]	187	16 (9)	n.d.	n.d.	n.d.	26 (14)	42 (22)
Denmark							
Christensen et al/2010 [39]	53	7 (13)	n.d.	n.d.	n.d.	n.d.	7 (13)
Christensen et al/2010 [27]	55	7 (13)	2 (4)	2 (4)	4 (7)	4 (7)	18 (33)
Finland							
Lahtinen et al/2008/2011 [8,40]	29	3 (10)	1 (3)	1 (3)	0 (0)	n.d.	5 (17)
China							
Qiu et al/2009 [41]	18	7 (39)	n.d.	n.d.	n.d.	n.d.	7 (39)
South Africa							
Watkins et al/2009 [7]	36	9 (25)	n.d.	n.d.	n.d.	n.d.	9 (25)

[a]The population was first tested negative for mutations in PKP2 or DSP and then screened for mutations in DSG2. [b]Other desmosomal genes were screened for but not reported. [c]JUP was only tested in patients negative for PKP2, DSP, DSG2 and DSC2 mutations.[e]DSC2 was only tested in patients negative for PKP2, DSP, DSG2 and JUP mutations. [f]PKP2 was only

tested in patients negative for DSP and JUP mutations. [g]DSG2 was only tested in patients negative for PKP2, DSP and JUP mutations. [h]DSG2 was only tested in patients negative for PKP2 and DSP mutations. n.d., not determined. Studies in grey analysed mutations in all five desmosomal genes and data are displayed graphically in Figure 4.2.

PubMed and the Cochrane Library databases were examined using combinations of the following search terms and abbreviations: arrhythmogenic right ventricular dysplasia/cardiomyopathy, prevalence, genetic mutations, mutational analysis, desmosomes, plakophilin-2 (PKP2), desmoplakin (DSP), desmoglein-2 (DSG2), desmocollin-2 (DSC2), and plakoglobin (JUP). We considered only full-length articles in English, published in the 2004-2011 period, which contained a sample size of more than 15 confirmed AC patients, according to the 1994 or 2010 Task Force Criteria (TFC).[10, 11]

Results

Table 4.1 summarises the relevant data from 28 studies, ordered according to the country/region from which the study population was derived. In most studies, potential mutations in *PKP2* were screened for, and in a subset of the studies (from The Netherlands, USA, Canada, United Kingdom, Denmark, Italy and France/Switzerland), patients were screened for all five desmosomal protein encoding genes. After removing double counted patients, necessary since some larger studies used a subset of previous study populations (i.e. Kapplinger et al.[12]) and some studies searched for additional mutations in patients scoring negative for *PKP2* mutation, we observed that of 931 individual patients (probands) screened for, 210 (22.6%) were found to carry a mutation in *PKP2*. When prevalence is ordered based on geographical distribution (Figure 4.1), relatively most *PKP2* mutations were found in The Netherlands, USA and China (39-52%), while rates below 10% were found in the UK and Greece/Cyprus.

When considering the subset of studies that screened for mutations in all AC associated desmosomal genes, i.e. *PKP2*, *DSP*, *DSG2*, *DSC2* and *JUP*, it was found that 46% of the AC patients carried a mutation in one or more of these genes. Figure 4.2 shows the results of mutation prevalence per country/region, again indicating a high prevalence of *PKP2* mutations in USA and The Netherlands while, especially in Italy, Denmark and UK, mutations in other desmosomal protein encoding genes are associated more frequently with the AC phenotype.

Mutation in the desmosomal gene *JUP* is associated with AC rarely, with the exception of Denmark and Greece/Cyprus (Table 4.1).

Discussion

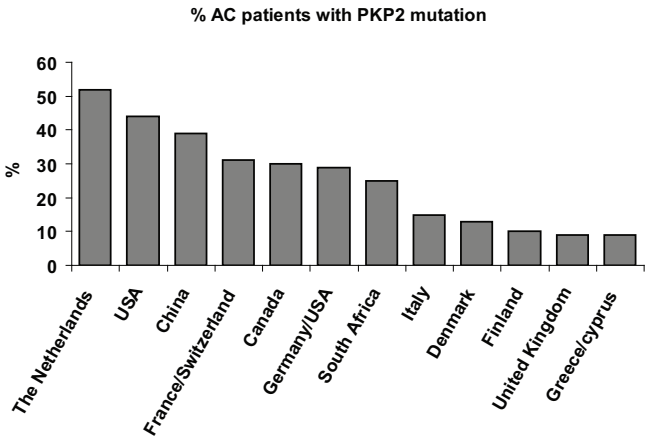

Figure 4.1 – Ranked prevalence of *PKP2* mutations associated with AC in different geographical regions

Our analysis indicates that approximately 46% of the AC cases can be linked to mutations in genes encoding desmosomal proteins. Mutations in 'non-desmosomal' genes coding for transforming growth factor b3[13] and ryanodine receptor,[14] transmembrane protein 43,[15] and the recently identified phospholamban mutation[16] may account in addition for cases of AC. However, the causal effects of transforming growth factor b3 and ryanodine receptor mutations in AC are currently disputed. Screening genes for other structural proteins in the ID, *i.e.* b-catenin, a-T-catenin and PERP, in a Danish population of 55 confirmed AC patients revealed no mutations.[17]

Some regions in our analysis have a large area size (USA, Canada) and/or contain populations from geographically distinct areas (e.g. Germany/USA), although in the latter the USA population is of West-European descent. In other studies, the population was derived from a relatively small region (Padua region, Italy). Therefore, data as presented here may not completely reflect the prevalence of the entire country as regional differences within one country are likely to be found in future. Furthermore, the patient population often included individuals

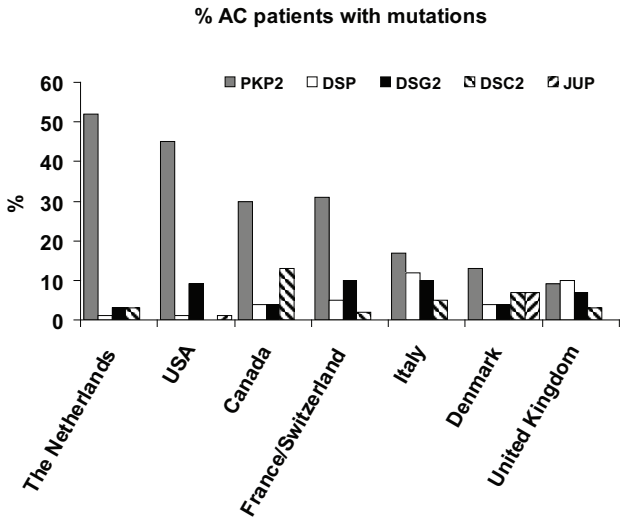

Figure 4.2 – Prevalence of plakophilin-2 (*PKP2*), desmoplakin (*DSP*), desmoglein-2 (*DSG2*), desmocollin-2 (*DSC2*) and junctional plakoglobin (*JUP*) mutations in seven geographic regions

from different origins. For example, Fressart et al.[18] included AC patients from Hispanic, Maghreb and Caribbean origin. Interesting in this respect are the findings of a recent study by Kapplinger et al.,[12] where it was shown that in the control population in the absence of heart disease manifestation, DNA variant prevalence in desmosomal protein encoding genes was approximately threefold lower in Caucasians than in non-Caucasians. However, so-called 'radical mutations' which are most likely associated with an AC phenotype showed a very low prevalence in both Caucasian (0%) and non-Caucasian (0.6%) controls. Finally, radical mutations, defined by the authors as insertions, deletions, splice junction or nonsense mutations, constitute the majority of genetic alterations in so-called mutation-positive AC patients, while many of the missense mutations found in controls and patients most likely have no causal effect with AC.[12]

Another complicating factor in comparing different studies is the use of new criteria in the revised TFC to include patients. For example, Sen-Chowdhry et al.[19] included probands with left ventricular or biventricular cardiomyopathy, which may explain the high prevalence of *DSP* mutations in this study population. However, patients with predominantly left ventricular involvement were often excluded by other authors, due to strict adherence to the TFC defined in 1994.[11] Previous

studies applied different criteria for mutational analysis. For example, Pilichou et al.[20] and Awad et al.[21] sequenced the *DSG2* gene only in patients who did not have *PKP2* or *DSP* mutations. In most new studies, all desmosomal protein encoding genes are screened.[18, 22-27]

When genetic screening is indicated, all desmosomal protein encoding genes should be included. *JUP* is only rarely associated with AC, except in Denmark and the Greece/Cyprus region. In the latter region the high incidence of *JUP* mutations may be due to Naxos disease, a specific condition of AC combined with woolly hair and cutaneous hyperkeratosis.

References

1. Basso C, Corrado D, Marcus FI, Nava A, Thiene G. Arrhythmogenic right ventricular cardiomyopathy. *Lancet*. 2009;373:1289-1300
2. Herren T, Gerber PA, Duru F. Arrhythmogenic right ventricular cardiomyopathy/dysplasia: A not so rare "Disease of the desmosome" With multiple clinical presentations. *Clin Res Cardiol*. 2009;98:141-158
3. Priori SG, Aliot E, Blomstrom-Lundqvist C, Bossaert L, Breithardt G, Brugada P, Camm AJ, Cappato R, Cobbe SM, Di Mario C, Maron BJ, McKenna WJ, Pedersen AK, Ravens U, Schwartz PJ, Trusz-Gluza M, Vardas P, Wellens HJ, Zipes DP. Task force on sudden cardiac death of the european society of cardiology. *Eur Heart J*. 2001;22:1374-1450
4. Noorman M, van der Heyden MA, van Veen TA, Cox MG, Hauer RN, de Bakker JM, van Rijen HV. Cardiac cell-cell junctions in health and disease: Electrical versus mechanical coupling. *J Mol Cell Cardiol*. 2009;47:23-31
5. Cheng L, Yung A, Covarrubias M, Radice GL. Cortactin is required for n-cadherin regulation of kv1.5 channel function. *J Biol Chem*. 2011;286:20478-20489
6. Gerull B, Heuser A, Wichter T, Paul M, Basson CT, McDermott DA, Lerman BB, Markowitz SM, Ellinor PT, MacRae CA, Peters S, Grossmann KS, Drenckhahn J, Michely B, Sasse-Klaassen S, Birchmeier W, Dietz R, Breithardt G, Schulze-Bahr E, Thierfelder L. Mutations in the desmosomal protein plakophilin-2 are common in arrhythmogenic right ventricular cardiomyopathy. *Nat Genet*. 2004;36:1162-1164
7. Watkins DA, Hendricks N, Shaboodien G, Mbele M, Parker M, Vezi BZ, Latib A, Chin A, Little F, Badri M, Moolman-Smook JC, Okreglicki A, Mayosi BM. Clinical features, survival experience, and profile of plakophylin-2 gene mutations in participants of the arrhythmogenic right ventricular cardiomyopathy registry of south africa. *Heart Rhythm*. 2009;6:S10-17
8. Lahtinen AM, Lehtonen E, Marjamaa A, Kaartinen M, Helio T, Porthan K, Oikarinen L, Toivonen L, Swan H, Jula A, Peltonen L, Palotie A, Salomaa V, Kontula K. Population-prevalent desmosomal mutations predisposing to arrhythmogenic right ventricular cardiomyopathy. *Heart Rhythm*. 2011;8:1214-1221
9. van der Zwaag PA, Cox MG, van der Werf C, Wiesfeld AC, Jongbloed JD, Dooijes D, Bikker H, Jongbloed R, Suurmeijer AJ, van den Berg MP, Hofstra RM, Hauer RN, Wilde AA, van Tintelen JP. Recurrent and founder mutations in The Netherlands : Plakophilin-2 p.Arg79x mutation causing arrhythmogenic right ventricular cardiomyopathy/dysplasia. *Neth Heart J*. 2010;18:583-591
10. Marcus FI, McKenna WJ, Sherrill D, Basso C, Bauce B, Bluemke DA, Calkins H, Corrado D, Cox MG, Daubert JP, Fontaine G, Gear K, Hauer R, Nava A, Picard MH, Protonotarios N, Saffitz JE, Sanborn

DM, Steinberg JS, Tandri H, Thiene G, Towbin JA, Tsatsopoulou A, Wichter T, Zareba W. Diagnosis of arrhythmogenic right ventricular cardiomyopathy/dysplasia: Proposed modification of the task force criteria. *Circulation*. 2010;121:1533-1541

11. McKenna WJ, Thiene G, Nava A, Fontaliran F, Blomstrom-Lundqvist C, Fontaine G, Camerini F. Diagnosis of arrhythmogenic right ventricular dysplasia/cardiomyopathy. Task force of the working group myocardial and pericardial disease of the european society of cardiology and of the scientific council on cardiomyopathies of the international society and federation of cardiology. *Br Heart J*. 1994;71:215-218
12. Kapplinger JD, Landstrom AP, Salisbury BA, Callis TE, Pollevick GD, Tester DJ, Cox MG, Bhuiyan Z, Bikker H, Wiesfeld AC, Hauer RN, van Tintelen JP, Jongbloed JD, Calkins H, Judge DP, Wilde AA, Ackerman MJ. Distinguishing arrhythmogenic right ventricular cardiomyopathy/dysplasia-associated mutations from background genetic noise. *J Am Coll Cardiol*. 2011;57:2317-2327
13. Beffagna G, Occhi G, Nava A, Vitiello L, Ditadi A, Basso C, Bauce B, Carraro G, Thiene G, Towbin JA, Danieli GA, Rampazzo A. Regulatory mutations in transforming growth factor-beta3 gene cause arrhythmogenic right ventricular cardiomyopathy type 1. *Cardiovasc Res*. 2005;65:366-373
14. Tiso N, Stephan DA, Nava A, Bagattin A, Devaney JM, Stanchi F, Larderet G, Brahmbhatt B, Brown K, Bauce B, Muriago M, Basso C, Thiene G, Danieli GA, Rampazzo A. Identification of mutations in the cardiac ryanodine receptor gene in families affected with arrhythmogenic right ventricular cardiomyopathy type 2 (arvd2). *Hum Mol Genet*. 2001;10:189-194
15. Merner ND, Hodgkinson KA, Haywood AF, Connors S, French VM, Drenckhahn JD, Kupprion C, Ramadanova K, Thierfelder L, McKenna W, Gallagher B, Morris-Larkin L, Bassett AS, Parfrey PS, Young TL. Arrhythmogenic right ventricular cardiomyopathy type 5 is a fully penetrant, lethal arrhythmic disorder caused by a missense mutation in the tmem43 gene. *Am J Hum Genet*. 2008;82:809-821
16. Groeneweg JA, van der Zwaag PA, van der Werf C, Cox MG, Jongbloed JD, Bezzina CR, Wiesfeld AC, van der Heijden JF, Doevendans PA, Wilde AA, van Tintelen JP, Dooijes D, Hauer R. Revised 2010 task force criteria for arvd/c diagnosis promote inclusion of non-desmosomal mutation carriers. *Circulation*. 2011;124
17. Christensen AH, Benn M, Tybjaerg-Hansen A, Haunso S, Svendsen JH. Screening of three novel candidate genes in arrhythmogenic right ventricular cardiomyopathy. *Genet Test Mol Biomarkers*. 2011;15:267-271
18. Fressart V, Duthoit G, Donal E, Probst V, Deharo JC, Chevalier P, Klug D, Dubourg O, Delacretaz E, Cosnay P, Scanu P, Extramiana F, Keller D, Hidden-Lucet F, Simon F, Bessirard V, Roux-Buisson N, Hebert JL, Azarine A, Casset-Senon D, Rouzet F, Lecarpentier Y,

Fontaine G, Coirault C, Frank R, Hainque B, Charron P. Desmosomal gene analysis in arrhythmogenic right ventricular dysplasia/cardiomyopathy: Spectrum of mutations and clinical impact in practice. *Europace*. 2010;12:861-868

19. Sen-Chowdhry S, Syrris P, Ward D, Asimaki A, Sevdalis E, McKenna WJ. Clinical and genetic characterization of families with arrhythmogenic right ventricular dysplasia/cardio-myopathy provides novel insights into patterns of disease expression. *Circulation*. 2007;115:1710-1720
20. Pilichou K, Nava A, Basso C, Beffagna G, Bauce B, Lorenzon A, Frigo G, Vettori A, Valente M, Towbin J, Thiene G, Danieli GA, Rampazzo A. Mutations in desmoglein-2 gene are associated with arrhythmogenic right ventricular cardiomyopathy. *Circulation*. 2006;113:1171-1179
21. Awad MM, Dalal D, Cho E, Amat-Alarcon N, James C, Tichnell C, Tucker A, Russell SD, Bluemke DA, Dietz HC, Calkins H, Judge DP. Dsg2 mutations contribute to arrhythmogenic right ventricular dysplasia/cardiomyopathy. *Am J Hum Genet*. 2006;79:136-142
22. den Haan AD, Tan BY, Zikusoka MN, Llado LI, Jain R, Daly A, Tichnell C, James C, Amat-Alarcon N, Abraham T, Russell SD, Bluemke DA, Calkins H, Dalal D, Judge DP. Comprehensive desmosome mutation analysis in north americans with arrhythmogenic right ventricular dysplasia/cardiomyopathy. *Circ Cardiovasc Genet*. 2009;2:428-435
23. Barahona-Dussault C, Benito B, Campuzano O, Iglesias A, Leung TL, Robb L, Talajic M, Brugada R. Role of genetic testing in arrhythmogenic right ventricular cardiomyopathy/dysplasia. *Clin Genet*. 2010;-77:37-48
24. Sen-Chowdhry S, Syrris P, McKenna WJ. Role of genetic analysis in the management of patients with arrhythmogenic right ventricular dysplasia/cardiomyopathy. *J Am Coll Cardiol*. 2007;50:1813-1821
25. Cox MG, van der Zwaag PA, van der Werf C, van der Smagt JJ, Noorman M, Bhuiyan ZA, Wiesfeld AC, Volders PG, van Langen IM, Atsma DE, Dooijes D, van den Wijngaard A, Houweling AC, Jongbloed JD, Jordaens L, Cramer MJ, Doevendans PA, de Bakker JM, Wilde AA, van Tintelen JP, Hauer RN. Arrhythmogenic right ventricular dysplasia/cardiomyopathy: Pathogenic desmosome mutations in index-patients predict outcome of family screening: Dutch arrhythmogenic right ventricular dysplasia/cardiomyopathy genotype-phenotype follow-up study. *Circulation*. 2011;123:2690-2700
26. Bauce B, Nava A, Beffagna G, Basso C, Lorenzon A, Smaniotto G, De Bortoli M, Rigato I, Mazzotti E, Steriotis A, Marra MP, Towbin JA, Thiene G, Danieli GA, Rampazzo A. Multiple mutations in desmosomal proteins encoding genes in arrhythmogenic right ventricular cardiomyopathy/dysplasia. *Heart Rhythm*. 2010;7:22-29
27. Christensen AH, Benn M, Bundgaard H, Tybjaerg-Hansen A, Haunso S, Svendsen JH. Wide spectrum of desmosomal mutations in danish patients with arrhythmogenic right ventricular cardiomyopathy. *J Med*

Genet. 2010;47:736-744
28. Dalal D, Molin LH, Piccini J, Tichnell C, James C, Bomma C, Prakasa K, Towbin JA, Marcus FI, Spevak PJ, Bluemke DA, Abraham T, Russell SD, Calkins H, Judge DP. Clinical features of arrhythmogenic right ventricular dysplasia/cardiomyopathy associated with mutations in plakophilin-2. *Circulation*. 2006;113:1641-1649
29. Yang Z, Bowles NE, Scherer SE, Taylor MD, Kearney DL, Ge S, Nadvoretskiy VV, DeFreitas G, Carabello B, Brandon LI, Godsel LM, Green KJ, Saffitz JE, Li H, Danieli GA, Calkins H, Marcus F, Towbin JA. Desmosomal dysfunction due to mutations in desmoplakin causes arrhythmogenic right ventricular dysplasia/cardiomyopathy. *Circ Res*. 2006;99:646-655
30. Marcus FI, Zareba W, Calkins H, Towbin JA, Basso C, Bluemke DA, Estes NA, 3rd, Picard MH, Sanborn D, Thiene G, Wichter T, Cannom D, Wilber DJ, Scheinman M, Duff H, Daubert J, Talajic M, Krahn A, Sweeney M, Garan H, Sakaguchi S, Lerman BB, Kerr C, Kron J, Steinberg JS, Sherrill D, Gear K, Brown M, Severski P, Polonsky S, McNitt S. Arrhythmogenic right ventricular cardiomyopathy/dysplasia clinical presentation and diagnostic evaluation: Results from the north american multidisciplinary study. *Heart Rhythm*. 2009;6:984-992
31. Heuser A, Plovie ER, Ellinor PT, Grossmann KS, Shin JT, Wichter T, Basson CT, Lerman BB, Sasse-Klaassen S, Thierfelder L, MacRae CA, Gerull B. Mutant desmocollin-2 causes arrhythmogenic right ventricular cardiomyopathy. *Am J Hum Genet*. 2006;79:1081-1088
32. Syrris P, Ward D, Evans A, Asimaki A, Gandjbakhch E, Sen-Chowdhry S, McKenna WJ. Arrhythmogenic right ventricular dysplasia/cardiomyopathy associated with mutations in the desmosomal gene desmocollin-2. *Am J Hum Genet*. 2006;79:978-984
33. Syrris P, Ward D, Asimaki A, Sen-Chowdhry S, Ebrahim HY, Evans A, Hitomi N, Norman M, Pantazis A, Shaw AL, Elliott PM, McKenna WJ. Clinical expression of plakophilin-2 mutations in familial arrhythmogenic right ventricular cardiomyopathy. *Circulation*. 2006;113:356-364
34. Syrris P, Ward D, Asimaki A, Evans A, Sen-Chowdhry S, Hughes SE, McKenna WJ. Desmoglein-2 mutations in arrhythmogenic right ventricular cardiomyopathy: A genotype-phenotype characterization of familial disease. *Eur Heart J*. 2007;28:581-588
35. van Tintelen JP, Entius MM, Bhuiyan ZA, Jongbloed R, Wiesfeld AC, Wilde AA, van der Smagt J, Boven LG, Mannens MM, van Langen IM, Hofstra RM, Otterspoor LC, Doevendans PA, Rodriguez LM, van Gelder IC, Hauer RN. Plakophilin-2 mutations are the major determinant of familial arrhythmogenic right ventricular dysplasia/cardiomyopathy. *Circulation*. 2006;113:1650-1658
36. Bhuiyan ZA, Jongbloed JD, van der Smagt J, Lombardi PM, Wiesfeld AC, Nelen M, Schouten M, Jongbloed R, Cox MG, van Wolferen M, Rodriguez LM, van Gelder IC, Bikker H, Suurmeijer AJ, van den Berg MP,

Mannens MM, Hauer RN, Wilde AA, van Tintelen JP. Desmoglein-2 and desmocollin-2 mutations in dutch arrhythmogenic right ventricular dysplasia/cardiomypathy patients: Results from a multicenter study. *Circ Cardiovasc Genet*. 2009;2:418-427

37. Basso C, Czarnowska E, Della Barbera M, Bauce B, Beffagna G, Wlodarska EK, Pilichou K, Ramondo A, Lorenzon A, Wozniek O, Corrado D, Daliento L, Danieli GA, Valente M, Nava A, Thiene G, Rampazzo A. Ultrastructural evidence of intercalated disk remodelling in arrhythmogenic right ventricular cardiomyopathy: An electron microscopy investigation on endomyocardial biopsies. *Eur Heart J*. 2006;27:1847-1854
38. Antoniades L, Tsatsopoulou A, Anastasakis A, Syrris P, Asimaki A, Panagiotakos D, Zambartas C, Stefanadis C, McKenna WJ, Protonotarios N. Arrhythmogenic right ventricular cardiomyopathy caused by deletions in plakophilin-2 and plakoglobin (naxos disease) in families from greece and cyprus: Genotype-phenotype relations, diagnostic features and prognosis. *Eur Heart J*. 2006;27:2208-2216
39. Christensen AH, Benn M, Tybjaerg-Hansen A, Haunso S, Svendsen JH. Missense variants in plakophilin-2 in arrhythmogenic right ventricular cardiomyopathy patients–disease-causing or innocent bystanders? *Cardiology*. 2010;115:148-154
40. Lahtinen AM, Lehtonen A, Kaartinen M, Toivonen L, Swan H, Widen E, Lehtonen E, Lehto VP, Kontula K. Plakophilin-2 missense mutations in arrhythmogenic right ventricular cardiomyopathy. *Int J Cardiol*. 2008;126:92-100
41. Qiu X, Liu W, Hu D, Zhu T, Li C, Li L, Guo C, Liu X, Wang L, Zheng H, Wang C, Diao Q, Shi D, Zhan P, Deng Y, Liu K, Wang Y, Liu B, Liu H, Zhang L. Mutations of plakophilin-2 in chinese with arrhythmogenic right ventricular dysplasia/cardiomyopathy. *Am J Cardiol*. 2009;103:1439-1444

CHAPTER 5

The end-stage of arrhythmogenic cardiomyopathy with severe involvement of the interventricular septum

Maartje Noorman[1,3,*], Judith A Groeneweg[2,3,*], Angeliki Asimaki[4], Stefania Rizzo[5], Maartje Papegaaij[1], Leonie van Stuijvenberg[1], Nicolaas de Jonge[2], Dennis Dooijes [6], Cristina Basso[5], Jeffrey E Saffitz[4], Toon AB van Veen[1], Aryan Vink[7], Richard NW Hauer[2,3]

1. Department of Medical Physiology, University Medical Center Utrecht, Utrecht, The Netherlands
2. Department of Cardiology, University Medical Center Utrecht, Utrecht, The Netherlands
3. Interuniversity Cardiology Institute of The Netherlands, Utrecht, The Netherlands
4. Department of Pathology, Beth Israel Deaconess Medical Center, Harvard Medical School, Boston, Massachusetts
5. Department of Cardiac, Thoracic, and Vascular Sciences, University of Padua Medical School, Padua, Italy
6. Department of Genetics, University Medical Center Utrecht, Utrecht, The Netherlands
7. Department of Pathology, University Medical Center Utrecht, Utrecht, The Netherlands

* *These authors contributed equally to this work*

Submitted

Abstract

Detailed histopathological, immunohistochemical and ultrastructural analysis is described in the heart of a 56-year old woman with end-stage arrhythmogenic cardiomyopathy with a pathogenic plakophilin-2 mutation. The explanted heart revealed severe fibrofatty replacement of nearly the entire right ventricular free wall. Also the left ventricle was severely affected, and most remarkable, there was massive involvement of the interventricular septum. Immunohistochemical and electron microscopy findings of intercalated disks revealed regions with a heterogeneous distribution of Cx43 and focal electron microscopic abnormalities amongst these regions. This illustrates again that arrhythmogenic cardiomyopathy is not limited to the right ventricle, but involves the entire myocardium, including the interventricular septum.

Introduction

Arrhythmogenic Cardiomyopathy (AC), also known as Arrhythmogenic Right Ventricular Dysplasia/Cardiomyopathy (ARVD/C), can present in 4 clinical stages which not necessarily proceed from one into the other: 1) concealed stage without or with minimal structural disease, although sudden cardiac death may occur, 2) overt stage with structural alterations of primarily the right ventricle (RV), and episodes of monomorphic ventricular tachycardia (VT), 3) overt stage with obvious structural biventricular involvement, and 4) the end-stage of the disease with heart failure.[1-3] Recently, left ventricular dominant variants have been described.[4]

A distinct histopathological feature of AC is fibrofatty replacement of the ventricular myocardium. Cardiomyocytolysis and replacement by fibrous and fatty tissue is a process that progresses from sub-epicardial and mid-myocardial layers to endocardium.[3, 5] These histopathological changes in the RV have been described for the left ventricle (LV) as well.[6] Remarkably, in AC the interventricular septum (IVS) is usually spared from these alterations.[4]

A tentative mechanism for the clinical phenotype and fibrofatty replacement is mechanical and electrical uncoupling of ventricular cardiomyocytes due to desmosomal dysfunction.[7-12] Desmosomes are proteins in the intercalated disk that connect adjacent cardiomyocytes, thereby providing mechanical integrity and electrical stability.[7-12] Alterations in 5 known desmosomal proteins, plakophilin-2 (PKP2), desmoplakin (DSP), plakoglobin (PKG), desmoglein-2 (DSG2), and desmocollin-2 (DSC2) have been related to AC.[13-21] Immunohistochemical analysis can be used to visualize the distribution of desmosomal proteins.[13]

Here we present an AC patient with a pathogenic *PKP2* mutation undergoing cardiac transplantation because of progressive heart failure. The explanted heart provided the opportunity to study the end-stage of the AC disease process in great detail. Macroscopically there was extensive damage to the RV, with LV and remarkable septal involvement. Histopathological, immunohistochemical, and electron microscopy analyses were performed.

Clinical findings and analysis

A 56-year old woman, since 15 years known with AC, underwent an orthotopic cardiac transplantation because of progressive RV and LV failure. In 1995, at age 41, a first episode of sustained VT was diagnosed. Sotalol treatment was initiated. Coronary angiography showed no abnormalities and LV cine-angiography showed an aneurysm of the LV apex. The following years displayed VT recurrences. Two VT morphologies were recorded: VT 1 had a left bundle branch block (LBBB) morphology, extreme superior axis, and cycle length 320 ms, VT 2 also had LBBB morphology with left superior axis, and cycle length 420 ms (Figure 5.1A).

She was referred to the Utrecht Cardiac Arrhythmia Unit in 1997 because of suspected AC. Diagnosis of AC was confirmed by the presence of epsilon waves in leads V1-3, negative T waves in all precordial leads (Figure 5.1B), and LBBB VT episodes with superior axis.

Further analysis showed a dilated RV with poor function and dyskinesia of the RV outflow tract and RV apex on RV cine-angiography. During electrophysiologic study the clinical VT 2 was inducible by programmed electrical stimulation. Body surface mapping, pace mapping, activation mapping, and entrainment of the VT confirmed the arrhythmogenic substrate at a right-sided paraseptal infero-basal location. Endocardial radio-frequency ablation was performed and VT 2 was no longer inducible. However, two other VT morphologies were inducible after ablation. Clinical VT 1 was not inducible at all.

Because of recurrent fast VT episodes during sotalol treatment, a cardioverter-defibrillator (ICD) was implanted in 1998. This procedure was complicated by an Addisonian crisis. Chronic treatment of the coincidentally found primary adrenocortical insufficiency significantly improved the patient's general condition.

Ventricular tachyarrhythmia episodes frequently recurred despite anti-arrhythmic drug treatment. VT recurrences were interrupted by anti-tachycardia pacing and shock therapy from the ICD.

In 2005, the heterozygous pathogenic *PKP2* mutation c.2386T>C (p.Cys796Arg) was found by molecular-genetic screening of 4 of the desmosomal genes (*PKP2*, *DSP*, *DSG2*, *DSC2*) and family screening was initiated. There were no known arrhythmias or sudden deaths in the family. DNA screening was negative for the *PKP2* mutation in the 3 asymptomatic sons of the patient.

Atrial arrhythmias (atrial fibrillation and flutter) were recorded at age 53. Echocardiography showed an extensively dilated, aneurysmatic

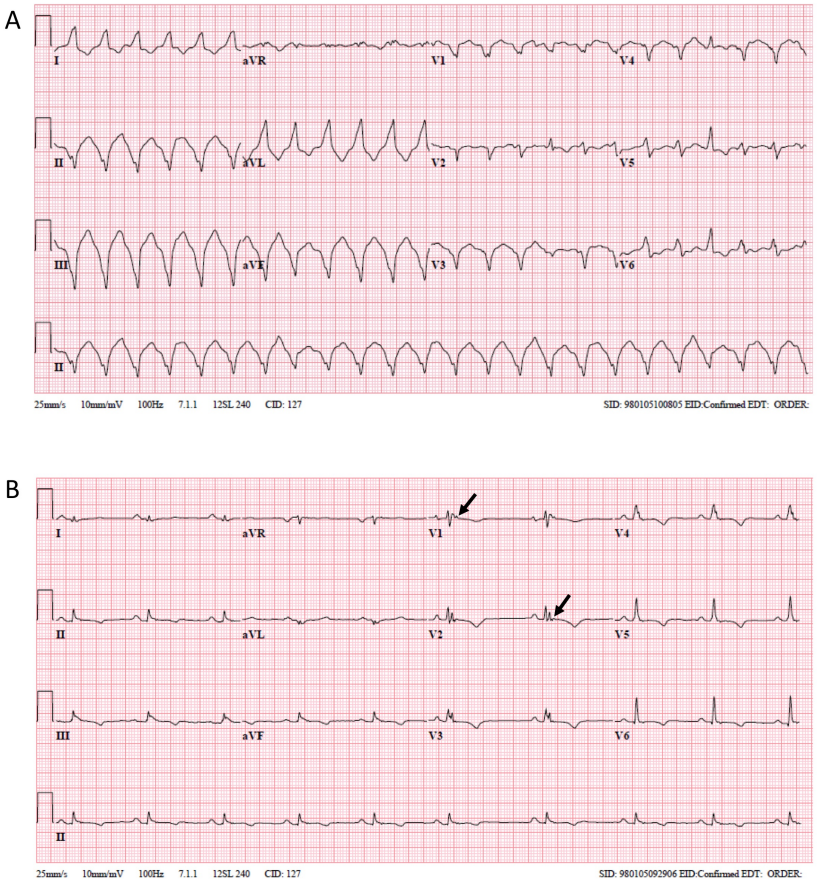

Figure 5.1 – **A.** Ventricular tachycardia with configuration 2: Left bundle branch block morphology, left superior axis (major task force criterion), and cycle length 420 ms. **B.** ECG of the index patient during sinus rhythm, while off drugs, with epsilon waves (indicated by arrows) in leads V1-2 (major task force criterion) and negative T waves in all precordial leads V1-6 (major task force criterion).

RV, significant tricuspid incompetence with volume overload of the RV, LV global and regional wall motion abnormalities with a reduced systolic LV function. An atrial lead was added to the ICD system.

Progression of heart failure and deterioration of the patient's condition started in 2009, at age 55. In September 2010 she was admitted in the hospital with backward and forward failure and later with cardiogenic shock. In December 2010, at age 56, she underwent a successful orthotopic cardiac transplantation. The ICD was explanted. At

present, the patient is doing well without any sign of rejection of the cardiac transplant.

Histopathological examination

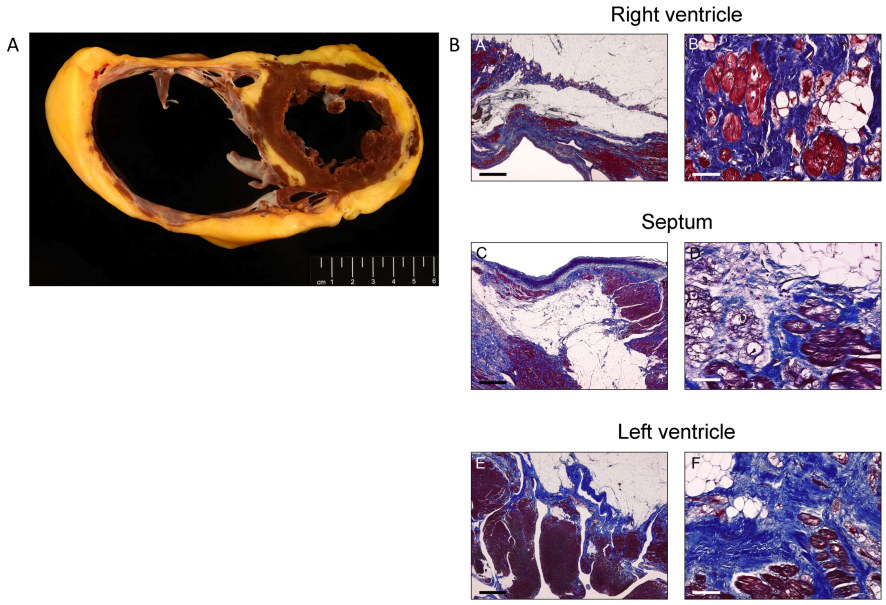

Figure 5.2 – **A.** Gross examination of the heart. Cross section through the ventricles of the explanted heart showing severe dilatation of the right ventricle with fibro-fatty replacement of nearly the entire free wall of the right ventricle. In addition, extensive fibro-fatty alteration in the left ventricle and the septum. **B.** Microscopic examination of the myocardium (Modified AZAN stain). A and B, Right ventricle. A, overview showing fibro-fatty replacement of the wall. Cardiomyocytes in red, fibrous tissue in blue and lipocytes. B, higher magnification of the same area showing large cardiomyocytes (in red) with vacuolar degeneration. C and D, fibrofatty replacement of the myocardium in the septum. C. E and F, fibrofatty replacement of the left ventricular wall. Scale bars in A, C, and E 1mm. Scale bars in B, D, and F 100μm.

Gross examination of the explanted heart (695 grams) revealed severe dilatation of the right ventricle with a maximal luminal diameter of 10.5 cm (Figure 5.2A). Severe fibro-fatty replacement of the free wall of the right ventricle was observed with almost complete absence of viable myocardium. Fibro-fatty replacement was also observed in the wall of the left ventricle, especially in the postero-lateral part. In addition to the

free walls of both ventricles, the septum also revealed massive subendocardial fibro-fatty replacement in the anterior and posterior parts. Microscopic examination confirmed the presence of vacuolar degeneration of cardiomyocytes with fibro-fatty replacement in the walls of both ventricles and in the septum (Figure 5.2B). The areas surrounding those with fibrofatty replacement showed hypertrophic cardiomyocytes with enlarged irregular nuclei and increased number of myofibrils. Very focally a minimal lymphohistiocytic infiltrate around degenerated cardiomyocytes was observed. The coronary arteries revealed concentric intimal fibrosis without significant stenoses.

Immunohistochemical analysis

Formalin-fixed, paraffin-embedded as well as frozen sections were used for immunohistochemical analysis as described previously.[13, 22] N-cadherin, a component of the adherens junction, was used as marker for the intercalated disk. Formalin-fixed, paraffin-embedded material was used for staining of PKG, DSP and PKP2 (Figure 5.3A). As shown in Figure 5.3A, specific immunoreactive signal for PKG was severely reduced both in IVS and LV. Also, signal for DSP was markedly reduced. Using an antibody that was able to recognize the C-terminus, the PKP2 signal was not reduced compared to control (Figure 5.3A).

Furthermore, double labeling on frozen material to visualize localization of Cx43 and the non-phosphorylated form of Cx43 (Cx43-NP) was performed. In the major part of the LV normal immunoreactive signal for Cx43 at the intercalated disks with only sporadic lateralization was observed (Figure 5.3B). In addition, heterogeneously diminished Cx43 signal at cell-cell junctions was found in the larger part of the IVS (Figure 5.3B bottom panel). However, several other specimen displayed normal Cx43 signals, (Figure 5.3B middle panel). In addition, at these spots with normal Cx43, Cx43-NP was absent (Figure 5.3C) which suggests a normal intercellular coupling.[23-25] Immunohistochemistry was not performed on the RV, since the wall of the RV showed severe fibrofatty replacement with only a few small areas with intact architecture of the myocardium.

Ultrastructural analsis

Electron microscopic evaluation of the left ventricular and septal myocardium showed focal myofibrillar lysis, T- tubule dilatation and mitochondrial clustering. No alteration in the mitochondrial or nuclear

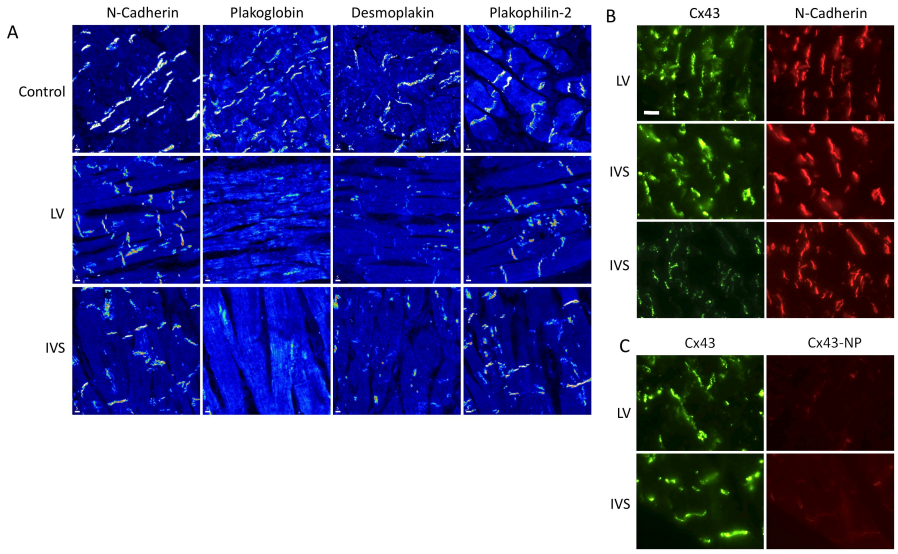

Figure 5.3 – **A.** Immunohistochemical stainings for N-cadherin, plakoglobin, desmoplakin and plakophilin-2 of control, and left ventricle (LV) and interventricular septum (IVS) in the patient. N-cadherin and PKP2 are comparable between control, LV and IVS. PKG and DSP are severely reduced in the patient. Scale bars 5μm. **B.** Immunohistochemical analysis of N-Cadherin/Connexin 43 (Cx43) and **C.** Cx43//the non-phosporylated form of Cx43 (Cx43-NP). Cx43 localization appears normal in the LV and down-regulated in the IVS. Cx43-NP is not present, indicating normal intercellular contact. Scale bars 25 μm.

structure was observed. Lipid droplets were rarely present in the myocardial cells. Longitudinal section of cardiomyocytes showed large amounts of dark lipofuscin granules located at the poles of nucleus and among the mitochondria. Abundant collagen fibers interspersed with cardiomyocytes, fibroblasts and inflammatory cells in the interstitial space were noted.

As far as the cell-cell junctions are concerned, highly convoluted intercalated disks and various degrees of intercellular space widening were found in both the LV and the interventricular septum (Figure 5.4A). Myofibril lysis at their points of attachment to the intercalated disk was also observed. Gap junctions appeared structurally normal in the samples analyzed, without any evidence of lateral localization at the membranes of cardiomyocytes. Proper alignment of sarcomeres, Z-lines, and myofilaments was observed in most cardiomyocytes, although fo-

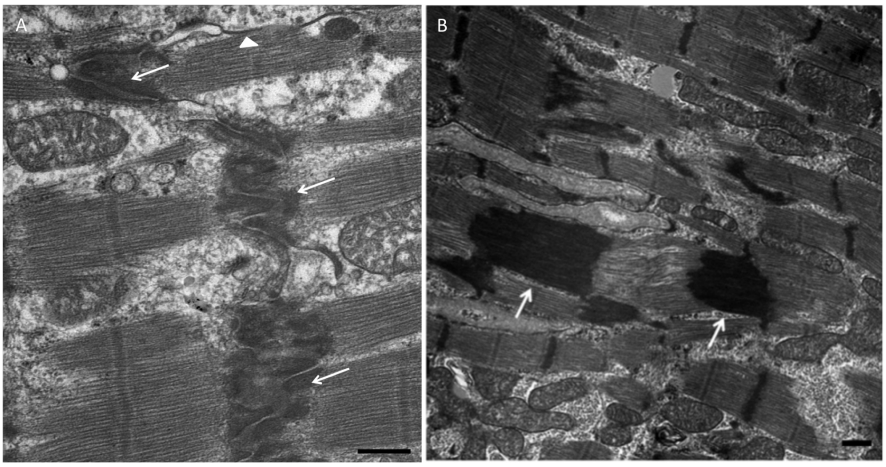

Figure 5.4 – Electron microscopy findings of ventricular cardiomyocytes from the explanted heart **A.** Intercalated disks in this sample show focal widening of the intercellular space at the level of the desmosome/fascia adherens (arrow), while the remaining spaces appear normal; gap junctions show a preserved structure (arrow head). Scale bar 500 nm; **B.** Enlarged Z-lines (arrows) due to focal accumulation of electron dense material are visible together with a region of more normal appearance. Scale bar 500 nm

cal accumulation of electron dense material at the Z-lines was observed (Figure 5.4B).

Discussion

We present a case of severe AC with a pathogenic mutation in the *PKP2* gene, leading to the necessity for a heart transplant. This opened the way to detailed histological, immunohistochemical and ultrastructural analyses on the explanted heart to study the end-stage of AC.

After the concealed phase, the overt stage of the disease developed in which the diagnosis was made based on depolarization and repolarization abnormalities on ECG, left bundle branch block morphology VT, and structural abnormalities of the RV. Gradually, increasing biventricular structural and functional abnormalities were observed, resulting in the end-stage: heart failure and ultimately cardiac transplantation.

Histopathologically, fibrofatty infiltration was found throughout the entire heart. Most severely affected was the RV, with hardly any

preservation of viable working myocardium. Furthermore, also the LV free wall showed extensive regions of fibrofatty replacement and, very remarkable, regions within the interventricular septum were severely affected.

Fibrosis or fatty infiltration of the interventricular septum has been previously described in AC, although at the microscopic histopathological level in endomyocardial biopsies or in imaging studies with magnetic resonance imaging with delayed enhancement analysis and never on the extensive macroscopic scale of the patient in the present study. On the contrary, previous studies in large cohorts of AC heart specimens suggested that the septum is usually spared from alterations.[4, 5] Septal fibrosis is nevertheless frequently observed in cardiac sarcoidosis, and cases of sarcoid myocarditis clinically mimicking AC have been reported.[26-29] However, in this patient there were no clinical signs of systemic sarcoidosis and no sarcoid granulomas were observed with histological analysis of the explanted heart. Moreover, a pathogenic *PKP2* mutation related to AC was identified.

Although this patient specific *PKP2* mutation (c.2386T>C, p.Cys796Arg) is a missense mutation, general consensus is that it is pathogenic. Both i*n silico* prediction algorithms SIFT and PolyPhen2 predict a deleterious effect of the amino acid substitution. Furthermore, the mutation has been found in 11 different Dutch families with AC: 11 probands and in addition 11/26 family members carrying solely this mutation fulfilled the revised 2010 Task Force Criteria for AC diagnosis. Even more important, biventricular involvement was identified in 6/37 mutation carriers. A founder effect of the c.2386T>C mutation has been suggested based on haplotype analysis.[15] Finally, in the patient no mutations in *DSP*, *DSG2*, and *DSC2* were identifiable. However, considering the severity of the AC phenotype with necessity for a cardiac transplantation, contribution of other yet unknown/unidentified genetic and/or environmental factors can not be ignored.

In agreement with the previously reported frequent down-regulation of PKG in AC[13], severely reduced signal for PKG was found with immunohistochemical analysis in regions *without* apparent fibrofatty infiltration, both in LV and IVS. In addition, down-regulation of DSP was observed. Normal staining patterns of the adherens junction protein N-cadherin and of the desmosomal protein PKP2 were found, despite the pathogenic *PKP2* mutation. Noteworthy was the heterogeneous staining pattern, particularly in the IVS, with focal abnormalities of the gap junction protein Cx43.

The remarkable finding of normal LV and heterogeneously downregulated IVS immunoreactive signal for Cx43 in end-stage of AC is in agreement with the report of Christensen *et al.* who also described severe cases of AC without gap junction remodeling.[30] However, gap junction remodeling has been described in all types of structural heart disease, and in AC even in regions without histopathological alteration.[7, 21]

The immunostaining of PKP2 with comparable signal intensities and distribution leads to the important suggestion that apparently both the wildtype protein (from the unaffected allele) and the mutant protein are expressed and localize simultaneously to the cell-cell junctions. This also stands in stark contrast to phenotypes seen in true haploinsufficient patients or in genetically engineered mouse models when there is either heterozygous or homozygous knock out (ie, loss of expression of the wildtype protein). To speculate, this observation suggests that heterozygous expression of the mutant protein is sufficient to cause severe disease and argues strongly for a dominant negative effect, much like that seen in hypertrophic cardiomyopathy.

In the left ventricular free wall and septum we observed focal involvement of myocardium with severe fibrofatty replacement in some regions, whereas other regions were not affected. On the ultrastructural level the intercalated disks of both the LV and septum revealed a heterogeneous appearance with a measured intercellular gap range that was partly close to the normal range and partly revealed extensively widened gaps. In all samples analyzed with electron microscopy, there was evidence for replacement-like fibrosis (i.e. collagen fibers and inflammatory cells in the interstitium).

The mysterious finding of accumulation of electron dense material within the sarcomere reminds of a finding previously reported in boxer dogs suffering from AC.[31] Noteworthy, the presence of electron dense material, corresponding to aggregation of alpha-actinin within sarcomeres, is a hallmark of nemaline myopathy, a disease due to mutations in genes encoding for actin filament proteins and affecting both skeletal and heart muscles.[32, 33] Future studies are needed to evaluate the origin and meaning of the electron dense material at the Z-lines in AC.

Conclusions

In conclusion, this presentation of the end-stage disease of a *PKP2* mutation associated AC shows that in addition to the right ventricular myocardium and the left ventricular free wall, the septal myocardium can be severely affected as well, not only on the microscopic but moreover on the macroscopic level.

References

1. Basso C, Corrado D, Marcus FI, Nava A, Thiene G. Arrhythmogenic right ventricular cardiomyopathy. *Lancet*. 2009;373:1289-1300
2. Marcus FI, Fontaine GH, Guiraudon G, Frank R, Laurenceau JL, Malergue C, Grosgogeat Y. Right ventricular dysplasia: A report of 24 adult cases. *Circulation*. 1982;65:384-398
3. Thiene G, Nava A, Corrado D, Rossi L, Pennelli N. Right ventricular cardiomyopathy and sudden death in young people. *N Engl J Med*. 1988;318:129-133
4. Sen-Chowdhry S, Syrris P, Prasad SK, Hughes SE, Merrifield R, Ward D, Pennell DJ, McKenna WJ. Left-dominant arrhythmogenic cardiomyopathy: An under-recognized clinical entity. *J Am Coll Cardiol*. 2008;-52:2175-2187
5. Basso C, Thiene G, Corrado D, Angelini A, Nava A, Valente M. Arrhythmogenic right ventricular cardiomyopathy. Dysplasia, dystrophy, or myocarditis? *Circulation*. 1996;94:983-991
6. Corrado D, Basso C, Thiene G, McKenna WJ, Davies MJ, Fontaliran F, Nava A, Silvestri F, Blomstrom-Lundqvist C, Wlodarska EK, Fontaine G, Camerini F. Spectrum of clinicopathologic manifestations of arrhythmogenic right ventricular cardiomyopathy/dysplasia: A multicenter study. *J Am Coll Cardiol*. 1997;30:1512-1520
7. Kaplan SR, Gard JJ, Carvajal-Huerta L, Ruiz-Cabezas JC, Thiene G, Saffitz JE. Structural and molecular pathology of the heart in carvajal syndrome. *Cardiovasc Pathol*. 2004;13:26-32
8. Saffitz JE. Dependence of electrical coupling on mechanical coupling in cardiac myocytes: Insights gained from cardiomyopathies caused by defects in cell-cell connections. *Ann N Y Acad Sci*. 2005;1047:336-344
9. Basso C, Czarnowska E, Della Barbera M, Bauce B, Beffagna G, Wlodarska EK, Pilichou K, Ramondo A, Lorenzon A, Wozniek O, Corrado D, Daliento L, Danieli GA, Valente M, Nava A, Thiene G, Rampazzo A. Ultrastructural evidence of intercalated disk remodelling in arrhythmogenic right ventricular cardiomyopathy: An electron microscopy investigation on endomyocardial biopsies. *Eur Heart J*. 2006;27:1847-1854
10. Garcia-Gras E, Lombardi R, Giocondo MJ, Willerson JT, Schneider MD, Khoury DS, Marian AJ. Suppression of canonical wnt/beta-catenin signaling by nuclear plakoglobin recapitulates phenotype of arrhythmogenic right ventricular cardiomyopathy. *J Clin Invest*. 2006;116:2012-2021
11. Oxford EM, Musa H, Maass K, Coombs W, Taffet SM, Delmar M. Connexin43 remodeling caused by inhibition of plakophilin-2 expression in cardiac cells. *Circ Res*. 2007;101:703-711
12. Sato PY, Musa H, Coombs W, Guerrero-Serna G, Patino GA, Taffet SM, Isom LL, Delmar M. Loss of plakophilin-2 expression leads to decreased sodium current and slower conduction velocity in cultured cardiac myocytes. *Circ Res*. 2009;105:523-526

13. Asimaki A, Tandri H, Huang H, Halushka MK, Gautam S, Basso C, Thiene G, Tsatsopoulou A, Protonotarios N, McKenna WJ, Calkins H, Saffitz JE. A new diagnostic test for arrhythmogenic right ventricular cardiomyopathy. *N Engl J Med*. 2009;360:1075-1084
14. Gerull B, Heuser A, Wichter T, Paul M, Basson CT, McDermott DA, Lerman BB, Markowitz SM, Ellinor PT, MacRae CA, Peters S, Grossmann KS, Drenckhahn J, Michely B, Sasse-Klaassen S, Birchmeier W, Dietz R, Breithardt G, Schulze-Bahr E, Thierfelder L. Mutations in the desmosomal protein plakophilin-2 are common in arrhythmogenic right ventricular cardiomyopathy. *Nat Genet*. 2004;36:1162-1164
15. van Tintelen JP, Entius MM, Bhuiyan ZA, Jongbloed R, Wiesfeld AC, Wilde AA, van der Smagt J, Boven LG, Mannens MM, van Langen IM, Hofstra RM, Otterspoor LC, Doevendans PA, Rodriguez LM, van Gelder IC, Hauer RN. Plakophilin-2 mutations are the major determinant of familial arrhythmogenic right ventricular dysplasia/cardiomyopathy. *Circulation*. 2006;113:1650-1658
16. Syrris P, Ward D, Asimaki A, Sen-Chowdhry S, Ebrahim HY, Evans A, Hitomi N, Norman M, Pantazis A, Shaw AL, Elliott PM, McKenna WJ. Clinical expression of plakophilin-2 mutations in familial arrhythmogenic right ventricular cardiomyopathy. *Circulation*. 2006;113:356-364
17. Rampazzo A, Nava A, Malacrida S, Beffagna G, Bauce B, Rossi V, Zimbello R, Simionati B, Basso C, Thiene G, Towbin JA, Danieli GA. Mutation in human desmoplakin domain binding to plakoglobin causes a dominant form of arrhythmogenic right ventricular cardiomyopathy. *Am J Hum Genet*. 2002;71:1200-1206
18. McKoy G, Protonotarios N, Crosby A, Tsatsopoulou A, Anastasakis A, Coonar A, Norman M, Baboonian C, Jeffery S, McKenna WJ. Identification of a deletion in plakoglobin in arrhythmogenic right ventricular cardiomyopathy with palmoplantar keratoderma and woolly hair (naxos disease). *Lancet*. 2000;355:2119-2124
19. Pilichou K, Nava A, Basso C, Beffagna G, Bauce B, Lorenzon A, Frigo G, Vettori A, Valente M, Towbin J, Thiene G, Danieli GA, Rampazzo A. Mutations in desmoglein-2 gene are associated with arrhythmogenic right ventricular cardiomyopathy. *Circulation*. 2006;113:1171-1179
20. Syrris P, Ward D, Evans A, Asimaki A, Gandjbakhch E, Sen-Chowdhry S, McKenna WJ. Arrhythmogenic right ventricular dysplasia/cardiomyopathy associated with mutations in the desmosomal gene desmocollin-2. *Am J Hum Genet*. 2006;79:978-984
21. Asimaki A, Syrris P, Wichter T, Matthias P, Saffitz JE, McKenna WJ. A novel dominant mutation in plakoglobin causes arrhythmogenic right ventricular cardiomyopathy. *Am J Hum Genet*. 2007;81:964-973
22. van Veen TA, van Rijen HV, Wiegerinck RF, Opthof T, Colbert MC, Clement S, de Bakker JM, Jongsma HJ. Remodeling of gap junctions in mouse hearts hypertrophied by forced retinoic acid signaling. *J Mol Cell Cardiol*. 2002;34:1411-1423

23. Beardslee MA, Lerner DL, Tadros PN, Laing JG, Beyer EC, Yamada KA, Kleber AG, Schuessler RB, Saffitz JE. Dephosphorylation and intracellular redistribution of ventricular connexin43 during electrical uncoupling induced by ischemia. *Circ Res.* 2000;87:656-662
24. Quan W, Rudy Y. Unidirectional block and reentry of cardiac excitation: A model study. *Circ Res.* 1990;66:367-382
25. Cabo C, Yao J, Boyden PA, Chen S, Hussain W, Duffy HS, Ciaccio EJ, Peters NS, Wit AL. Heterogeneous gap junction remodeling in reentrant circuits in the epicardial border zone of the healing canine infarct. *Cardiovasc Res.* 2006;72:241-249
26. Roberts WC, McAllister HA, Jr., Ferrans VJ. Sarcoidosis of the heart. A clinicopathologic study of 35 necropsy patients (group 1) and review of 78 previously described necropsy patients (group 11). *Am J Med.* 1977;63:86-108
27. Ott P, Marcus FI, Sobonya RE, Morady F, Knight BP, Fuenzalida CE. Cardiac sarcoidosis masquerading as right ventricular dysplasia. *Pacing Clin Electrophysiol.* 2003;26:1498-1503
28. Ladyjanskaia GA, Basso C, Hobbelink MG, Kirkels JH, Lahpor JR, Cramer MJ, Thiene G, Hauer RN, MF VO. Sarcoid myocarditis with ventricular tachycardia mimicking arvd/c. *J Cardiovasc Electrophysiol.* 2010;21:94-98
29. Vasaiwala SC, Finn C, Delpriore J, Leya F, Gagermeier J, Akar JG, Santucci P, Dajani K, Bova D, Picken MM, Basso C, Marcus F, Wilber DJ. Prospective study of cardiac sarcoid mimicking arrhythmogenic right ventricular dysplasia. *J Cardiovasc Electrophysiol.* 2009;20:473-476
30. Christensen AH, Andersen CB, Tybjaerg-Hansen A, Haunso S, Svendsen JH. Mutation analysis and evaluation of the cardiac localization of tmem43 in arrhythmogenic right ventricular cardiomyopathy. *Clin Genet.* 2011;80:256-264
31. Oxford EM, Danko CG, Kornreich BG, Maass K, Hemsley SA, Raskolnikov D, Fox PR, Delmar M, Moise NS. Ultrastructural changes in cardiac myocytes from boxer dogs with arrhythmogenic right ventricular cardiomyopathy. *J Vet Cardiol.* 2011;13:101-113
32. Jennekens FG, Roord JJ, Veldman H, Willemse J, Jockusch BM. Congenital nemaline myopathy. I. Defective organization of alpha-actinin is restricted to muscle. *Muscle Nerve.* 1983;6:61-68
33. Clarkson E, Costa CF, Machesky LM. Congenital myopathies: Diseases of the actin cytoskeleton. *J Pathol.* 2004;204:407-417

CHAPTER 6

Remodeling of the cardiac sodium channel, Connexin43 and Plakoglobin at the intercalated disk in patients with arrhythmogenic cardiomyopathy

Maartje Noorman[1,5*], Sara Hakim[1*], Elise Kessler[1*], Judith A Groeneweg[2,5], Moniek GPJ Cox[2,5], Angeliki Asimaki[7], Harold VM van Rijen[1], Leonie van Stuijvenberg[1], Halina Chkourko[9], Marcel AG van der Heyden[1], Marc A Vos[1], Nicolaas de Jonge[2], Jasper J van der Smagt[3], Dennis Dooijes[3], Aryan Vink[4], Roel A de Weger[4], Andras Varro[6], Jacques MT de Bakker[5], Jeffrey E Saffitz[7], Tomas J Hund[8], Peter J Mohler[8], Mario Delmar[9], Richard NW Hauer[2,5], Toon AB van Veen[1]

1. Department of Medical Physiology, University Medical Center Utrecht, The Netherlands
2. Department of Cardiology, University Medical Center Utrecht, The Netherlands
3. Department of Genetics, University Medical Center Utrecht, The Netherlands
4. Department of Pathology, University Medical Center Utrecht, The Netherlands
5. Interuniversity Cardiology Institute of The Netherlands, Utrecht, The Netherlands
6. Department of Pharmacology & Pharmacotherapy, Faculty of Medicine, University of Szeged, Hungary
7. Department of Pathology, Beth Israel Deaconess Medical Center and Harvard Medical School, Boston, USA
8. Dorothy M. Davis Heart and Lung Research Institute, Departments of Internal Medicine, Division of Cardiovascular Medicine, Physiology & Cell Biology, The Ohio State University Medical Center, Columbus, OH, USA
9. The Leon H Charney Division of Cardiology, New York University School of Medicine, New York, NY, USA

* *These authors contributed equally to this study*

Submitted

Abstract

Background: Arrhythmogenic cardiomyopathy (AC), is tightly associated with desmosomal mutations in the majority of patients. Arrhythmogenesis in AC patients is likely related to remodeling of cardiac gap junctions and increased levels of fibrosis. Recently, using experimental models, we also identified sodium channel dysfunction secondary to desmosomal dysfunction. The aim of the present study was to assess the immunoreactive signal levels of the sodium channel protein $Na_V1.5$, as well as Connexin43 and Plakoglobin, in myocardial specimens obtained from AC patients.
Methods: Left and right ventricular free wall (LVFW/RVFW) postmortem material was obtained from 5 AC patients and 5 age and sex-matched controls. From another 15 AC patients RV septal biopsies (RVSB) were taken. All patients fulfilled the 2010 revised Task Force Criteria for AC diagnosis. Immunohistochemical analyses were performed using antibodies against Connexin43 (Cx43), Plakoglobin, $Na_V1.5$, Plakophilin-2 and N-Cadherin.
Results: N-Cadherin and Desmoplakin immunoreactive signals and distribution were normal in AC patients compared to control. Plakophilin-2 signals were unaffected, unless a PKP2 mutation predicting haploinsufficiency was present. Distribution was unchanged compared to control. Immunoreactive signal levels of PKG, Cx43 and $Na_V1.5$ were affected in 74%, 70% and 65% of the patients, respectively.
Conclusions: Reduced immunoreactive signal of PKG, Cx43 and $Na_V1.5$ at the intercalated disks can be observed in a large majority of the patients. Decreased levels of $Na_V1.5$ might contribute to arrhythmia vulnerability and provides a new clinically relevant tool for future risk assessment strategies.

Introduction

Arrhythmogenic Cardiomyopathy (AC), previously known as Arrhythmogenic Right Ventricular Cardiomyopathy/Dysplasia (ARVC/D), is a heart muscle disease characterized by replacement of predominantly the right ventricle (RV) with fibro-fatty scar tissue. In later stages of the disease, also the left ventricle (LV) and the interventricular septum (IVS) can be affected. Recently, also patients with a predominant LV involvement have been described.[1] Patients generally present with syncope, palpitations and sudden cardiac death.[2] Mutations in genes encoding for desmosomal proteins, which are important for intercellular mechanical coupling, are associated with this disease in about 60% of the patients.[3-9]

The arrhythmogenic phenotype of AC suggests that, although the mutated genes do not code for channel proteins, these gene products associate with molecules that are relevant for electrical function. In particular, several studies have identified a disturbed immuno-localization of Connexin43 (Cx43), the major ventricular gap junction protein, in AC myocardium.[10-12] In several other forms of cardiomyopathy, a heterogeneous downregulation and de-phosphorylation of Cx43 are strongly associated with an increased propensity for development of life-threatening ventricular arrhythmias.[13-16]

AC is clinically diagnosed according to the revised Task Force Criteria (TFC),[17] based on global or regional dysfunction and structural alterations, tissue characterization of the ventricular wall, re- and depolarization or conduction abnormalities, arrhythmias, genetics and family history. Still, many cases remain un- or misdiagnosed, because of the multiple facets of the clinical manifestation of the disease.

It has been described that immunoreactivity of plakoglobin (PKG) was reduced in a high percentage of AC patients compared either to controls, or to patients with other underlying cardiac disease such as dilated or hypertrophic cardiomyopathy.[12] This early reduction in immunoreactivity for PKG appeared not only present in the RV, but also in the macroscopically unaffected LV and IVS. Based on this finding it was suggested that immunoreactivity of PKG could be a tool to discriminate AC patients from healthy subjects and patients with other forms of heart disease. However, more recent studies have shown that PKG signals are also reduced in sarcoidosis and giant cell myocarditis.[18, 19]

Recently we reported that a reduction in Cx43 protein can lead to reduced sodium channel ($Na_V1.5$) expression and function in a mouse

model of severely reduced Cx43 and in isolated neonatal rat ventricular cardiomyocytes.[20] Furthermore, *in vitro* silencing of plakophilin-2 (PKP2), one of the desmosomal proteins that is often mutated in AC patients, also leads to a decreased sodium current.[21] In addition, PKP2-haploinsufficent mice showed a significant sodium current deficit.[22] Whether desmosomal deficiency and the AC phenotype correlate with changes in the distribution of proteins relevant to the sodium channel complex in the human heart, remains to be defined. This knowledge could also be relevant to the indication or contraindication of sodium channel blockers in these patients.

In this study we used immunohistochemistry to identify the immunoreactive signal levels and distribution of Cx43, PKG and $Na_V1.5$ in AC patients as compared to controls. Our data show that these levels and distribution of Cx43, PKG and $Na_V1.5$ are affected in the large majority of AC patients.

Methods

Patient samples and tissue processing

Left and right ventricular free wall (LVFW and RVFW) myocardium (on average 2-4 cm^3) was obtained from 5 AC patients (AC1-5, post-mortem) and from 5 age and sex matched controls with no underlying heart disease (C1-5). Right ventricular septal biopsies (RVSB, 2-4 mm^3) were obtained from another 15 AC patients (AC6-20). All patients consented to clinical evaluation according to the TFC. All material used in this study was flash frozen in liquid nitrogen. Frozen samples were cryo-sectioned at a thickness of 10 μm.

Patient screening

From 18/20 AC patients, DNA was available to screen for mutations in the *PKP2, DSP, DSG2, DSC2, PKG, TMEM43* and *PLN* genes by direct sequencing. In addition, using multiple ligation-dependent probe amplification, the *PKP2* gene was screened for large exon deletions. Genetic screening was performed upon the patients' written consent.

Immunohistochemistry

Immunohistochemistry was performed as described previously.[23] Primary antibodies against N-Cadherin (mouse, Sigma, 1:800), PKP2

(mouse, Progen, undiluted-1:1000), PKG (mouse, Sigma, 1:100,000), $Na_V1.5$ (rabbit, custom-made,[24] 1:100), and Cx43 (mouse, Transduction Labs, 1:200 and rabbit, Zymed, 1:250) were used. Secondary labeling was performed with appropriate Texas Red (1:100) and FITC (1:250) conjugated whole IgG antibodies (Jackson Laboratories). Blinded cross-evaluation for $Na_V1.5$ labeling of material from 9 patients was performed in Utrecht and in New York.

Results

Patient characteristics

Characteristics of the 5 controls and the 15 AC patients are shown in Table 6.1. Molecular-genetic analysis of 18 out of 20 AC patients revealed 5 different *PKP2* mutations in 11 patients. In addition to a pathogenic *PKP2* mutation, one of those patients also carried unclassified variants in *TMEM43* (p.Arg240Cys) and *DSG2* (p.Ala358Thr). One patient had unclassified variants in *DSC2* and *DSG2*, 2 showed a mutation in *PLN* (p.Arg14del) and 4 did not present any mutations in the analyzed genes.

In Table 6.2 additional clinical characteristics of the AC patients are provided, including age at which first symptoms occurred, and separate Task Force criteria for AC diagnosis.

Immunoreactive signals and distribution of desmosomal proteins

As depicted in Figure 6.1, double-labeling with antibodies against N-Cadherin (N-Cad) and PKP2 revealed that the immunoreactive proteins co-localized at the intercalated disks (IDs) of AC patients (exampled by AC8, -9 and -10), identical to the pattern seen in controls (see C1 as an example). N-Cad, an adherens junction protein in which no mutations in humans have been documented, was used as a marker for the ID. Reduced immunoreactive signals have never been documented in AC patients, and as such, also serves as a control to verify tissue quality/preservation. Indeed, in all controls and patients we studied the distribution of immunoreactive N-cadherin was similar.

Next, we studied the signals and distribution of PKP2 in tissue from AC patients with deletion of exons 1-4 of PKP2, which likely causes PKP2 haplo-insufficiency (AC6, -7, and -8). Results were compared to those obtained from controls, AC patients with no identified

Table 6.1 – Clinical characteristics of Control and Arrhythmogenic Cardiomyopathy patients

Patient	Age	Age 1st symptoms	Sex	TFC	Mutation
Control 1	36	NA	M	NA	NA
Control 2	38	NA	M	NA	NA
Control 3	40	NA	M	NA	NA
Control 4	35	NA	F	NA	NA
Control 5	44	NA	F	NA	NA
AC 1	27	16	M	autopsy	None
AC 2	43	24	M	8	None
AC 3	63	55	F	autopsy	None
AC 4	63	59	M	HTX	ND
AC 5	25	25	M	autopsy	ND
AC 6	16	16	M	9	*PKP2* deletion exons 1-14, *DSG2* uv, *TMEM43* p.Arg240Cys uv
AC 7	39	34	M	10	*PKP2* deletion exons 1-4
AC 8	72	69	M	8	*PKP2* deletion exons 1-4
AC 9	74	65	M	9	*PKP2* p.Cys796Arg
AC 10	77	76	M	7	None
AC 11	47	43	F	5	PLN c.40_42delAGA p.Arg14del
AC 12	38	37	M	7	UV in DSC2 and UV in DSG2 (not pathogenic)
AC 13	30	22	F	5	PKP2 c.235C>T p.Arg79X
AC 14	65	59	F	8	PKP2 c.235C>T p.Arg79X
AC 15	39	17	F	6	PKP2 c.2146-1G>C p.IVS10-1G>C
AC 16	49	48	F	6	PKP2 c.1211-1212insT p.Leu404fs
AC 17	58	34	M	10	PKP2: c.1211-1212insT p. Leu404fs
AC 18	48	41	M	4	PLN c.40_42delAGA p.Arg14del
AC 19	41	29	F	9	PKP2 c.2146-1G>C p.IVS10-1G>C
AC 20	23	17	F	7	PKP2: c.1211-1212insT p. Leu404fs

Right and left ventricular free wall post-mortem material was used from control 1-5 and AC 1-5. Right ventricular septal biopsies were examined from AC 6-20. All AC patients had a TFC score $\geq$4 or were diagnosed after autopsy or heart transplantation. Abbreviations: NA: not applicable, ND: not determined, HTX: heart transplantation. TFC: Task Force Criteria (TFC value indicates number of criteria; major criterion counts for 2 points, minor criterion for 1 point).

Table 6.2 – Patient characteristics

Patient	Age	Sex	1st Symptoms + age (yrs)	Diagnostic Task Force Criteria	
				Major	Minor
AC 1	27	M	VF (16)	Autopsy	
AC 2	43	M	LBBB VT (24)	Epsilon waves, structural abnormalities	Negative T waves in V4-6, prolonged TAD, LBBB VT
AC 3	63	F	Decompensation (55)	Autopsy	
AC 4	63	M	Decompensation (59)	Heart Transplant	
AC 5	25	M	VF (25)	Autopsy	
AC 6	16	M	LBBB VT (16)	LBBB VT with superior axis, negative T waves V1-4, akinesia in dilatated RV	Late potentials
AC 7	39	M	LBBB VT (34)	LBBB VT with superior axis, negative T waves V1-3, akinesia in dilated RV	
AC 8	72	M	Syncope (69)	akinetic areas in dilated RV, son with AC.	Late potentials, >500PVCs/24h, negative T waves V1-2,
AC 9	74	M	LBBB VT (65)	Epsilon waves, negative T waves V1-3, akinesia in dilated RV.	LBBB VT, late potentials
AC 10	77	M	LBBB VT (76)	LBBB VT with superior axis, dyskinesia in dilated RV	Late potentials
AC 11	47	F	NSVT (43)	LBBB VT with superior axis, negative T waves V1-3, structural major abnormalities	Minor abnormalities on biopsy
AC 12	38	M	RBBB VT (37)	LBBB VT with superior axis, negative T waves V1-3, structural major abnormalities	Prolonged TAD, late potentials
AC 13	30	F	Palpitations (22)	Father with AC, structural major abnormalities	LBBB VT with inferior axis, minor abnormalities on biopsy
AC 14	65	F	Palpitations (59)	Negative T waves V1-3, epsilon waves V1-3, brother with AC, structural major abnormalities	LBBB VT with inferior axis
AC 15	39	F	Palpitations (17)	Father with AC, structural major abnormalities	Prolonged TAD, late potentials, LBBB VT with inferior axis
AC 16	49	F	Negative T waves in V1-3 (48)	Negative T waves in V1-3, LBBB VT with superior axis, brother with AC	Minor abnormalities on biopsy
AC 17	58	M	LBBB VT (34)	Epsilon waves V1-3, LBBB VT with superior axis, structural major abnormalities	Negative T waves V1-2
AC 18	48	M	LBBB VT (41)	Structural major abnormalities	Prolonged TAD, LBBB VT with inferior axis
AC 19	41	F	LBBB VT (29)	Negative T waves V1-3, LBBB VT with superior axis, father with AC, structural major abnormalities	Prolonged TAD, minor abnormalities on biopsy
AC 20	23	F	Palpitations (17)	Negative T waves V1-3, father with AC, structural major abnormalities	Prolonged TAD, >500 PVCs/24h

Major and minor criteria according to the Task Force Criteria and age of first symptoms are shown. Abbreviations: VF: ventricular fibrillation, LBBB: left bundle branch block, VT: ventricular tachycardia, TAD: terminal activation duration, PVC: premature ventricular complex.

mutation (AC10), or AC patients having a missense mutation that thus

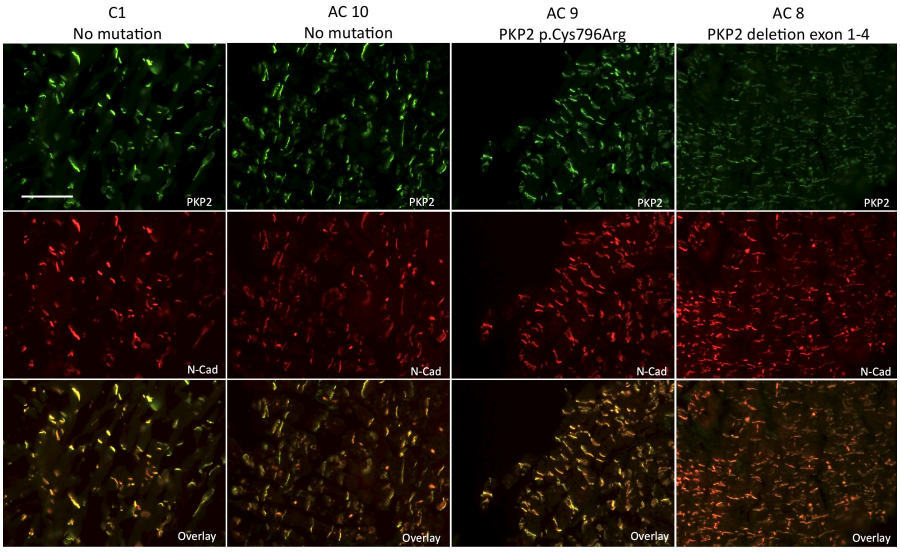

Figure 6.1 – *Undisturbed Plakophilin2 distribution in AC regardless of mutations.* PKP2 is normally present in the intercalated disk in AC patients, regardless of whether a mutation is present in the *PKP2* gene. Haploinsuffiency of PKP2 (in AC8) also showed undisturbed PKP2 distribution. However, reduced signal intensity of PKP2 was identified. N-Cad is used as a marker for the intercalated disk. Scale bar equals 100 μm.

far has not been associated with trafficking defects (AC9). In controls, as well as in tissue from AC patients without identified *PKP2* mutation (AC10) or a p.Cys796Arg mutation (AC9), PKP2 immunoreactive signal levels and distribution were highly comparable. However, in the two AC patients with a deletion of *PKP2* exons 1-4 (AC7 and -8) and one with a deletion of exons 1-14 (AC6), the intensity of the PKP2 immunoreactive signal was clearly reduced (see Figure 6.1 at AC 8). In contrast to this decreased signal intensity, distribution of PKP2 was not affected, since it still showed a complete overlap with N-Cad at the ID.

Distribution and immunoreactive signal levels of PKG, Cx43 and $Na_V1.5$

Previous studies have shown that alterations in PKG expression and distribution can serve as biomarkers, to facilitate diagnosis of AC.[12] Complementary studies also revealed that tissue preservation and di-

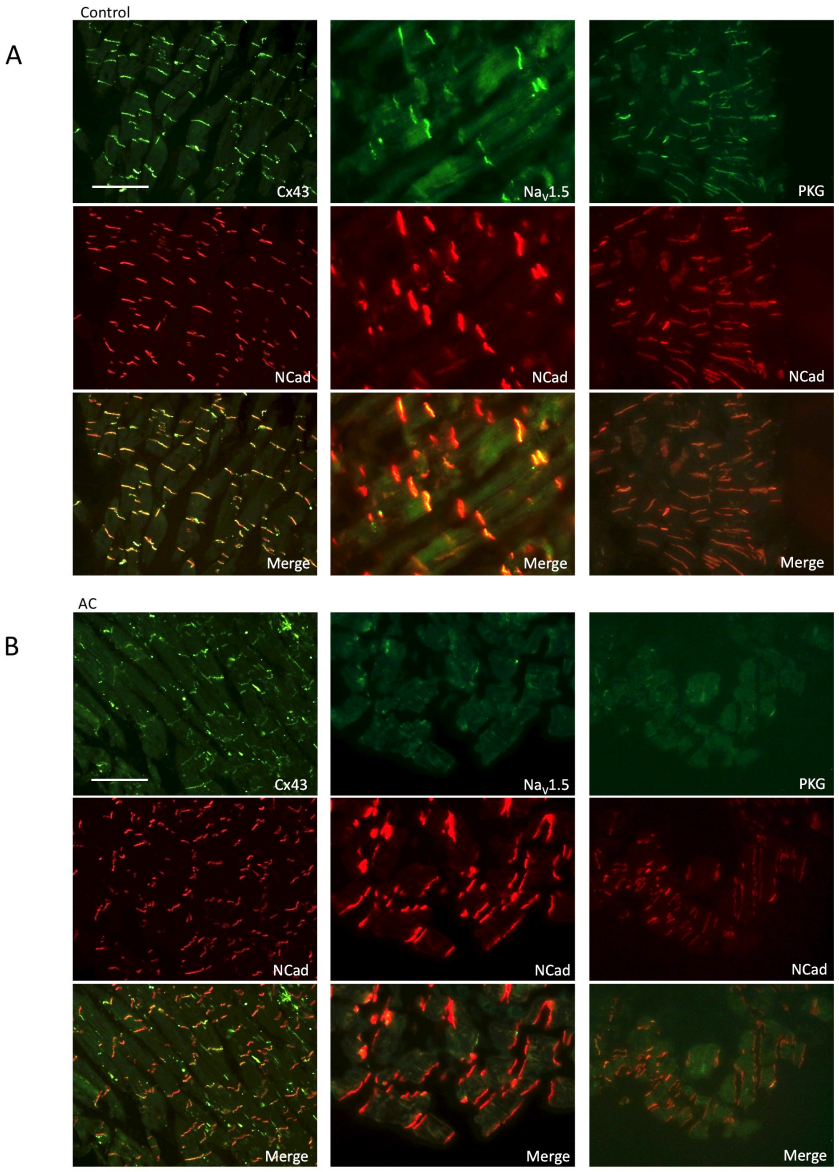

Figure 6.2 – *Expression patterns for Cx43, $Na_V1.5$ and PKG.* A. Double labelings with N-Cadherin. A large subset of the patients (B) showed reduced immunoreactive signal levels for Cx43, $Na_V1.5$ and/or PKG compared to control (A).

lution of the anti-PKG antibody critically determined the appropriateness of evaluation.[25] Serial antibody dilutions were therefore used to determine the best conditions under which the presence or absence of a PKG signal at the intercalated disk, segregated with the clinical diagnosis of AC. At a dilution of 1:100,000 PKG signals were clearly present in the 5 control patients where they co-localized with N-Cad at the ID (Figure 6.2A, right panels). In 5/19 AC patients, PKG labeling was comparable to controls but in 14/19 (74%) patients, PKG signals were clearly reduced and sometimes even completely absent whereas double labeling with antibodies raised against N-Cad always revealed a normal pattern of N-Cad at the ID (Figure 6.2B, right panel).

Analysis of cryo-material from the RVFW (AC 1-5) and RVSB (ARVC 6-20) revealed that Cx43 immunoreactive signal was disturbed (ranging from mild to severe) in 14/20 (70%) patients when compared to the pattern found in the 5 control individuals. Figure 6.2A shows that in control material (left panels), Cx43 and N-Cad closely overlap, while this overlay is partially disrupted in a large percentage of AC patients (Figure 6.2B, left panels). In AC patients, labeling of Cx43 was not only reduced but also clearly heterogeneously distributed. In controls, Cx43 was found almost exclusively at the ID. However, in AC patients, Cx43 signal was not only reduced at the ID, but also sparely present at the lateral sides of the myocytes.

Similarly, double labeling of $Na_V1.5$ and N-Cad revealed a reduced immunoreactive signal of $Na_V1.5$ in 12/17 (65%) patients with labeling in all 5 controls being normal (Figure 6.2A, mid panels). Again, the alterations ranged from reduced signal intensity of $Na_V1.5$ (with normal N-Cad counterstaining) to complete absence of $Na_V1.5$ (Figure 6.2B, mid panels). A blinded cross- evaluation on material of 9 AC patients, performed by the group in NYU (New York) confirmed the assessment made in a separate center in 8/9 cases. Three patients classified as unaffected were recognized as such, and only in 1/6 affected patients the evaluation of $Na_V1.5$ downregulation was not independently confirmed (patient AC18).

We also performed a double labeling of $Na_V1.5$ and Cx43 (Figure 6.3). In areas where Cx43 was normally present in the intercalated disk (upper panels) both in controls and in patients, $Na_V1.5$ was also present at the intercalated disk. We expected, based on previous results in mice,[20] that in areas with a disturbed Cx43 signal, $Na_V1.5$ would also show a disturbed pattern. In Figure 6.2B (lower panels) an area of disturbed Cx43 expression is shown (arrows) and in this place also

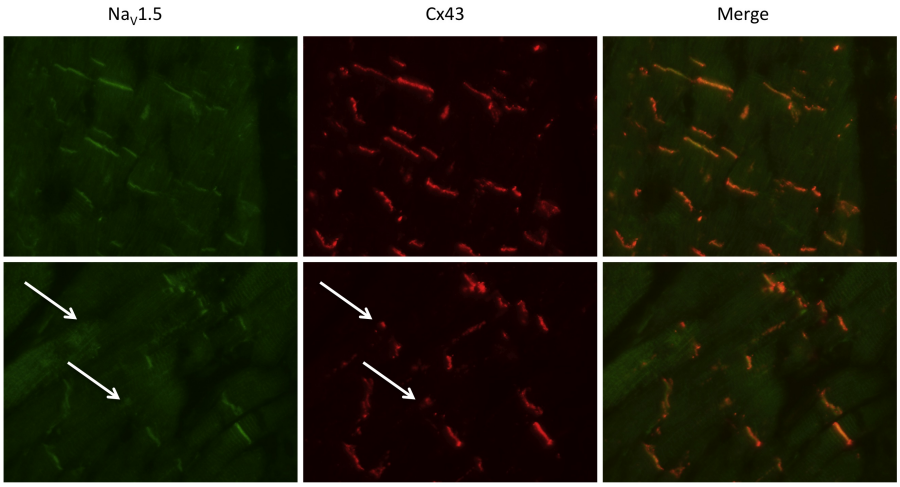

Figure 6.3 – *Double labeling of Cx43 and $Na_V1.5$.* Upper panels show a region with unaffected Cx43 and $Na_V1.5$, whereas lower panels show a region of disturbed Cx43 signal, where also immunoreactive signal intensity of $Na_V1.5$ is reduced.

$Na_V1.5$ signal is reduced. However, we were unable to confirm that in every patient with a disturbed pattern of Cx43, $Na_V1.5$ was concomitantly reduced. We also identified patients that presented a disturbance in Cx43 pattern, without a reduced $Na_V1.5$, and the other way around: patients with reduced $Na_V1.5$ and unchanged Cx43.

Discussion

We have used an immunohistochemical approach to assess the signal intensity and distribution of immunoreactive proteins in samples of human tissue obtained from patients with clinical diagnosis of AC. Our results showed that in a large majority of tissue specimens, signal intensities for Cx43, PKG, and/or $Na_V1.5$ were substantially reduced. In addition, Cx43 and $Na_V1.5$ were often heterogeneously distributed. The observations were apparent, regardless of whether mutations in desmosomal genes were found. In contrast, signal intensities and distribution of N-Cadherin and PKP2 remained unchanged, except in the case of tissue from patients with a genotype that likely would lead to PKP2 haploinsufficiency through deletion of the first 4, or all of the exons.

Several studies have shown a connection between disturbances in mechanical coupling, electrical coupling and excitability of cardiomyocytes.[20, 21, 26] These observations were merely derived from artificial systems, where an extreme reduction of one of the components was induced. In the present study, we have used human AC patient material where immunoreactive signals of the mechanical components appeared generally unaffected, despite the fact that mutations in the mechanical components were present in a large proportion of cases. Since the protein immunoreactivity is highly subjected to tissue preservation and experimental conditions, we assessed detection of a given protein with various antibody dilutions. The observed reduction of PKP2 signal-intensity in patients predicted to be haplo-insufficient suggests that the PKP2 antibody dilution was adequate to detect variations in signal intensity (see Figure 6.1). In addition, control experiments in which the antibody used against PKP2 was further diluted up to 1000 times more than the regular concentration used, still revealed equal but lower intensities of PKP2 in control and patients without a mutation in PKP2 (data not shown).

Mutations in desmosomal proteins are associated with the AC phenotype. A common occurrence is a heterogeneous distribution of cardiac Cx43 at the intercalated disks.[10-12] In the present study, we show for the first time that also junctional immunoreactive signal of $Na_V1.5$ expression is decreased in a large subset of our patients. In general, safe and normal conduction depends on appropriate excitability (facilitated through the $Na_V1.5$ channels), cell-to-cell conduction through Cx43 gap junctions, and tissue geometry (preferred absence of massive insulating fibrosis). Pro-arrhythmic alterations in the latter two factors have been recognized in AC patients before. The common disturbance of Cx43 signals but not of the desmosomal proteins that we described is consistent with the results of Fidler et al,[27] which showed that RVSB of four patients with a *PKP2* mutation all displayed a disturbed Cx43 pattern, with no changes in PKP2 distribution in 3 of the four cases. Of note, the *PKP2* mutations included in our study and those described in the study of Fidler *et al* are different. In the latter case, the mutations were not expected to impair the trafficking of pKP2 to the intercalated disk.

Though multiple components involved in the molecular basis of AC have been identified, the sequence of events that lead to disruption of the macromolecular complex that is situated at the ID still remains fairly unresolved. Whether the molecules of the desmosome, the gap

junctions and the sodium channel complex interact directly, or through unknown molecular partners, remains to be defined. In vitro studies in which PKP2 was deleted by interference strategies revealed a concomitant decrease in intercellular communication, excitability and impulse propagation.[21, 28] On the other hand, reduced presence of PKG (also known as γ-catenin) at the ID may lead to replacement with β-catenin which in turn reduces intra-nuclear levels of β-catenin and as such transcriptional reduction of Cx43.[29, 30] Animal studies in genetically engineered mice have shown that a combination of genetically reduced $Na_V1.5$ and Cx43 levels did induce conduction slowing without, however, exhausting conduction reserve and a resulting increased propensity to arrhythmias.[31] Genetically reduced Cx43 levels on its own appeared also able to induce a reduction of $Na_V1.5$ dependent sodium current.[20, 32] When these conditions were exacerbated in a model of aged mice with reduced levels of Cx43 and $Na_V1.5$, as well as increased amounts of fibrosis, conduction reserve exhausted and a significant incidence of arrhythmias could be recorded.[33] The latter situation fits very well with the progressive deterioration as seen in the AC disease model where increasing amounts of fibrosis are found in the later phase of the disease. Additional insight into the inter-relation of Cx43 and the preservation of cardiac structure was provided in a follow up study in which we showed enhanced fibrosis in mice with reduced Cx43 expression; the latter seemed consequent to enhanced fibroblast activity rather than increased proliferation of these cells.[34]

Though the present study concentrated on a few molecules thought to be relevant to the electrical phenotype, the spectrum of molecular remodeling in AC hearts is likely to be much broader. Within our limitations, our data do suggest that a reduced abundance of $Na_V1.5$ immunoreactive protein at the intercalated disk may be a component of the molecular profile in some AC cases. The latter may, in turn, be a component of the electrophysiological substrate present in AC patients. As in the case of patients suspected of Brugada syndrome, a sodium channel blocker challenge might help for identification and/or stratification of patients at risk of AC, particularly those in the concealed phase of the disease. As a proof of principle, we recently showed that flecainide administration to young heterozygous PKP2 mice with structurally normal hearts (no fibrosis or adiposis detected) led to a high incidence of ventricular arrhythmias and sudden death, whereas the same flecainide challenge did not cause either arrhythmias or death in control littermates.[22]

Study limitations

The immunohistochemical data presented in this study merely show qualitative differences between controls and patients. Immunoreactive signal intensity and distribution of several intercalated disk-associated proteins has been studied in autopsy material from controls and patients and these data have been compared to data obtained with RVSB. These septal biopsies were taken from AC patients that were still under clinical evaluation and were both limited in amount and size, which excludes introduction of additional quantification methodology via Western blotting or by patch clamp. We also did not include a detailed analysis of the degree of fibro-fatty replacement. Though fibrosis was apparent in al biopsies studied, the septal tissue is regarded to be less representative in this aspect.

Conclusion

Immunohistochemical analysis in AC reveals reduced signals for Cx43, PKG and/or $Na_V1.5$ in a majority of patients. The newly identified reduction of $Na_V1.5$ sodium channels might importantly contribute to arrhythmia vulnerability in AC patients and could, in the future, be added as an element of evaluation for risk stratification. Our data further support the notion that deficiency in the abundance and/or function of the sodium channel complex may be one of the multiple arrhythmogenic substrates present in the hearts of patients afflicted with mutations in desmosomal proteins and as such, at risk of ventricular fibrillation and sudden cardiac death.

References

1. Sen-Chowdhry S, Syrris P, Prasad SK, Hughes SE, Merrifield R, Ward D, Pennell DJ, McKenna WJ. Left-dominant arrhythmogenic cardiomyopathy: An under-recognized clinical entity. *J Am Coll Cardiol*. 2008;-52:2175-2187
2. Saffitz JE. The pathobiology of arrhythmogenic cardiomyopathy. *Annu Rev Pathol*. 2011;6:299-321
3. Asimaki A, Syrris P, Wichter T, Matthias P, Saffitz JE, McKenna WJ. A novel dominant mutation in plakoglobin causes arrhythmogenic right ventricular cardiomyopathy. *Am J Hum Genet*. 2007;81:964-973
4. Heuser A, Plovie ER, Ellinor PT, Grossmann KS, Shin JT, Wichter T, Basson CT, Lerman BB, Sasse-Klaassen S, Thierfelder L, MacRae CA, Gerull B. Mutant desmocollin-2 causes arrhythmogenic right ventricular cardiomyopathy. *Am J Hum Genet*. 2006;79:1081-1088
5. Syrris P, Ward D, Evans A, Asimaki A, Gandjbakhch E, Sen-Chowdhry S, McKenna WJ. Arrhythmogenic right ventricular dysplasia/cardiomyopathy associated with mutations in the desmosomal gene desmocollin-2. *Am J Hum Genet*. 2006;79:978-984
6. Pilichou K, Nava A, Basso C, Beffagna G, Bauce B, Lorenzon A, Frigo G, Vettori A, Valente M, Towbin J, Thiene G, Danieli GA, Rampazzo A. Mutations in desmoglein-2 gene are associated with arrhythmogenic right ventricular cardiomyopathy. *Circulation*. 2006;113:1171-1179
7. Rampazzo A, Nava A, Malacrida S, Beffagna G, Bauce B, Rossi V, Zimbello R, Simionati B, Basso C, Thiene G, Towbin JA, Danieli GA. Mutation in human desmoplakin domain binding to plakoglobin causes a dominant form of arrhythmogenic right ventricular cardiomyopathy. *Am J Hum Genet*. 2002;71:1200-1206
8. Gerull B, Heuser A, Wichter T, Paul M, Basson CT, McDermott DA, Lerman BB, Markowitz SM, Ellinor PT, MacRae CA, Peters S, Grossmann KS, Drenckhahn J, Michely B, Sasse-Klaassen S, Birchmeier W, Dietz R, Breithardt G, Schulze-Bahr E, Thierfelder L. Mutations in the desmosomal protein plakophilin-2 are common in arrhythmogenic right ventricular cardiomyopathy. *Nat Genet*. 2004;36:1162-1164
9. Cox MG, van der Zwaag PA, van der Werf C, van der Smagt JJ, Noorman M, Bhuiyan ZA, Wiesfeld AC, Volders PG, van Langen IM, Atsma DE, Dooijes D, van den Wijngaard A, Houweling AC, Jongbloed JD, Jordaens L, Cramer MJ, Doevendans PA, de Bakker JM, Wilde AA, van Tintelen JP, Hauer RN. Arrhythmogenic right ventricular dysplasia/cardiomyopathy: Pathogenic desmosome mutations in index-patients predict outcome of family screening: Dutch arrhythmogenic right ventricular dysplasia/cardiomyopathy genotype-phenotype follow-up study. *Circulation*. 2011;123:2690-2700
10. Kaplan SR, Gard JJ, Carvajal-Huerta L, Ruiz-Cabezas JC, Thiene G, Saffitz JE. Structural and molecular pathology of the heart in carvajal syndrome. *Cardiovasc Pathol*. 2004;13:26-32

11. Kaplan SR, Gard JJ, Protonotarios N, Tsatsopoulou A, Spiliopoulou C, Anastasakis A, Squarcioni CP, McKenna WJ, Thiene G, Basso C, Brousse N, Fontaine G, Saffitz JE. Remodeling of myocyte gap junctions in arrhythmogenic right ventricular cardiomyopathy due to a deletion in plakoglobin (naxos disease). *Heart Rhythm*. 2004;1:3-11
12. Asimaki A, Tandri H, Huang H, Halushka MK, Gautam S, Basso C, Thiene G, Tsatsopoulou A, Protonotarios N, McKenna WJ, Calkins H, Saffitz JE. A new diagnostic test for arrhythmogenic right ventricular cardiomyopathy. *N Engl J Med*. 2009;360:1075-1084
13. van Rijen HV, Eckardt D, Degen J, Theis M, Ott T, Willecke K, Jongsma HJ, Opthof T, de Bakker JM. Slow conduction and enhanced anisotropy increase the propensity for ventricular tachyarrhythmias in adult mice with induced deletion of connexin43. *Circulation*. 2004;-109:1048-1055
14. Gutstein DE, Morley GE, Vaidya D, Liu F, Chen FL, Stuhlmann H, Fishman GI. Heterogeneous expression of gap junction channels in the heart leads to conduction defects and ventricular dysfunction. *Circulation*. 2001;104:1194-1199
15. Wiegerinck RF, van Veen TA, Belterman CN, Schumacher CA, Noorman M, de Bakker JM, Coronel R. Transmural dispersion of refractoriness and conduction velocity is associated with heterogeneously reduced connexin43 in a rabbit model of heart failure. *Heart Rhythm*. 2008;5:1178-1185
16. Boulaksil M, Winckels SK, Engelen MA, Stein M, van Veen TA, Jansen JA, Linnenbank AC, Bierhuizen MF, Groenewegen WA, van Oosterhout MF, Kirkels JH, de Jonge N, Varro A, Vos MA, de Bakker JM, van Rijen HV. Heterogeneous connexin43 distribution in heart failure is associated with dispersed conduction and enhanced susceptibility to ventricular arrhythmias. *Eur J Heart Fail*. 2010;12:913-921
17. Marcus FI, McKenna WJ, Sherrill D, Basso C, Bauce B, Bluemke DA, Calkins H, Corrado D, Cox MG, Daubert JP, Fontaine G, Gear K, Hauer R, Nava A, Picard MH, Protonotarios N, Saffitz JE, Sanborn DM, Steinberg JS, Tandri H, Thiene G, Towbin JA, Tsatsopoulou A, Wichter T, Zareba W. Diagnosis of arrhythmogenic right ventricular cardiomyopathy/dysplasia: Proposed modification of the task force criteria. *Circulation*. 2010;121:1533-1541
18. Winterfield JR, Lee J, Asimaki A, Inada K, Ellinor PT, Tedrow UB, Saffitz J, Stevenson WG. Plakoglobin abnormalities and arrhythmogenesis in idiopathic cardiomyopathies. *Heart Rhythm*. 2010;7:S113
19. Asimaki A, Tandri H, Duffy ER, Winterfield JR, Mackey-Bojack S, Picken MM, Cooper LT, Wilber DJ, Marcus FI, Basso C, Thiene G, Tsatsopoulou A, Protonotarios N, Stevenson WG, McKenna WJ, Gautam S, Remick DG, Calkins H, Saffitz JE. Altered desmosomal proteins in granulomatous myocarditis and potential pathogenic links to arrhythmogenic right ventricular cardiomyopathy. *Circ Arrhythm Electrophysiol*. 2011;4:743-752

20. Jansen JA, Noorman M, Musa H, Stein M, de Jong S, van der Nagel R, Hund TJ, Mohler PJ, Vos MA, van Veen TA, de Bakker JM, Delmar M, van Rijen HV. Reduced heterogeneous expression of cx43 results in decreased $Na_V1.5$ expression and reduced sodium current that accounts for arrhythmia vulnerability in conditional cx43 knockout mice. *Heart Rhythm*. 2012;9:600-607
21. Sato PY, Musa H, Coombs W, Guerrero-Serna G, Patino GA, Taffet SM, Isom LL, Delmar M. Loss of plakophilin-2 expression leads to decreased sodium current and slower conduction velocity in cultured cardiac myocytes. *Circ Res*. 2009;105:523-526
22. Cerrone M, Noorman M, Lin X, Chkourko H, Liang FX, van der Nagel R, Hund T, Birchmeier W, Mohler P, van Veen TA, van Rijen HV, Delmar M. Sodium current deficit and arrhythmogenesis in a murine model of plakophilin-2 haploinsufficiency. *Cardiovasc Res*. 2012
23. van Veen TA, van Rijen HV, Wiegerinck RF, Opthof T, Colbert MC, Clement S, de Bakker JM, Jongsma HJ. Remodeling of gap junctions in mouse hearts hypertrophied by forced retinoic acid signaling. *J Mol Cell Cardiol*. 2002;34:1411-1423
24. Hund TJ, Koval OM, Li J, Wright PJ, Qian L, Snyder JS, Gudmundsson H, Kline CF, Davidson NP, Cardona N, Rasband MN, Anderson ME, Mohler PJ. A beta(iv)-spectrin/camkii signaling complex is essential for membrane excitability in mice. *J Clin Invest*. 2010;120:3508-3519
25. Munkholm J, Christensen AH, Svendsen JH, Andersen CB. Usefulness of immunostaining for plakoglobin as a diagnostic marker of arrhythmogenic right ventricular cardiomyopathy. *Am J Cardiol*. 2012;109:272-275
26. Oxford EM, Musa H, Maass K, Coombs W, Taffet SM, Delmar M. Connexin43 remodeling caused by inhibition of plakophilin-2 expression in cardiac cells. *Circ Res*. 2007;101:703-711
27. Fidler LM, Wilson GJ, Liu F, Cui X, Scherer SW, Taylor GP, Hamilton RM. Abnormal connexin43 in arrhythmogenic right ventricular cardiomyopathy caused by plakophilin-2 mutations. *J Cell Mol Med*. 2009;13:4219-4228
28. Sato PY, Coombs W, Lin X, Nekrasova O, Green KJ, Isom LL, Taffet SM, Delmar M. Interactions between ankyrin-g, plakophilin-2, and connexin43 at the cardiac intercalated disk. *Circ Res*. 2011;109:193-201
29. van der Heyden MA, Rook MB, Hermans MM, Rijksen G, Boonstra J, Defize LH, Destree OH. Identification of connexin43 as a functional target for wnt signalling. *J Cell Sci*. 1998;111 (Pt 12):1741-1749
30. Garcia-Gras E, Lombardi R, Giocondo MJ, Willerson JT, Schneider MD, Khoury DS, Marian AJ. Suppression of canonical wnt/beta-catenin signaling by nuclear plakoglobin recapitulates phenotype of arrhythmogenic right ventricular cardiomyopathy. *J Clin Invest*. 2006;116:2012-2021
31. Stein M, van Veen TA, Remme CA, Boulaksil M, Noorman M, van Stuijvenberg L, van der Nagel R, Bezzina CR, Hauer RN, de Bakker

JM, van Rijen HV. Combined reduction of intercellular coupling and membrane excitability differentially affects transverse and longitudinal cardiac conduction. *Cardiovasc Res*. 2009;83:52-60

32. Desplantez T, McCain ML, Beauchamp P, Rigoli G, Rothen-Rutishauser B, Parker KK, Kleber AG. Connexin43 ablation in foetal atrial myocytes decreases electrical coupling, partner connexins, and sodium current. *Cardiovasc Res*. 2012;94:58-65
33. Stein M, Boulaksil M, Jansen JA, Herold E, Noorman M, Joles JA, van Veen TA, Houtman MJ, Engelen MA, Hauer RN, de Bakker JM, van Rijen HV. Reduction of fibrosis-related arrhythmias by chronic renin-angiotensin-aldosterone system inhibitors in an aged mouse model. *Am J Physiol Heart Circ Physiol*. 2010;299:H310-321
34. Jansen JA, van Veen TA, de Jong S, van der Nagel R, van Stuijvenberg L, Driessen H, Labzowski R, Oefner CM, Bosch AA, Nguyen TQ, Goldschmeding R, Vos MA, de Bakker JM, van Rijen HV. Reduced cx43 expression triggers increased fibrosis due to enhanced fibroblast activity. *Circ Arrhythm Electrophysiol*. 2012

CHAPTER 7

Immunohistochemical analysis of septal biopsies to diagnose AC requires a highly standardized methodology

Maartje Noorman[1,5*], Sara Hakim[1*], Angeliki Asimaki[2], Moniek GPJ Cox[3,5], Harold VM van Rijen[1], Marcel AG van der Heyden[1], Nicolaas de Jonge[3], Aryan Vink[4], Roel A de Weger[4], Andras Varro[6], Richard NW Hauer[3,5], Jeffrey E Saffitz[2#], Toon AB van Veen[1#]

1. Department of Medical Physiology, University Medical Center Utrecht, Utrecht, The Netherlands.
2. Department of Pathology, Beth Israel Deaconess Medical Center and Harvard Medical School, Boston, USA
3. Department of Cardiology, University Medical Center Utrecht, Utrecht, The Netherlands.
4. Department of Pathology, University Medical Center Utrecht, Utrecht, The Netherlands.
5. Interuniversity Cardiology Institute of The Netherlands, Utrecht, The Netherlands
6. Department of Pharmacology & Pharmacotherapy, Faculty of Medicine, University of Szeged, Hungary

*, # *These authors contributed equally to this work*

Submitted

Abstract

Background: Arrhythmogenic cardiomyopathy (AC) is considered to be a desmosomal disease with a predominant right ventricular (RV) phenotype. Reduced signal intensity for plakoglobin (PKG) has been proposed as a marker that contributes to diagnosis of the disease. In this technical study we investigated how methodology-related differences caused by tissue preservation and antibody dilutions affect an appropriate diagnosis.
Methods: Autopsy- and biopsy material was obtained from 5 control and 10 AC patients that fulfilled the diagnostic Task Force Criteria as proposed in 2010. Immunohistochemical analysis was performed on cryo-sections and formalin fixed material using antibodies against PKG and N-Cadherin.
Results: Immunohistochemistry on formalin-fixed material showed a reduced signal for Plakoglobin in 7/10 AC patients in a bidirectional, double-blinded exchange experiment in which 77% were correctly classified. Unmasking this disturbed PKG pattern was highly dependent on tissue-preservation and antibody-dilution since on cryo-sections the reduced presence in patients could only be found at very strong antibody dilutions.
Conclusions: Reduced immunoreactive signal Plakoglobin at the intercalated disks can be observed in a large majority of AC patients. These changes can comparably be detected on both cryo- and formalin-fixed material but demand a different, highly defined and uniformly used approach.

Introduction

Arrhythmogenic Right Ventricular Cardiomyopathy (ARVC), in more recent terminology known as Arrhythmogenic Cardiomyopathy (AC), is a progressive disease associated with arrhythmias, sudden cardiac death and heart failure. Though left ventricular predominance in phenotypes is also known, histologically it is considered to present as a predominant right ventricular (RV) phenotype which is characterized by fibro-fatty replacement of the myocardium, especially in the triangle of dysplasia in the RV.[1] In about 60% of the cases, AC is associated with mutations in genes encoding desmosomal proteins like Plakophilin2 (PKP2),[2, 3] Desmoplakin (DSP),[4] Desmoglein2 (DSG2),[5] Desmocollin2 (DSC2),[6, 7] and Plakoglobin (PKG).[8] The desmosome is one of the intercellular junctions situated in the intercalated disk, at the longitudinal ends of cardiomyocytes. There it ensures the mechanical interaction of myocytes, through linkage with desmin within the cytoskeleton.[9]

Historically, the universal standard for diagnosis of AC has been the demonstration of fibro-fatty infiltration at autopsy, or after heart transplantation. To facilitate early clinical diagnosis in patients suspected of AC, McKenna *et al* proposed the Task Force Criteria for AC in 1994,[10] which have been revised recently.[11, 12] These criteria, subdivided in major and minor, include structural abnormalities and regional dysfunction within the heart, tissue characteristics, electrical abnormalities, and family history.

One of the major criteria concerns the histopathological status of tissue. For this, analysis of endomyocardial biopsies taken from the thin right ventricular free wall (RVFW) is relevant but potentially hazardous because of the risk of perforation. In contrast, to collect right ventricular septal biopsies (RVSB) biopsies is a relatively safe procedure but is considered of limited value for diagnosis of AC based on fibro-fatty replacement since in that perspective the septum often is not or only mildly affected.[13]

In the last few years, PKG immunoreactivity has been identified as a tool to discriminate tissue (taken as biopsy or at autopsy) from AC patients, healthy controls and, importantly, also from patients with other structural heart diseases (hypertrophic, dilated and ischemic cardiomyopathy). PKG signals appeared to be strongly reduced in AC patients exclusively, and not in other cardiomyopathies.[14] In a follow-up, PKG signals also appeared to be reduced in AC-related cardiac diseases like sarcoidosis and giant cell myocarditis.[15, 16] Interestingly,

PKG signals appeared not only reduced in the affected RVFW, but also in macroscopically healthy and histologically not affected left ventricular free wall (LVFW) and interventricular septum. The latter aspect opens new possibilities to use these RVSB for additive immunohistochemical analysis to support the complex diagnosis of AC.

To follow up on the previous observations, in the present study we have addressed several important technical issues required for an appropriate immunohistochemical analysis of AC tissue. Using immunohistochemistry on both formalin fixed and cryo-sections derived from healthy controls and AC patients, we determined expression and distribution of PKG in the RVFW as well as in RVSB.

Methods

Right ventricular free wall (RVFW) myocardium (on average 2-4 cm^3) was obtained from 5 patients, with diagnosis confirmed at autopsy or heart transplantation and from 5 age and sex matched controls (without any cardiovascular history). This material was flushed with PBS and rapidly frozen in liquid nitrogen. In addition, during cardiovascular intervention using a disposable Jawz forceps (Argon Medical Devices, Athens Tx, USA), a maximum of 6 RVSB (2-4 mm^3) were taken from another 5 patients that were diagnosed according to clinical Task Force criteria [11, 12]. At least one biopsy sample was routinely formalin-fixed and embedded in paraffin. Additional biopsy samples were mildly fixed following a slightly modified protocol as published by Bajanca *et al.*[17] Finally, biopsies were frozen in liquid nitrogen and cryo-sectioned at a thickness of 10 μm whereas paraffin-embedded samples were sectioned at 4 μm. All patients consented to clinical evaluation according to the Task Force criteria. For this study, numbers and types of diagnostic tests undergone by the patients were not influenced by inclusion in this study. Therefore, no review by the ethical committee was required.

Cryo-sections were rehydrated in phosphate-buffered saline (PBS), and permeabilized in 0.2% Triton X-100/PBS (1 h). Subsequently, sections were blocked in 2% bovine serum albumin (BSA, Sigma)/PBS for 30 min. Then, sections were double-labeled overnight with primary antibodies against PKG (mouse, P-8087 Sigma, 1:100-1:150,000) and N-Cadherin (rabbit, C-3678 Sigma, 1:800), dissolved in PBS in presence of 10% normal goat serum, (NGS). After another block with 2% BSA for 30 min, a 2 h secondary labeling was performed with appropriate Texas Red (TR)- (1:100) and fluorescein isothiocyanate (FITC)-conjugated

(1:250) antibodies (715-075-150 and 11-095-144 respectively, Jackson Laboratories) in presence of 10% NGS. All procedures were performed at RT and between all subsequent steps sections were washed with PBS. After immunolabeling, sections were mounted in Vectashield (Vector Laboratories) and examined with a Nikon Optipot-2 light microscope.

Formalin-fixed sections were de-paraffinized in xylol and rehydrated. Antigen was retrieved by heating in citrate buffer (10 mmol/l, pH 6.0) in a microwave for 11 min. Subsequently, sections were permeabilized and blocked by incubating for 40 min at RT in PBS containing 1% Triton X-100, 3% NGS and 1% BSA. Next, sections were double-labeled with primary antibodies against PKG (mouse, P-8087 Sigma, 1:200-1:50,000) and N-Cadherin (rabbit, C-3678 Sigma, 1:800) (overnight at 4ºC) followed by secondary antibody incubation at RT for 2 h. Secondary labeling was performed with appropriate Texas Red and FITC conjugated whole IgG antibodies (715-075-150 and 11-095-144 respectively, Jackson Laboratories, 1:400). Finally, sections were mounted in Vectashield.

Results and Discussion

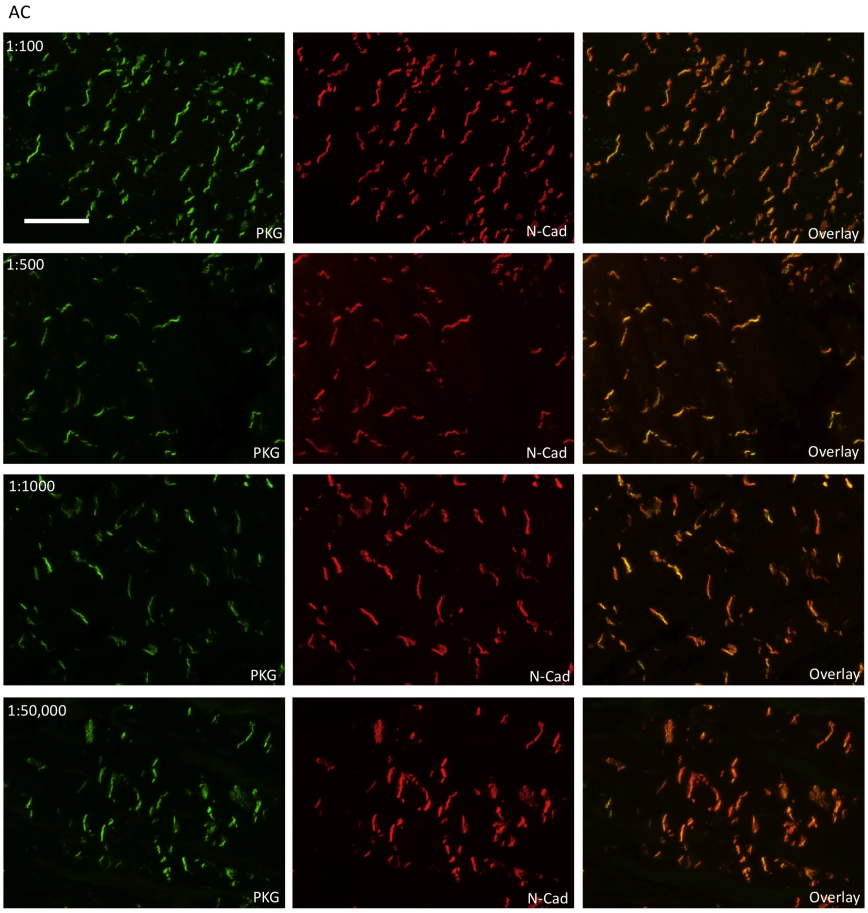

Figure 7.1 – Dilutions of the PKG antibody up to 1:50,000 still allowed to visualize PKG at the intercalated disks on cryo-sections of AC patients.Digital pictures of tissue incubated with the strongest dilutions of PKG-antibody were taken using longer exposure times, which means that labeling intensities are not comparable between subsequent dilutions. Scale bar equals 100 μm.

In order to evaluate the expression of PKG, cryo-sections of controls and patients were incubated with the PKG-antibody at dilutions ranging from 1:100 to 1:50,000. As illustrated in Figure 7.1, all patients (both at RVFW autopsy material and RVSB) displayed PKG at the intercalated disk. Signal intensities were equal to those found in con-

trols (not shown), and had a high degree of overlay when double labeled with N-Cadherin. The latter served as a stable and positive control to assure presence of intact intercalated disks. To understand the outcome of those initial experiments and more specifically, the noticed difference with the previously reported data regarding down regulation of PKG labeling in AC,[14] additional (stronger) dilutions of the PKG-antibody were tested and experiments were also repeated on sections derived from formalin fixed materials. When the PKG-antibody was even further diluted (up to 1:150,000) the previously reported differences between controls and AC patients with respect to PKG expression became also apparent when tested on those cryo-sections. As depicted in Figure 7.2 labeling intensities of PKG were clearly reduced in 65% of the patients as compared to controls at a dilution of 1:100,000 whereas intensities were always indistinguishable at the dilution of 1:50,000.

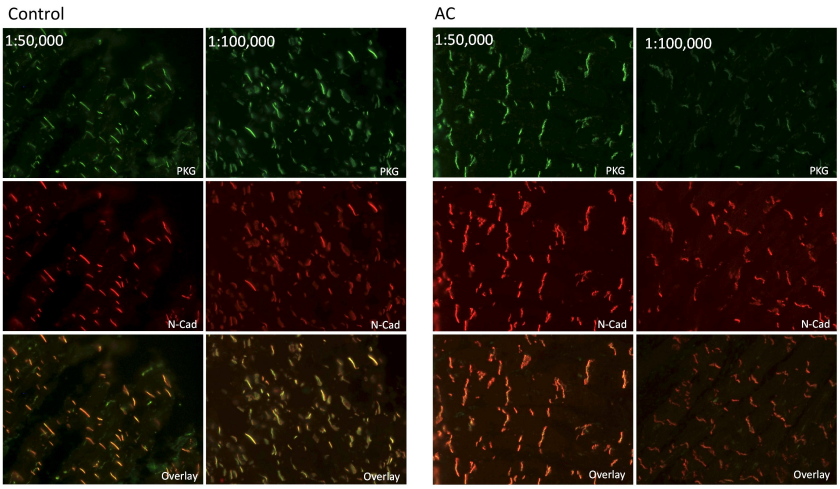

Figure 7.2 – **a:** controls and **b:** patients. Dilution of 1:50,000 of the PKG antibody still allows PKG to be visible in the intercalated disk in both controls and patients in cryo-material. Further dilution to 1:100,000 showed a difference in PKG intensity between controls and patients.

To evaluate the effect of different concentrations of the PKG-antibody on thinner and differently prepared tissue sections, experiments were repeated on formalin fixed autopsy material. As shown in Figure 7.3A, dilution of the PKG-antibody revealed that in controls, the PKG signals were clearly present at a dilution of 1:1000 whereas they disappeared when antibodies were even further diluted (data not shown).

As a reminder, positive signals on cryo-sections could still be detected at dilutions up to 1:150,000. Clearly, on formalin fixed material, the signal to noise ratio was compromised compared to that on cryo-material. Labeling on formalin-fixed AC material resulted in similar diminished signals upon increasing dilution. At a dilution of 1:1000, PKG signals were absent or clearly reduced in 60% of AC patients (Figure 7.3B), but still present in all controls. To further substantiate these findings, a bidirectional double-blinded exchange of formalin fixed material was arranged between the labs in Boston (Saffitz) and Utrecht (van Veen). To discriminate controls from AC, immunolabeling against PKG (1:1000) on RV sections of 13 individuals (3 controls and 10 AC patients) resulted in an appropriate diagnosis in 10/13 cases (77%), which is in line with previously reported data.[14] The 3 controls showed normal PKG labeling of the intercalated disks and were all identified as 'control'. Based on a similar pattern of PKG labeling, from the 10 diagnosed patients 3 were inappropriately classified as 'controls' (one in Utrecht and the other 2 in Boston). In the remaining 7, PKG signals appeared to be completely absent or severely disturbed and as such those patients were correctly identified as AC.

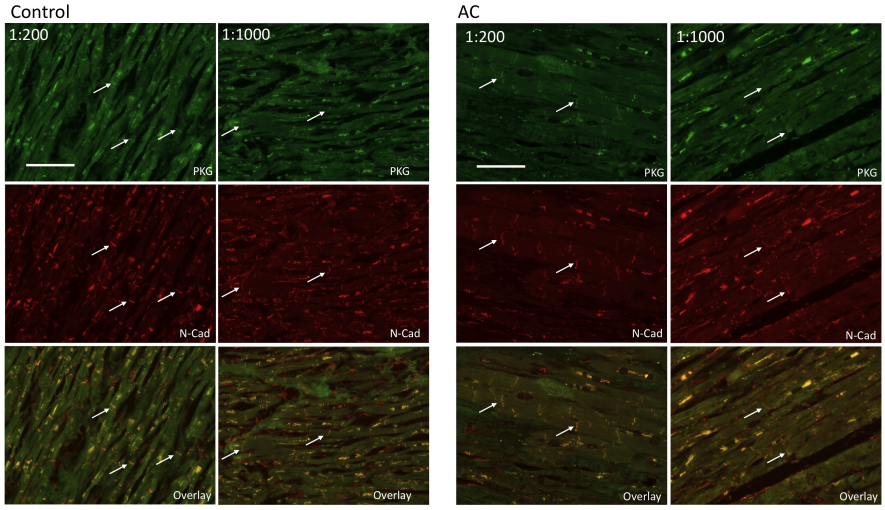

Figure 7.3 – **a**: controls and **b**: patients. On formalin fixed material, dilutions of the PKG antibody below 1:1000 failed to visualize PKG at the intercalated disks on sections of both control- and AC material. Scale bar equals 100 μm.

This significant dependence on the experimental conditions and tech-

niques used was also applicable to the mentioned study where the antibody had to be diluted up to 1:50,000 when peroxidase-based labeling was applied whereas 1:1000 was used for fluorescent labeling.[14] Another factor that in the present study may have contributed to the initial absence of differences in PKG signals between controls and AC patients when analyzed on frozen sections is based on the fact that the frozen sections were of 10 μm thickness, whereas the paraffin-embedded sections were only 4 μm thick. This most likely means that in the frozen sections much more epitope is available, leading to increased signal intensities which compromises detection of potential differences between controls and patients. Not unlikely, the difference in antibody dilution suitable to detect PKG in either cryo-sections (1:100,000) or formalin-fixed sections (1:1000) may be influenced by this difference in thickness of the sections. Finally, it should also be emphasized that the absence of immunohistochemical signal does not prove that the protein is absent. The ability to detect an immunohistochemical signal depends on the local concentration and accessibility of the epitope, the titer and binding affinity of the antibody, and the specific reaction conditions used in the immunostaining experiments.

Conclusion

The current data derived upon analysis of tissues that have been preserved differently (cryo-frozen versus formalin fixed), demands a highly defined immunohistochemical procedure to allow a predictive and universal contribution of such data in characterization of AC. To make meaningful comparisons, controls and patient samples must be batched and immunostained under identical conditions. Furthermore, the great dependence of signal intensity on the immunostaining conditions (antibody titer and characteristics, tissue preservation and thickness of the material) must always be a point of consideration.

References

1. Thiene G, Nava A, Corrado D, Rossi L, Pennelli N. Right ventricular cardiomyopathy and sudden death in young people. *N Engl J Med.* 1988;318:129-133
2. Gerull B, Heuser A, Wichter T, Paul M, Basson CT, McDermott DA, Lerman BB, Markowitz SM, Ellinor PT, MacRae CA, Peters S, Grossmann KS, Drenckhahn J, Michely B, Sasse-Klaassen S, Birchmeier W, Dietz R, Breithardt G, Schulze-Bahr E, Thierfelder L. Mutations in the desmosomal protein plakophilin-2 are common in arrhythmogenic right ventricular cardiomyopathy. *Nat Genet.* 2004;36:1162-1164
3. van Tintelen JP, Entius MM, Bhuiyan ZA, Jongbloed R, Wiesfeld AC, Wilde AA, van der Smagt J, Boven LG, Mannens MM, van Langen IM, Hofstra RM, Otterspoor LC, Doevendans PA, Rodriguez LM, van Gelder IC, Hauer RN. Plakophilin-2 mutations are the major determinant of familial arrhythmogenic right ventricular dysplasia/cardiomyopathy. *Circulation.* 2006;113:1650-1658
4. Rampazzo A, Nava A, Malacrida S, Beffagna G, Bauce B, Rossi V, Zimbello R, Simionati B, Basso C, Thiene G, Towbin JA, Danieli GA. Mutation in human desmoplakin domain binding to plakoglobin causes a dominant form of arrhythmogenic right ventricular cardiomyopathy. *Am J Hum Genet.* 2002;71:1200-1206
5. Pilichou K, Nava A, Basso C, Beffagna G, Bauce B, Lorenzon A, Frigo G, Vettori A, Valente M, Towbin J, Thiene G, Danieli GA, Rampazzo A. Mutations in desmoglein-2 gene are associated with arrhythmogenic right ventricular cardiomyopathy. *Circulation.* 2006;113:1171-1179
6. Syrris P, Ward D, Evans A, Asimaki A, Gandjbakhch E, Sen-Chowdhry S, McKenna WJ. Arrhythmogenic right ventricular dysplasia/cardiomyopathy associated with mutations in the desmosomal gene desmocollin-2. *Am J Hum Genet.* 2006;79:978-984
7. Heuser A, Plovie ER, Ellinor PT, Grossmann KS, Shin JT, Wichter T, Basson CT, Lerman BB, Sasse-Klaassen S, Thierfelder L, MacRae CA, Gerull B. Mutant desmocollin-2 causes arrhythmogenic right ventricular cardiomyopathy. *Am J Hum Genet.* 2006;79:1081-1088
8. Asimaki A, Syrris P, Wichter T, Matthias P, Saffitz JE, McKenna WJ. A novel dominant mutation in plakoglobin causes arrhythmogenic right ventricular cardiomyopathy. *Am J Hum Genet.* 2007;81:964-973
9. Noorman M, van der Heyden MA, van Veen TA, Cox MG, Hauer RN, de Bakker JM, van Rijen HV. Cardiac cell-cell junctions in health and disease: Electrical versus mechanical coupling. *J Mol Cell Cardiol.* 2009;47:23-31
10. McKenna WJ, Thiene G, Nava A, Fontaliran F, Blomstrom-Lundqvist C, Fontaine G, Camerini F. Diagnosis of arrhythmogenic right ventricular dysplasia/cardiomyopathy. Task force of the working group myocardial and pericardial disease of the european society of cardiology

and of the scientific council on cardiomyopathies of the international society and federation of cardiology. *Br Heart J*. 1994;71:215-218

11. Marcus FI, McKenna WJ, Sherrill D, Basso C, Bauce B, Bluemke DA, Calkins H, Corrado D, Cox MG, Daubert JP, Fontaine G, Gear K, Hauer R, Nava A, Picard MH, Protonotarios N, Saffitz JE, Sanborn DM, Steinberg JS, Tandri H, Thiene G, Towbin JA, Tsatsopoulou A, Wichter T, Zareba W. Diagnosis of arrhythmogenic right ventricular cardiomyopathy/dysplasia: Proposed modification of the task force criteria. *Circulation*. 2010;121:1533-1541
12. Cox MG, van der Smagt JJ, Noorman M, Wiesfeld AC, Volders PG, van Langen IM, Atsma DE, Dooijes D, Houweling AC, Loh P, Jordaens L, Arens Y, Cramer MJ, Doevendans PA, van Tintelen JP, Wilde AA, Hauer RN. Arrhythmogenic right ventricular dysplasia/cardiomyopathy diagnostic task force criteria: Impact of new task force criteria. *Circ Arrhythm Electrophysiol*. 2010;3:126-133
13. Basso C, Ronco F, Marcus F, Abudureheman A, Rizzo S, Frigo AC, Bauce B, Maddalena F, Nava A, Corrado D, Grigoletto F, Thiene G. Quantitative assessment of endomyocardial biopsy in arrhythmogenic right ventricular cardiomyopathy/dysplasia: An in vitro validation of diagnostic criteria. *Eur Heart J*. 2008;29:2760-2771
14. Asimaki A, Tandri H, Huang H, Halushka MK, Gautam S, Basso C, Thiene G, Tsatsopoulou A, Protonotarios N, McKenna WJ, Calkins H, Saffitz JE. A new diagnostic test for arrhythmogenic right ventricular cardiomyopathy. *N Engl J Med*. 2009;360:1075-1084
15. Winterfield JR, Lee J, Asimaki A, Inada K, Ellinor PT, Tedrow UB, Saffitz J, Stevenson WG. Plakoglobin abnormalities and arrhythmogenesis in idiopathic cardiomyopathies. *Heart Rhythm*. 2010;7:S113
16. Asimaki A, Tandri H, Duffy ER, Winterfield JR, Mackey-Bojack S, Picken MM, Cooper LT, Wilber DJ, Marcus FI, Basso C, Thiene G, Tsatsopoulou A, Protonotarios N, Stevenson WG, McKenna WJ, Gautam S, Remick DG, Calkins H, Saffitz JE. Altered desmosomal proteins in granulomatous myocarditis and potential pathogenic links to arrhythmogenic right ventricular cardiomyopathy. *Circ Arrhythm Electrophysiol*. 2011;4:743-752
17. Bajanca F, Luz M, Duxson MJ, Thorsteinsdottir S. Integrins in the mouse myotome: Developmental changes and differences between the epaxial and hypaxial lineage. *Dev Dyn*. 2004;231:402-415

CHAPTER 8

Sodium current deficit and arrhythmogenesis in a murine model of Plakophilin-2 haploinsufficiency

Marina Cerrone[1*], Maartje Noorman[2,3*], Xianming Lin[1], Halina Chkourko[1], Feng-Xia Liang[4], Roel van der Nagel[2], Thomas J Hund[5], Peter J Mohler[5], Toon AB van Veen[2], Harold VM van Rijen[2], Mario Delmar[1]

1. Division of Cardiology, New York University School of Medicine. New York, NY, USA
2. Department of Medical Physiology, University Medical Center Utrecht, Utrecht, The Netherlands
3. Interuniversity Cardiology Institute of The Netherlands, Utrecht, The Netherlands
4. Office of Collaborative Science Microscopy Core, New York University School of Medicine, New York, NY, USA
5. Dorothy M. Davis Heart and Lung Research Institute, Departments of Internal Medicine, Division of Cardiovascular Medicine, Physiology & Cell Biology, The Ohio State University Medical Center, Columbus, OH, USA

** These authors contributed equally to this work*

Cardiovascular Research 2012

Abstract

Aims: shRNA-mediated loss of expression of the desmosomal protein plakophilin-2 leads to sodium current (I_{Na}) dysfunction. Whether *pkp2* gene haploinsufficiency leads to I_{Na} deficit *in vivo*, remains undefined. Mutations in *pkp2* are detected in Arrhythmogenic Cardiomyopathy. Ventricular fibrillation and sudden death often occur in the "concealed phase" of the disease, prior to overt structural damage. The mechanisms responsible for these arrhythmias remain poorly understood. We sought to characterize the morphology, histology and ultrastructural features of PKP2-heterozygous-null (PKP2-Hz) murine hearts, and explore the relation between PKP2 abundance, I_{Na} function and cardiac electrical synchrony.

Methods and Results: Hearts of PKP2-Hz mice were characterized by multiple methods. We observed ultrastructural, but not histological or gross anatomical differences in PKP2-Hz hearts, compared to wild-type littermates. Yet, in myocytes, decreased amplitude and a shift in gating and kinetics of I_{Na} were observed. To further unmask I_{Na} deficiency, we exposed myocytes, Langendorff-perfused hearts and anesthetized animals to a pharmacological challenge (flecainide). In PKP2-Hz hearts, the extent of flecainide-induced I_{Na} block, impaired ventricular conduction, and altered electrocardiographic parameters were larger than controls. Flecainide provoked ventricular arrhythmias and death in PKP2-Hz animals, but not in wild-type.

Conclusions: PKP2 haploinsufficiency leads to I_{Na} deficit in murine hearts. Our data support the notion of a cross-talk between desmosome, and sodium channel complex. They also suggest that I_{Na} dysfunction may contribute to generation and/or maintenance of arrhythmias in PKP2-deficient hearts. Whether pharmacological challenges could help unveil arrhythmia risk in patients with mutations or variants in PKP2, remains undefined.

Introduction

The first descriptions of the intercalated disk defined three structures, all involved in cell-cell communication (desmosomes, adherens junctions and gap junctions). It is now generally accepted that molecules not involved in forming a physical continuum between neighboring cells also populate the intercalated disk. Key among them is $Na_v1.5$, the pore-forming subunit of the sodium channel most abundant in heart. Recent studies have shown that $Na_v1.5$ functionally and physically interacts with other intercalated disk proteins such as SAP-97,[1] Connexin43 (Cx43),[2, 3] and the desmosomal protein plakophilin-2 (PKP2).[3, 4] The latter studies further showed that siRNA-mediated loss of PKP2 expression affects the amplitude and kinetics of the sodium current. These observations, however, were limited to studies in isolated cells, where PKP2 expression was acutely disrupted in vitro. Whether PKP2 deficiency and in particular, *pkp2* haploinsufficiency, leads to sodium current deficit in vivo, remains undefined.

The importance of PKP2 in cardiac function is highlighted by the fact that mutations in the *pkp2* gene are found in several cases of arrhythmogenic cardiomyopathy (AC; also known as "arrhythmogenic right ventricular cardiomyopathy" or "ARVC"). Of relevance, ventricular fibrillation and sudden death in patients with AC often occur in the "concealed phase" of the disease, prior to overt structural damage (see [5] for review). The mechanisms responsible for life-threatening arrhythmias in the concealed phase of AC, remain unclear. We postulate that sodium channel function is disrupted by PKP2 haploinsufficiency. As such, we propose that sodium channel dysfunction may be a contributing factor to arrhythmogenesis in PKP2-deficient hearts.

Germline knockout of PKP2 in mice leads to embryonic lethality.[6] However, heterozygous animals are viable and live through adulthood. The structural and functional consequences of PKP2 deficiency in the murine heart remain to be defined. In the present study, we conducted a general characterization of the anatomical, histological and ultrastructural features of the hearts of mice heterozygous-null for PKP2 (PKP2-Hz). Our studies revealed that the PKP2-Hz hearts showed ultrastructural, but not histological or gross anatomical differences, when compared with wild-type (WT) littermates. Yet, in myocytes from these structurally normal hearts, a sodium current deficit was observed. Previous studies have shown that the consequences of sodium current deficiency on cardiac electrophysiology can be unmasked by exposure to sodium channel blockers, such as flecainide.[7-12] We there-

fore exposed isolated myocytes, Langendorff-perfused hearts and anesthetized whole animals with the PKP2-Hz genotype, and their control littermates, to this drug. Our results show that in PKP2-Hz hearts, the extent of flecainide-induced use-dependent I_{Na} block, impaired ventricular conduction, and altered electrocardiographic parameters were larger than in controls. The pharmacological challenge also provoked ventricular arrhythmias and death in PKP2-Hz animals, but not in the WT controls. The possible implications of these findings to the pathophysiology of AC are discussed.

Methods

Determination of mice genotype

Mice heterozygous-null for the *pkp2* gene (PKP2-Hz) were generated as described previously[6] and kindly provided by Dr. Walter Birchmeier (Berlin, Germany). PCR genotyping for the wildtype allele was performed using oligonucleotides 5'-GATCCTGGGTCACCTGGACA-3' and 5'-AGGGTCTGCTGCACCTGCT-3'. Identification of the mutant allele was performed by PCR using oligonucleotides 5'-GATCCTGGGTCACCTGGACA-3' and 5'-CTTCTGAGGGGATCGGCAATA-3'. Mice were bred in the C57Bl6 background.

Protein identification in murine heart lysate

Total murine heart lysate was prepared as described previously.[13] Equal amounts of protein (25 μg/lane) of each sample were separated on 7% (for $Na_V1.5$) or 10% SDS-polyacrylamide gels (for the remaining proteins) and transferred by electrophoresis to nitrocellulose membranes (Biorad). Equal protein loading was assessed by Ponceau S staining. After first and second antibody incubation, immuno-reactivity was detected using ECL chemiluminescence kit (Amersham). The following antibodies were used for Western blots: Plakophilin-2 (PKP2; 1:1000; Progen), plakoglobin (PKG; 1:100; Sigma), connexin43 (Cx43; 1:250; Transduction Laboratories), N-cadherin (N-Cad; 1:800; Sigma), GAPDH (1:1000, Millipore), and $Na_V1.5$ (1:200).[14] Secondary labeling was performed with peroxidase-conjugated secondary antibodies (1:7000, Jackson ImmunoResearch).

Data were obtained from a total of 6 WT and 6 PKP2-Hz murine hearts. Each protein was assessed separately (separate gels). Autoradiography images for each Western blot, and the corresponding Pon-

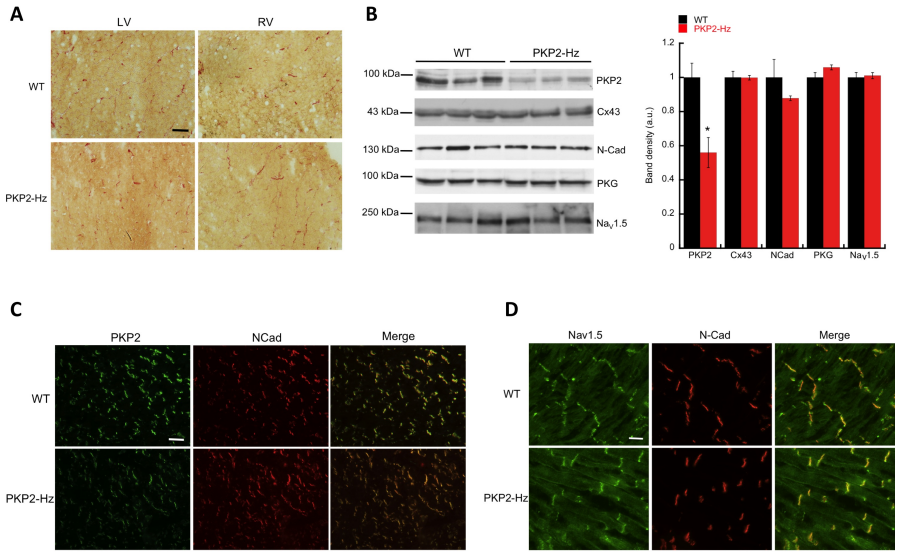

Figure 8.1 – *Characterization of PKP2-Hz hearts.* **A:** Picrosirius red staining to determine collagen abundance. Images obtained from either left (LV; left) or right ventricle (RV; right) of mice wildtype (WT; top) or PKP2-Hz (bottom). Extent of Picrosirius-red staining was determined from the fraction of Sirius red-positive pixels within a field. Data for each field sampled in a WT heart normalized to the average value of 12 random fields in the same heart. Data for PKP2-Hz hearts measured relative to the average value of the littermate WT heart, processed in parallel. No difference was observed between genotypes when compared to the respective ventricle: RV-WT: 1.0±0.16, RV-PKP2-Hz: 0.77±0.08; pNS. LV-WT: 1.0±0.15, LV-PKP2-Hz 1.25±0.16; pNS (ANOVA). N=4, n=48. Calibration bar, 50 μm. **B**: Western blots for intercalated disk proteins. For quantification (right panel), band densities were corrected by total protein, and PKP2-Hz data measured relative to WT on same exposure. *p<0.05 compared to WT. All other comparisons, **C and D**: Immunofluorescence images for PKP2 (green) and N-Cad (red; C; Calibration bar, 50 μm) and for $Na_V1.5$ (green) and N-Cad (red; D; Calibration bar 25 μm) in WT and PKP2-Hz hearts. No difference was apparent between groups.

ceau S stainings were imported into ImageJ (2008, NIH, Bethesda, MD). The density of each band in the Western blot was normalized to the corresponding Ponceau S signal (after background subtraction), to correct for loading. The average density of the six WT samples (after loading correction) was used as a unit. Each band density (from both WT and PKP2-Hz hearts) was then normalized relative to such a unit.

The normalized data were then averaged to generate the bar graph shown in Figure 8.1B.

Immunohistochemistry and histology

For detection of protein localization by immunofluorescence, hearts were rapidly frozen in liquid nitrogen and stored at -80 ˚ C. Hearts were sectioned (thickness: 10μm) in a direction parallel to the long axis of the heart. Sections displaying a four-chamber view were used for immunostaining, as previously described.[13] Samples were exposed to polyclonal antibody against $Na_V1.5$ (1:100)[14] and mouse monoclonal antibody against N-Cadherin (1:800, Sigma, Aldrich), or PKP2 (1:1000, Progen) PKG (1:1000, Sigma), Cx43 (1:200, Transduction Labs) for primary labeling. Afterwards, sections were incubated with FITC-conjugated anti rabbit whole IgG and Texas Red-conjugated anti mouse whole IgG. After labeling, sections were mounted in Vectashield (Vector Laboratories) and visualized by conventional epifluorescence microscopy (Nikon optiphot-2).

To evaluate the extent of fibrosis, sections were fixed with 4% paraformaldehyde in PBS, stained with Picrosirius Red and examined by light microscopy. Four WT and four littermate PKP2-Hz hearts were used for the analysis. For each heart, twelve random pictures from the left ventricular free wall, and twelve from the right ventricular wall, were acquired at a magnification of 200x, and digitized into RGB stacks for analysis (ImageJ). Picrosirius-positive pixels were defined as those with intensities, in the red channel, between 90 and 190 in the 256 scale. For each WT heart, the data collected from the 12 different frames was averaged and used as the unit. The value of each frame, both from the WT hearts and from the PKP2-Hz littermate hearts that were processed in parallel, was then referred to that unit. Compiled data on each genotype group were then averaged for statistical analysis (two-tailed Student's t test).

Electron microscopy and electron tomography

Mouse hearts were fixed in situ with 4% paraformaldehyde in 0.1M PBS (pH 7.4); after an initial period, hearts were excised and maintained in the same fixative. Small pieces were cut with a tissue puncher, rapidly frozen with a high-pressure freezer (HPM 010; Bal-Tec AG, Liechtenstein) and stored under liquid nitrogen with 2% Osmium Tetroxide in acetone. For freeze substitution, specimen carriers containing frozen

tissue were placed into anhydrous acetone containing 2% OsO_4 and 0.1% uranyl acetate at -80°C for 96 hr. By using an automated freeze substitution machine (EM AFS; Leica Microsystems), the samples were slowly warmed (5°C/hr) to -60°C and incubated for 12 hr, then to -30°C for an additional 12 hr, to 0°C for 4 hr, and finally to room temperature for 1 hr. Samples were rinsed 1hr in acetone for 3 times and infiltrated with acetone:EMbed 812 resin = 1:1 (Electron Microscopy Sciences, Hatfield, PA) for 1hr, followed by acetone:Embed 812 = 1:2 overnight. The samples were then incubated in twice pure Embed 812 for 4 hr before being polymerized at 60°C. Thin sections (120 nm; UC6 microtome; Leica Microsystems) were collected on slotted copper grids (Electron Microscopy Sciences, Hatfield, PA) coated with a formvar membrane. The sections were counterstained by incubation with 3% uranyl acetate[15] in 50% methanol for 20 min, followed by washing in water, and incubation with Renold's lead citrate for 5 min. A thin layer of carbon was evaporated on top of the sections to minimize beam-induced specimen shrinkage (Auto306 Vacuum Evaporator; Edwards BOC).

Collection and Analysis of Tomograms

Samples were tilted between -70° and +70° at one - degree intervals and electron micrographs were recorded at 15,000 to 25,000 fold magnifications with a Tecnai TF20 microscope (FEI Corporation, Hillsboro, OR, USA) equipped with a 4k x 4k CCD camera (TVIPS, Gauting, Germany). Dual-axis tilt series were collected with a high-tilt tomography holder (Fischione, Export, PA, USA) and the serial EM program for automated data collection.[16] A second tilt series of the same area was collected after manually rotating the specimen support by ninety degrees. Dual-axis tomographic images were reconstructed by IMOD.[17]

Myocyte isolation and cell electrophysiology

Adult mouse ventricular myocytes were obtained by enzymatic dissociation following standard procedures.[19] Briefly, after thoracotomy, hearts were placed in a Langendorf column and perfused sequentially with low calcium, and with a collagenase-containing (Worthington) solution. Ventricles were cut into small pieces, and gently minced with a Pasteur pipette. Ca^{2+} concentration was then increased gradually to normal values. Cells were used for electrophysiological recording within 8 hours after isolation.

Electrophysiological recordings

All electrophysiological recordings were conducted in the whole-cell configuration.[4] Pipette resistance was maintained within the range of 1.5 to 1.8 MΩ. Recording pipettes were filled with a solution containing (in mmol/l): NaCl 5, CsF 135, EGTA 10, MgATP 5 and HEPES 5, pH 7.2 with CsOH. Cells were maintained in a solution containing (in mM): NaCl 5 (20 for HEK293 cells), CsCl 132.5 (117.5 for HEK293 cells), $CaCl_2$ 1, $MgCl_2$ 1, $CdCl_2$ 0.1, HEPES 20 and Glucose 11, pH 7.35 with CsOH. Voltage clamp protocols were as follows: for determination of peak current voltage relation, 200 msec voltage pulses were applied to V_m -90 mV to +30 mV in 5 mV voltage steps, from a holding potential of V_m = -120 mV. Interval between voltage steps was 3 sec. For analysis of steady-state activation, I_{Na} at each membrane potential was divided by the electrochemical driving force for sodium ions and normalized to the maximal sodium conductance. The normalized conductance was then plotted against V_m. Steady state inactivation was determined by stepping V_m from -130 mV to -40 mV, followed by a 30 msec test pulse to V_m = -40mV to elicit I_{Na}. Both the steady state voltage-dependent activation and inactivation curves were fitted to Boltzmann's functions. Recovery from inactivation was studied by applying paired voltage clamp steps. Two 20-msec test pulses (S1, S2) to V_m = -40mV (holding potential = -120 mV) were separated by increasing increments of 2 msec to a maximum S1-S2 interval of 100 msec. The S1-S1 interval was kept constant at 3 sec. The time-dependent recovery from inactivation curves were fit with exponential functions.

For experiments assessing the effect of flecainide on peak sodium current amplitude, voltage clamp steps from -120 mV to -30 mV in amplitude and 100 ms in duration were applied repetitively every 300 ms. Control recordings (no drug added) were obtained for a total duration of 50-60 seconds after patch break. After that period, voltage clamp was switched off, and flecainide was added to the superfusate. Three minutes after addition of the drug, the voltage clamp was switched back on. Re-initiation of the voltage pulses elicited currents of progressively decreasing amplitude, reflecting the use-dependence of flecainide block. The time-dependent peak sodium current amplitude decay curves were fit with bi-exponential functions. All recordings were obtained utilizing an Axon multiclamp 700B Amplifier coupled to a pClamp system (versions 10.2, Axon Instruments, Foster City, CA).

Epicardial activation mapping in Langendorf-perfused murine hearts

For epicardial activation mapping experiments, mice were anesthetized (4% isoflurane in oxygen) and the hearts quickly excised, rinsed and placed on a Langendorf column for retrograde coronary perfusion, as described previously.[20] Hearts were continuously perfused with a Tyrode solution containing: (in mmol/l): NaCl 116, KCl 5, $MgSO_4$ 1.1, NaH_2PO_4 0.35, $NaHCO_3$ 27, glucose 10, mannitol 16 and $CaCl_2$ 1.8 at 37 ˚ C. Solution was continuously gassed with 95% O_2, 5% CO_2.

Extracellular electrograms were recorded using a 247-point multiterminal electrode (19x13 grid, 0.3 mm spacing) placed over both LV and RV, as described previously. Recordings were made during stimulation (2 ms pulse duration, 2x diastolic stimulation threshold) from the center of the grid at basic cycle length (BCL) of 120 ms. Effective refractory period (ERP), defined as the longest coupling interval of the premature stimulus that failed to activate the entire heart, was determined as in[21]. Measurements were repeated on the same hearts after 5 minutes of continuous perfusion of a Tyrode solution containing 0.53 μmol/l of flecainide.

The moment of maximal negative dV/dt in the unipolar electrograms was selected as the time of local activation and determined using customized software.[22] Activation times were used to construct activation maps. Conduction velocities parallel (CV_L) and perpendicular (CV_T) to fiber orientation were determined from activation maps generated from BCL-pacing. Activation times of at least 4 consecutive electrode terminals along lines perpendicular to intersecting isochronal lines were used to calculate CVs. Anisotropic ratio was defined as CV_L/CV_T.

Flecainide challenge and electrocardiographic recordings in anesthetized whole animal preparations

Twelve (6 males) PKP2-Hz and 11 (5 males) littermate wild-type mice, between 3 and 6 months of age, were used for the in vivo experiments. Mice were anesthetized with 1.5% isoflurane in 700 ml O_2/minute via a nose cone (following induction in a chamber containing isoflurane 4-5%). Rectal temperature was continuously monitored and maintained at 37-38 °C using a heat pad. A “lead II” ECG was recorded from sterile needle electrodes inserted subcutaneously in each forelimb and hindlimb. The signal was then acquired and analyzed using a digital ac-

quisition and analysis system (Power Lab; AD Instruments; LabChart 7Pro software version). After control (baseline) recordings, 83 μmol/kg (40 mg/Kg) of flecainide were administered intraperitoneally in a single bolus and the ECG recorded for 20 minutes following drug administration. ECG parameters were quantified at baseline, five and ten minutes from the average of ten beats. Arrhythmia incidence and its characteristics were monitored for the entire 20 minutes of recording (except for three arrhythmic deaths prior to the end of the experimental period). QT interval was defined as the time elapsed from the beginning of the major deflection representing the QRS to the end of the secondary slow deflection, as described by Danik et al[23] and as used by other groups in similar experimental settings.[24] This choice was due to the lack of a consistent visualization of the third negative deflection.[23, 24] QT intervals were corrected for RR interval, according to Mitchell et al[25] ($QTc=QT/(RR/100)^{1/2}$). Criteria for exclusion of an animal from the data set used to quantify a particular ECG parameter were as follows (see also legend of Figure 8.8): For P duration and PR interval, an animal was excluded from data set if, at the specific time point analyzed, ECG showed at least one of the following: 1) ventricular tachycardia, 2) advanced AV block, 3) atrial tachycardia, diagnosed from altered P polarity and shorter PR interval compared to baseline or 4) P wave inversion, likely signaling a low atrial rhythm. First two criteria (ventricular tachycardia; advanced AV block) were applied to determine exclusion from QTc data set. For QRS duration, animals in VT were excluded; animals in second-degree AV block were included, with parameters measured only from conducted sinus beats.

Results

General characterization of the animal model

PKP2-Hz mice and their WT littermates were used for the study. PKP2-Hz animals showed normal size and appearance. No difference in survival was observed when compared to WT littermates. Hearts from PKP2-Hz animals were also normal in appearance and in weight ($HW/BW=0.58\pm0.02;n=12$ and $0.62\pm0.02;n=13$ for WT and PKP2-Hz, respectively). Histological examination revealed no evidence of fibrotic infiltrates in the PKP2-Hz compared to control (Figure 8.1A). Western blot analysis showed the expected decrease in PKP2 protein abundance, and no differences in the abundance of other intercalated disk proteins (Cx43, N-Cadherin, plakoglobin or $Na_V1.5$; see

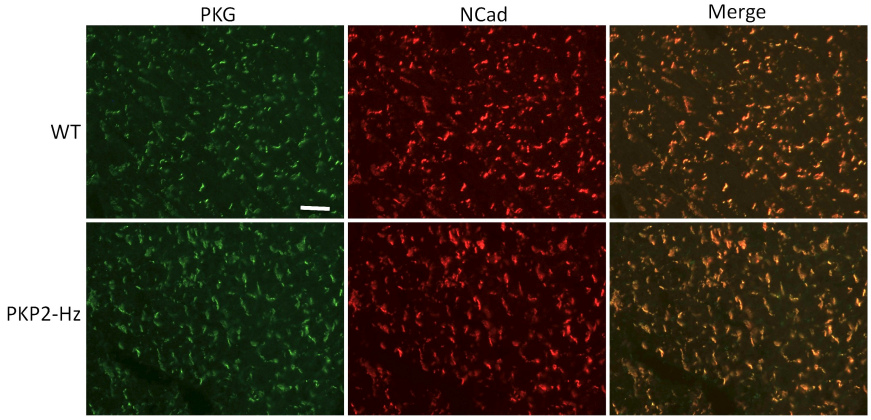

Figure 8.2 – Immunofluorescence images for Plakoglobin (PKG, green) and N-cadherin (NCad, red) in WT and PKP2-Hz hearts. No difference was apparent between groups. Calibration bar 50 μm.

Figure 8.1B). Immunofluorescence studies showed an apparent decrease in the intensity of PKP2 signals, which remained localized to the intercalated disk (Figure 8.1C). Similarly, no changes in localization of $Na_V1.5$, Cx43, Plakoglobin or N-Cadherin were observed at this level of resolution (Figure 8.1D, Figure 8.2 and Figure 8.3). However, ultra-

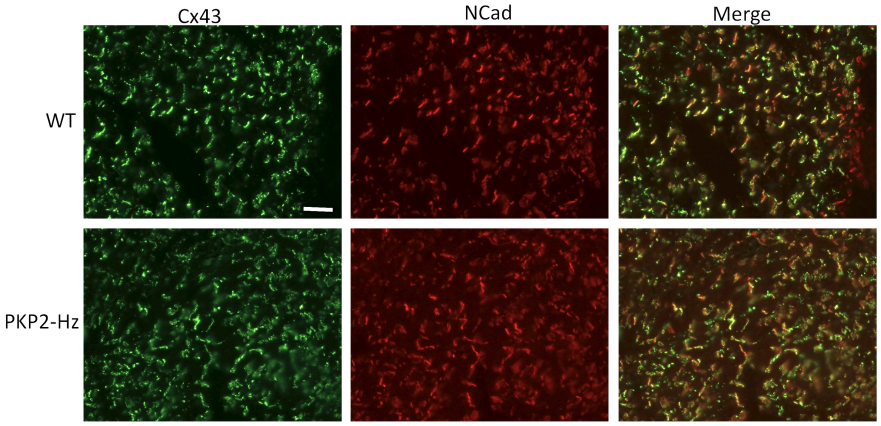

Figure 8.3 – Immunofluorescence images for Connexin 43 (Cx43, green) and N-cadherin (NCad, red) in WT and PKP2-Hz hearts. No difference was apparent between groups. Calibration bar 50 μm.

structural analysis of sections that ran parallel to the direction of the fibers showed that desmosomes were sporadic or absent, and the di-

mension of the intercellular space between structures was non-uniform and expanded in some areas, particularly at the crests of the area composita (see Figure 8.4; left panels). These observations were consistent with those from other models of desmosomal deficiency.[26] Furthermore, tomographic electron microscopy (T-EM; Figure 8.4) revealed that the expanded intercellular space coincided with the presence of membrane invaginations in one side of the intercalated disk. Figure 8.4A-F show selected planes of the same section, revealing that the invaginations extended several nanometers into the intracellular space; in some planes, the invaginations seemed to "pinch off," leaving a healed membrane continuum facing the intercellular cleft. This observation was confirmed in three separate samples analyzed by T-EM, and was not found in the controls (see, for example, [27]).

Sodium current properties in adult ventricular myocytes of PKP2-Hz mice

Previous studies have demonstrated that acute loss of PKP2 expression leads to a decrease in amplitude and a shift in gating and kinetics of the sodium current (I_{Na}).[4] We therefore explored whether a similar effect would be observed in myocytes from PKP2-Hz hearts. As shown in Figure 8.5, whole-cell patch clamp experiments revealed that average peak sodium current density in PKP2-Hz cells was significantly reduced when compared to control (A). There was no difference in the voltage-dependence of activation (B) but we observed a negative shift in steady state inactivation (panel C) and a slower recovery from inactivation (panel D) in cells from PKP2-Hz animals when compared to control. Overall, our studies showed impairment of cardiac sodium current in cells from animals with reduced abundance of PKP2.

Flecainide-induced decrease in I_{Na} is more pronounced in PKP2-Hz myocytes

Sodium channel blockers such as flecainide can help unveil an -otherwise masked or minimal- sodium current deficit.[7, 8, 10-12, 28] We explored whether the use-dependence of flecainide block could be more pronounced in PKP2-Hz cells than in control. Figure 8.6A depicts the time course of average peak I_{Na} density, relative to that at the onset of recording, measured by 100 ms voltage clamp steps from -120 mV to -30 mV applied repetitively every 300 ms. Control recordings (no drug added) were obtained for a total duration of 50-60 seconds af-

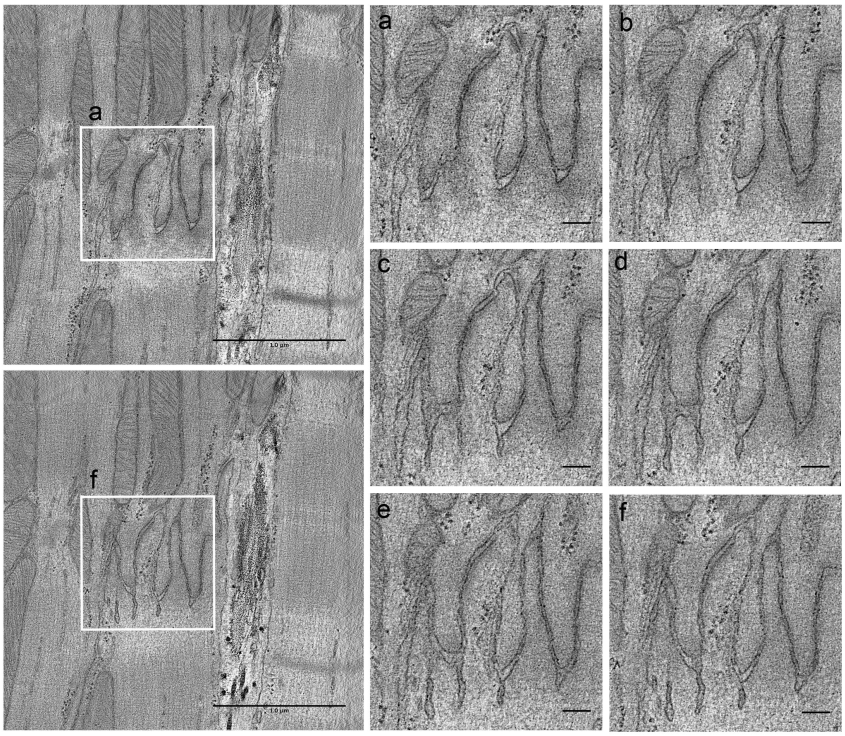

Figure 8.4 – *Tomographic electron microscopy images of the intercalated disk region in a PKP2-Hz adult heart.* Outlined region in left panels, enlarged for insets a-f. Each frame corresponding to different plane of visualization. Notice membrane invaginations, extending into the intracellular space and detaching from a healed membrane in some of the sectional planes.

ter patch break. Flecainide (1 μmol/L) was added to the superfusate at the time indicated by the upward arrow. No voltage clamp steps were applied for the first three minutes after addition of the drug (voltage clamp off; cell at resting membrane potential). After that period, membrane voltage was clamped again and the repetitive pulse protocol reinitiated. The peak current density elicited by the first pulse following the period of quiescence reflected the magnitude of the "tonic" (as opposed to "use-dependent") blocking effect of the drug. Subsequent pulses elicited currents of progressively decreasing amplitude, reflecting the use-dependence of flecainide block. The reduction in I_{Na} density was significantly larger in PKP2-Hz cells (red) than control

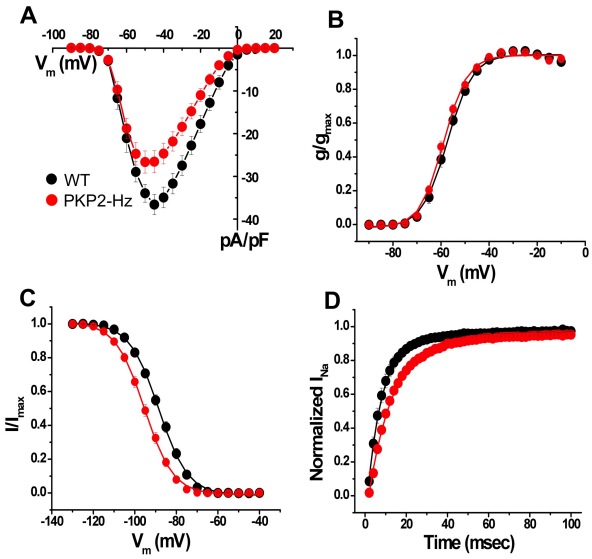

Figure 8.5 – *Sodium current properties recorded from adult cardiac myocytes isolated from PKP2-Hz hearts.* **A:** Average peak sodium current density as a function of voltage command. Peak current amplitude at -45 mV: WT: -36.1±2.4 pA/pF; n=12. PKP2-Hz: -26.3±2.6 pA/pF; n=16. P<0.01. **B**: Voltage dependence of steady-state activation curves. Voltage for half-maximal activation ($V_{1/2}$): -57.4±0.9 mV for WT and -58.9±0.7 mV for PKP2-Hz (pNS). **C**: Voltage dependence of steady-state inactivation. Voltage for half-maximal inactivation ($V_{1/2}$): -89.6±1.4 mV for WT and -95.3±1.1 mV for PKP2-Hz (p <0.005). **D**: Time course of recovery from inactivation. Time constant (one exponential function): 8.5±0.9 msec for WT and 11.9±0.7 msec for PKP2-Hz (p < 0.002).

(black). Compiled data obtained from experiments testing three different flecainide concentrations (only one concentration tested per cell) are shown in Figure 8.6B and C. The bar graphs in Figure 8.6B show the extent of use-dependent block, whereas Figure 8.6C compares the time course. The black and red bars represent data from control and PKP2-Hz cells, respectively. The results show that flecainide caused a more pronounced, and faster block in cells deficient in PKP2 (all numerical parameters are presented in Table 8.1).

Table 8.1 – Percent of flecainide-induced INa block in wild-type (WT) and PKP2-heterozygous (PKP2-Hz) mice.

	Tonic block (%)		Use-dependent block (%)		t fast (sec)		**t slow (sec)**	
Flecainide	WT	PKP2 -Hz	WT	PKP2 -Hz	WT	PKP2 -Hz	WT	PKP2 -Hz
1 mM	8.4±1.0 (n=8)	10±0.8 (n=10)	17.5±2.7 (n=8)	24.3±2.2* (n=10)				
10 mM	18.1±1.7 (n=9)	16.5±1.9 (n=9)	33±3.0 (n=9)	43.5±2.6* (n=9)	6.9±2.0 (n=9)	5.8±1.5 (n=9)	39.4±6.0 (n=9)	39.6±5.6 (n=9)
100 mM	44±3.3 (n=8)	47.4±2.5 (n=9)	84.3±4.1 (n=8)	92.3±4.3* (n=9)	2.8±0.5 (n=8)	1.7±0.1* (n=9)	24.3±10.0 (n=8)	27.1±9.0 (n=9)

*p<0.05 Student's t-test. All values expressed as Mean±SEM.

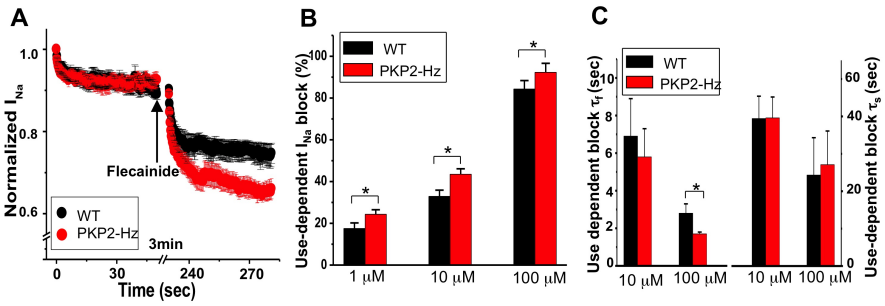

Figure 8.6 – *PKP2 deficiency and use-dependent, flecainide-induced I_{Na} block.* Panels A-C: Data from adult ventricular myocytes dissociated from either PKP2-Hz (red) or WT littermates (black). **A:** Time course of I_{Na}, relative to current density at patch break. After sixty seconds of regular pacing, voltage clamp pulses were interrupted, and Flecainide (1 μmol/L) added (arrow). Repetitive pulses were re-initiated three minutes after addition of the drug. SEM noted for each time point. **B:** Compiled data for fraction of current decrease consequent to use-dependent flecainide block. WT, n= 8, 9, 8 and PKP2-Hz n=10 ,9, 9 for 1, 10 and 100 μmol/L flecainide, respectively. (*p<0.05 for each concentration). **C:** Fast and slow time constants of use-dependent flecainide block (*p<0.05).

Flecainide-induced slow conduction velocity is more pronounced in PKP2-Hz hearts

Additional experiments explored the effect of flecainide on electrophysiological parameters recorded by electrical epicardial activation mapping of Langendorff-perfused whole heart preparations. Figure 8.7A shows examples of an activation map from a littermate control (WT;

left) and a PKP2-Hz mouse (right), in the absence or in the presence of 0.53 μmol/L of flecainide (drug concentrations of 1 μmol/L led to loss of propagated activity in some of our preparations). The crowding of the isochrones reflects the fact that flecainide caused a decrease in longitudinal propagation velocity, which was most prominent in PKP2-Hz hearts. Cumulative data are shown in Table 8.2. Graphs depicting the measurements of longitudinal conduction velocity for the right and left ventricle are shown in Figure 8.7B and C, respectively. The data show that the flecainide-induced decrease was most prominent for right ventricular propagation along the fiber direction ($p<0.02$ versus littermate controls), with the consequent decrease in anisotropic ratio for the RV (Table 8.2). A similar tendency was observed for left ventricular propagation, though the difference was not statistically significant. Qualitatively, these results were reminiscent of those obtained in SCN5A haploinsufficient hearts.[29]

Table 8.2 – Electrophysiological parameters recorded by epicardial activation maps of Langendorf-perfused wild-type (WT) and PKP2-Heterozygous (PKP2-Hz) murine hearts, at baseline and in the presence of 0.53 μmoles/l of flecainide.

	WT	**PKP2-Hz**	**WT Flec**	**PKP2-Hz Flec**
N (% male)	12 (33)	13 (61)		
HW/BW (g/g)	0.58 ± 0.02	0.62 ± 0.02		
LV CV_L (cm/s)	71.9 ± 4.0	71.1 ± 3.1	70.6 ± 2.8	63.5 ± 3.2
RV CV_L(cm/s)	66.7 ± 2.2	69.6 ± 1.9	64.9 ± 1.7	56.1 ± 2.3*
LV CV_T(cm/s)	44.1 ± 1.4	40.7 ± 2.4	37.5 ± 4.0	41.1 ± 3.3
RV CV_T (cm/s)	47.3 ± 2.3	50.1 ± 3.0	44.4 ± 1.7	44.9 ± 2.4
LV AR (CV_L/CV_T)	1.6 ± 0.1	1.8 ± 0.1	1.9 ± 0.2	1.6 ± 0.2
RV AR (CV_L/CV_T)	1.4 ± 0.1	1.5 ± 0.1	1.5 ± 0.1	1.2 ± 0.1*
LV ERP (ms)	54.0 ± 2.7	60.0 ± 4.1	63.3 ± 6.1	71.0 ± 6.7
RV ERP (ms)	42.0 ± 3.9	46.9 ± 3.5	60.0 ± 5.8	59.2 ± 4.2

* $p<0.05$ vs WT Flecainide. Student's t test. HW/BW: heart weight/body weight. CVL : Longitudinal conduction velocity. CVT: Transverse conduction velocity. AR: Anisotropic ratio. ERP: Effective refractory period. All values expressed as Mean±SEM.

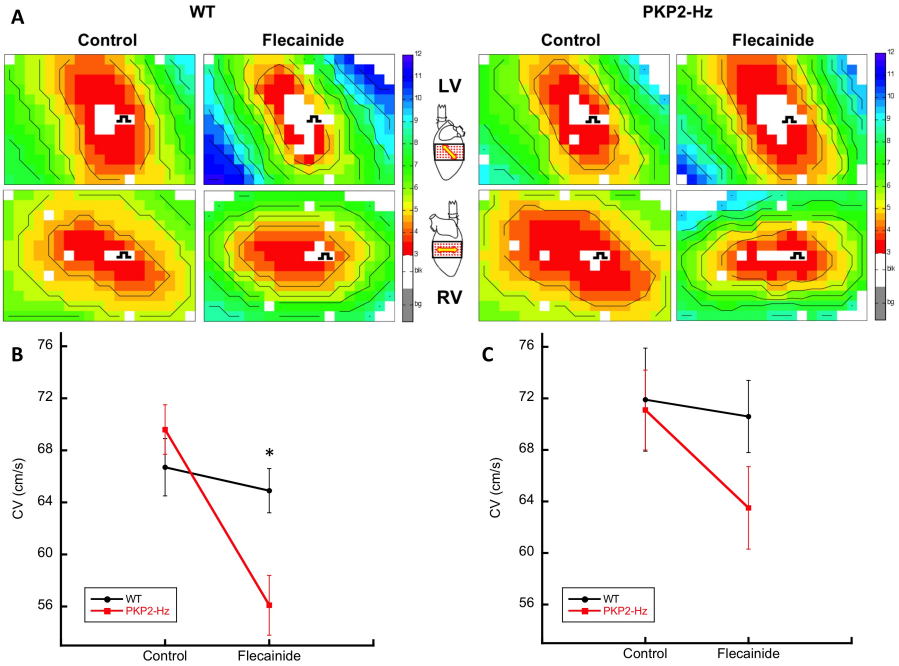

Figure 8.7 – *Epicardial activation maps in PKP2-Hz hearts and control littermates.* **A:** Examples of activation maps for left (LV; top) and right ventricle (RV; bottom) of a WT (left) and a PKP2-Hz heart in the absence (control) or presence of flecainide. Colors indicate activation times. Isochrones outlined by black lines. Area depicted within each frame: 5.4 by 3.6 mm. Site of stimulation indicated by square-pulse symbol. **B** and **C**: Average longitudinal conduction velocity (CV), measured in right (RV; panel B) or left ventricle (LV; panel C) of either WT (black symbols) or PKP2-Hz mice (red symbols). For additional details see Table 8.2. *p<0.05.

Flecainide-induced electrocardiographic changes and ventricular arrhythmias in PKP2-Hz mice

Our results in isolated cells and in whole heart preparations led us to explore whether genotype-dependent electrocardiographic differences are apparent in the mice. Single-lead, surface ECGs were recorded from anesthetized animals. At baseline, we detected a significant difference in the duration of the P wave (longer in PKP2-Hz animals); other ECG baseline parameters recorded from PKP2-Hz animals were similar to control (see Table 8.3 and Figure 8.8). A flecainide challenge (83 μmol/kg i.p.) caused a prolongation of the P and QRS durations,

Table 8.3 – Baseline ECG parameters in anesthetized mice.

	WT	**PKP2-Hz**	**p**
Number of animals	11 (5 males)	12 (6 males)	
RR (ms)	149.54±3.27	145.33±3.77	NS
P duration (ms)	11.45±0.28	13.0±0.59	0.02*
PR (ms)	41.09±0.91	42.72±0.76	NS
QRS (ms)	12.36±0.3	12.16±0.11	NS
QT (ms)	22.18±6.58	26±7.85	NS
QTc (ms)	17±0.26	17.58±0.41	NS
P ampl (V)	0.027±0.003	0.033±0.003	NS
R ampl (V)	0.29±0.03	0.261±0.04	NS
S ampl (V)	0.1±0.02	0.06±0.009	NS
T ampl (V)	0.039±0.009	0.041±0.005	NS
QRS ampl	0.397±0.03	0.326 ±0.04	NS

All values expressed as Mean±SEM. p value from unpaired Student's t test. pNS if p>0.05.
*indicates statistical significance.

and of the PR and QTc intervals. In average, the flecainide effect was significantly more pronounced in PKP2-Hz animals than in control (Figure 8.8A shows an example; cumulative data recorded at baseline, five and ten minutes after the single bolus injection of flecainide, is shown in Figure 8.8B and in Table 8.4). A similar result was obtained when the relative increase in a given variable (as percent of its magnitude at baseline), rather than the absolute value, was analyzed (see Figure 8.9 and Table 8.5). Flecainide also induced second degree AV block in 8 out of 12 PKP2-Hz and 5 out of 11 WT animals. Two out of twelve PKP2-Hz (and 0/11 WT controls) showed atrial arrhythmias. More importantly, 6 out of 12 PKP2-Hz animals showed ventricular arrhythmias, an outcome that was not observed in any of the 11 WT mice tested (p=0.01; Two-sided Fisher test vs WT; see Figure 8.8A for examples of ventricular arrhythmias in PKP2-Hz mice). Arrhythmic death during recording occurred in three PKP2-Hz animals; none of the WT animals died during the procedure. Overall, the electrocardiographic response to flecainide, and the susceptibility to ventricular arrhythmias following the flecainide challenge, segregated according to the specific genotype of the tested mice.

Table 8.4 – Absolute values (in ms) of ECG parameters recorded from anesthetized mice 5 and 10 minutes after flecainide bolus (83 μmol/kg i.p.).

	5 mins			10 mins		
	WT (ms)	**PKP2-Hz (ms)**	**p**	**WT (ms)**	**PKP2-Hz (ms)**	**p**
P	17±0.9 (n=11)	21.7±0.9 (n=10)	0.002*	20±1.3 (n=6)	28±2.1 (n=4)	0.01*
PR	65±2.4 (n=11)	72.2±2.9 (n=10)	0.07	69±4.0 (n=6)	89±4.4 (n=4)	0.01*
QRS	20.4±0.7 (n=11)	22±0.6 (n=12)	0.12	24.5±1.1 (n=11)	28.7±0.8 (n=8)	0.01*
QTc	28.3±1.4 (n=11)	33.4±1.0 (n=12)	0.007*	32.6±2.7 (n=6)	40.8±2.7 (n=5)	0.06

All values expressed as Mean±SEM. p values from paired Student's t test. pNS if p>0.05.

*indicates statistical significance.

Discussion

We have shown that a decrease in PKP2 abundance associates with sodium channel dysfunction in mice. A significant difference in sodium current properties was observed in control conditions (Figure 8.5); the sodium current deficit was amplified by superfusion with flecainide (Figure 8.6). Flecainide also lead to genotype-dependent slowing of longitudinal conduction (Figure 8.7), electrocardiographic changes (Figure 8.8), and increased susceptibility to ventricular arrhythmias and death (Figure 8.8). The electrophysiological phenotype was observed in an animal model void of overt structural heart disease (Figure 8.1), though with an ultrastructural phenotype (Figure 8.4). Overall, our data support the notion that a genetically-mediated decrease in PKP2 abundance can directly impair the function of the voltage-gated sodium channel complex, cardiac electrophysiological behavior, even when structural integrity of the cardiac tissue is not compromised. Together with our studies on the molecular interactions between PKP2 and components of the voltage-gated sodium channel complex,[3] and all differences between an animal model and a human disease being noted, our data provide a potential mechanistic insight into the origin of arrhythmias that occur in patients with mutations

Table 8.5 – Increment (as percent of baseline) in ECG parameters recorded from anesthetized mice 5 and 10 minutes after flecainide bolus (83 μmol/kg i.p.).

	5 mins			10 mins		
	WT (%)	**PKP2** (%)	**p**	**WT** (%)	**PKP2-Hz** (%)	**p**
P	49±9 (n=11)	67±10 (n=10)	0.2	73±11 (n=6)	135±22 (n=4)	0.025*
PR	58±5 (n=11)	67±6 (n=10)	0.3	69±6 (n=6)	113±9 (n=4)	0.004*
QRS	66±6 (n=11)	80±5 (n=12)	0.09	98±7 (n=11)	137±7 (n=8)	0.002*
QTc	66±8 (n=11)	95±7 (n=12)	0.01*	96±16 (n=6)	132±17 (n=5)	0.16

All values expressed as Mean±SEM. p values from paired Student's t test. pNS if p>0.05.
*indicates statistical significance.

in the *pkp2* gene and no overt structural disease. Yet, sodium current may not be the only affected variable. Further studies will be necessary to determine whether junctional conductance, amplitude/kinetics of repolarizing currents, and/or extent of electrical heterogeneity, are affected by loss of PKP2 in a manner similar to what has been observed after loss of other junctional molecules.[15, 30-32]

Flecainide has primary effects as a use-dependent sodium channel blocker, and our results further found a genotype-dependent effect (Figure 8.6). Both flecainide and PKP2 deficiency lead to slow recovery from I_{Na} inactivation.[4, 33] We therefore speculate that the combination of both factors leads to a more extensive impairment of I_{Na} during repetitive activation. Based on our results on isolated cells, we further speculate that the flecainide-induced changes in conduction velocity (Figure 8.7 and Table 8.2) were primarily consequent to the sodium current deficit. We also observed that flecainide had a more pronounced effect on conduction velocity in the right ventricle (Figure 8.7B). This is consistent with other studies showing that sodium current deficit leads to preferential impairment of propagation in the right ventricle.[34, 35] The mechanism for this effect is unknown, though it has been speculated that it relates to the fact that the RV free wall is thinner, and it

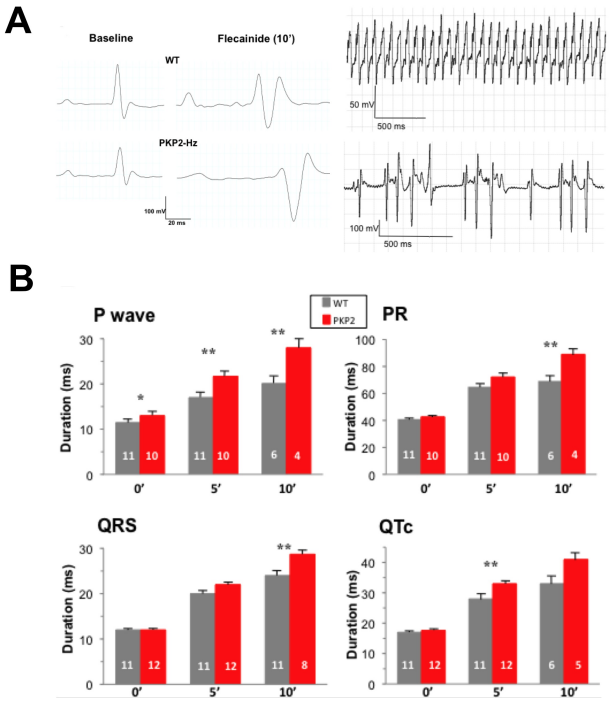

Figure 8.8 – *Electrocardiographic features of PKP2-Hz mice at baseline, and in response to flecainide.* **A**: left, example of ECG traces from WT (top) and PKP2-Hz mouse, (bottom). Recordings obtained at baseline (left) and 10 minutes after flecainide (40 mg/Kg i.p., right). Right: VT in PKP2-Hz mice. Recordings obtained from two animals, 10' (top) and 9' (bottom) after flecainide ip. **B**: Graph bars show average P wave duration, PR interval, QRS duration and QTc interval measured at baseline, 5' and 10' after flecainide injection. A total of 11 WT and 12 PKP2-Hz animals were studied. Criteria for exclusion from data set: For P duration and PR interval, subject excluded from data set if ECG showed at least one of the following (number of excluded subjects from a given time point, in parentheses): 1) ventricular tachycardia, VT (4 PKP2-Hz at 10'), 2) second-degree AV block (5 WT, 3 PKP2-Hz at 10'), 3) atrial tachycardia, diagnosed for altered P polarity and shorter PR interval (one PKP2-Hz at 5' and at 10') or 4) P wave inversion, likely signaling a low atrial rhythm (two PKP2-Hz at baseline and at 5'). First two criteria also applied to QTc data set. For QRS duration, animals in VT were excluded; animals in second degree AV block were included, with parameters measured only from conducted sinus beats. n values indicated in each bar. *$p<0.05$; **$p\leq0.01$. Additional data in Table 8.3, Table 8.4 and Figure 8.9.

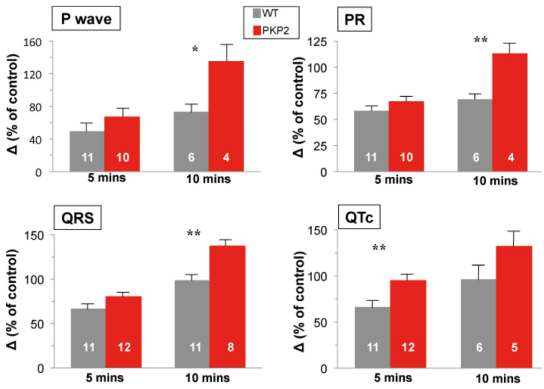

Figure 8.9 – Relative changes in ECG parameters. Bar graphs correspond to data collected from mice wild-type (WT; grey) or heterozygous-null for PKP2 (PKP2-Hz; red). Data measured as the percentual increment (Δ) in a given parameter, relative to the value measured at baseline. Same data set used for Figure 8.8. Baseline data in Table 8.3. Values used for this graph, can be found in Table 8.5.

also shows sharp shifts in fiber orientation across the wall. The larger layer-to-layer rotational anisotropy may be associated with poor electrical coupling and preferential sites for conduction block.[36, 37] Moreover, the right-versus-left heterogeneity may have facilitated the initiation, and maintenance of ventricular arrhythmias (Figure 8.8). The heterogeneous distribution of the sodium channel protein in the conduction system and across the ventricular wall, may have also contributed to arrhythmogenesis.[34] Our results are also consistent with in silico studies demonstrating that PKP2-dependent changes in I_{Na} can lead to initiation and sustainment of vortex activity.[38] It should be noted, however, that flecainide also has effects on other currents;[39-42] moreover, disruption of the area composita (see our Figure 8.4) may affect potassium channels.[32] Whether PKP2 deficiency also affects other ion currents, and their response to flecainide treatment, remains to be determined. The experimental data, however, point to the sodium current deficit as a primary mechanism for the observed effects.

A deficiency in PKP2 abundance has been associated with various cases of familial arrhythmogenic cardiomyopathy (AC).[5] It has been suggested that arrhythmias in patients with AC are consequent to reentrant activity around anatomical obstacles. While such a mechanism is certainly possible, life-threatening ventricular arrhythmias or sudden death often occur in the concealed phase of the disease, prior to overt

structural damage.[5] The intimate mechanisms responsible for these arrhythmias are less clear. Decreased gap junction-mediated electrical coupling could be an adjuvant to arrhythmogenesis, though it is unlikely to be the only cause (see [29, 43, 44]). Obvious differences between animal models and clinical cases notwithstanding, the data presented in this study support the notion that patients with haploinsufficiency in the *pkp2* gene (mutation R79x, for example; see [45, 46]) may present a sodium current deficit. As in the case of the PKP2-Hz mice, this deficit may remain masked, but could be unveiled by an external trigger. In that regard, it is important to note that hearts from patients that have succumbed to ventricular fibrillation often reveal the presence of inflammatory infiltrates. Separate studies have revealed elevated levels of serum inflammatory mediators, and myocardial expression of IL-17 and TNF-alpha, in patients with AC.[47] Previous data suggest that cytokines can alter sodium current function.[48, 49] Future studies will address whether PKP2 is involved in modulating the response of I_{Na} to cytokines, in a manner that would facilitate loss of the cardiac rhythm in the setting of an inflammatory response in a PKP2-deficient heart.

It is interesting to note that, as opposed to other animal models of desmosomal deficiency, PKP2-Hz mice do not develop a structural disease. The reason as to why decreased *pkp2* gene dose and decreased PKP2 protein do not lead to the structural manifestations of AC in mice is unclear; yet, the observation is consistent with the limited penetrance of the structural disease,[5, 50] and supports the idea that epigenetic factors (e.g., an inflammatory response; see [47]) perhaps not present in the "sterile" environment of the laboratory animals, may be necessary to trigger the fibrofatty infiltration. On the other hand, the model allows us to study the arrhythmogenic substrates related to PKP2 deficiency in the absence of structural involvement, a feature particularly helpful to understand the electrical phenotype of the desmosome-deficient heart in the concealed phase of the disease.

The present study focused on the phenotype of the PKP2-Hz hearts. Whether other desmosomal proteins also interact with $Na_V1.5$, and whether these interactions occur in the human heart, is currently a matter of investigation. Recently, Gomes et al[51] reported that desmoplakin-heterozygous mice present average peak sodium current density similar to control; yet, careful analysis of their results suggests the possibility of technical limitations in their voltage clamp recordings, which could have masked small differences between the groups (see timing of peak current in the traces at the bottom of their Figure 1F, left-shift in Vm

for peak current in the IV plot, and overall shape of IV curve; experiments carried out at [Na]o= 25 mM; [Na]i = 5 mM with patch electrodes of 3-4 MW); moreover, gating and kinetic properties were not thoroughly studied. On the other hand, patients with heterozygous mutations in desmoplakin and without overt structural disease showed significant regional conduction delays and a heterogeneous $Na_V1.5$ distribution.[51] In summary, there is new evidence in support of the hypothesis, first proposed by our laboratory,[4] that I_{Na} is affected by desmosomal mutations. Additional studies are necessary to better understand this interaction. Furthermore, characterizing the role of I_{Na} in desmosome disease will be important as guidance on the indication or contraindication of sodium channel blockers in patients affected with AC. Finally, sodium channel blockers (including flecainide) are used as a diagnostic tool in humans suspect of Brugada syndrome, a disease often associated with primary deficiency in sodium channel function.[9] Whether flecainide would aid in the evaluation of arrhythmia risk in patients suspect of AC, is an interesting area that deserves further investigation.

References

1. Petitprez S, Zmoos AF, Ogrodnik J, Balse E, Raad N, El-Haou S, Albesa M, Bittihn P, Luther S, Lehnart SE, Hatem SN, Coulombe A, Abriel H. Sap97 and dystrophin macromolecular complexes determine two pools of cardiac sodium channels nav1.5 in cardiomyocytes. *Circ Res*. 2011;108:294-304
2. Malhotra JD, Thyagarajan V, Chen C, Isom LL. Tyrosine-phosphorylated and nonphosphorylated sodium channel beta1 subunits are differentially localized in cardiac myocytes. *J Biol Chem*. 2004;279:40748-40754
3. Sato PY, Coombs W, Lin X, Nekrasova O, Green KJ, Isom LL, Taffet SM, Delmar M. Interactions between ankyrin-g, plakophilin-2, and connexin43 at the cardiac intercalated disk. *Circ Res*. 2011;109:193-201
4. Sato PY, Musa H, Coombs W, Guerrero-Serna G, Patino GA, Taffet SM, Isom LL, Delmar M. Loss of plakophilin-2 expression leads to decreased sodium current and slower conduction velocity in cultured cardiac myocytes. *Circ Res*. 2009;105:523-526
5. Delmar M, McKenna WJ. The cardiac desmosome and arrhythmogenic cardiomyopathies: From gene to disease. *Circ Res*. 2010;107:700-714
6. Grossmann KS, Grund C, Huelsken J, Behrend M, Erdmann B, Franke WW, Birchmeier W. Requirement of plakophilin 2 for heart morphogenesis and cardiac junction formation. *J Cell Biol*. 2004;167:149-160
7. Martin CA, Guzadhur L, Grace AA, Lei M, Huang CL. Mapping of reentrant spontaneous polymorphic ventricular tachycardia in a scn5a+/- mouse model. *Am J Physiol Heart Circ Physiol*. 2011;300:H1853-1862
8. Stokoe KS, Balasubramaniam R, Goddard CA, Colledge WH, Grace AA, Huang CL. Effects of flecainide and quinidine on arrhythmogenic properties of scn5a+/- murine hearts modelling the brugada syndrome. *J Physiol*. 2007;581:255-275
9. Meregalli PG, Ruijter JM, Hofman N, Bezzina CR, Wilde AA, Tan HL. Diagnostic value of flecainide testing in unmasking scn5a-related brugada syndrome. *J Cardiovasc Electrophysiol*. 2006;17:857-864
10. Scicluna BP, Tanck MW, Remme CA, Beekman L, Coronel R, Wilde AA, Bezzina CR. Quantitative trait loci for electrocardiographic parameters and arrhythmia in the mouse. *J Mol Cell Cardiol*. 2011;50:380-389
11. Antzelevitch C, Brugada P, Borggrefe M, Brugada J, Brugada R, Corrado D, Gussak I, LeMarec H, Nademanee K, Perez Riera AR, Shimizu W, Schulze-Bahr E, Tan H, Wilde A. Brugada syndrome: Report of the second consensus conference: Endorsed by the heart rhythm society and the european heart rhythm association. *Circulation*. 2005;111:659-670
12. Brugada R, Brugada J, Antzelevitch C, Kirsch GE, Potenza D, Towbin JA, Brugada P. Sodium channel blockers identify risk for sudden death in patients with st-segment elevation and right bundle branch block but

structurally normal hearts. *Circulation*. 2000;101:510-515
13. van Veen TA, van Rijen HV, Wiegerinck RF, Opthof T, Colbert MC, Clement S, de Bakker JM, Jongsma HJ. Remodeling of gap junctions in mouse hearts hypertrophied by forced retinoic acid signaling. *J Mol Cell Cardiol*. 2002;34:1411-1423
14. Hund TJ, Koval OM, Li J, Wright PJ, Qian L, Snyder JS, Gudmundsson H, Kline CF, Davidson NP, Cardona N, Rasband MN, Anderson ME, Mohler PJ. A beta(iv)-spectrin/camkii signaling complex is essential for membrane excitability in mice. *J Clin Invest*. 2010;120:3508-3519
15. Danik SB, Rosner G, Lader J, Gutstein DE, Fishman GI, Morley GE. Electrical remodeling contributes to complex tachyarrhythmias in connexin43-deficient mouse hearts. *FASEB J*. 2008;22:1204-1212
16. Mastronarde DN. Automated electron microscope tomography using robust prediction of specimen movements. *J Struct Biol*. 2005;152:36-51
17. Kremer JR, Mastronarde DN, McIntosh JR. Computer visualization of three-dimensional image data using imod. *J Struct Biol*. 1996;116:71-76
18. Ruan Y, Denegri M, Liu N, Bachetti T, Seregni M, Morotti S, Severi S, Napolitano C, Priori SG. Trafficking defects and gating abnormalities of a novel scn5a mutation question gene-specific therapy in long qt syndrome type 3. *Circ Res*. 2010;106:1374-1383
19. Maass K, Chase SE, Lin X, Delmar M. Cx43 ct domain influences infarct size and susceptibility to ventricular tachyarrhythmias in acute myocardial infarction. *Cardiovasc Res*. 2009;84:361-367
20. van Rijen HV, van Veen TA, van Kempen MJ, Wilms-Schopman FJ, Potse M, Krueger O, Willecke K, Opthof T, Jongsma HJ, de Bakker JM. Impaired conduction in the bundle branches of mouse hearts lacking the gap junction protein connexin40. *Circulation*. 2001;103:1591-1598
21. van Rijen HV, Eckardt D, Degen J, Theis M, Ott T, Willecke K, Jongsma HJ, Opthof T, de Bakker JM. Slow conduction and enhanced anisotropy increase the propensity for ventricular tachyarrhythmias in adult mice with induced deletion of connexin43. *Circulation*. 2004;109:-1048-1055
22. Potse M, Linnenbank AC, Grimbergen CA. Software design for analysis of multichannel intracardial and body surface electrocardiograms. *Comput Methods Programs Biomed*. 2002;69:225-236
23. Danik S, Cabo C, Chiello C, Kang S, Wit AL, Coromilas J. Correlation of repolarization of ventricular monophasic action potential with ecg in the murine heart. *Am J Physiol Heart Circ Physiol*. 2002;283:H372-381
24. Martin CA, Zhang Y, Grace AA, Huang CL. In vivo studies of scn5a+/- mice modeling brugada syndrome demonstrate both conduction and repolarization abnormalities. *J Electrocardiol*. 2010;43:433-439
25. Mitchell GF, Jeron A, Koren G. Measurement of heart rate and q-t interval in the conscious mouse. *Am J Physiol*. 1998;274:H747-751
26. Kant S, Krull P, Eisner S, Leube RE, Krusche CA. Histological and

ultrastructural abnormalities in murine desmoglein 2-mutant hearts. *Cell Tissue Res.* 2012
27. Delmar M, Liang FX. Connexin43 and the regulation of intercalated disk function. *Heart Rhythm.* 2011
28. Leoni AL, Gavillet B, Rougier JS, Marionneau C, Probst V, Le Scouarnec S, Schott JJ, Demolombe S, Bruneval P, Huang CL, Colledge WH, Grace AA, Le Marec H, Wilde AA, Mohler PJ, Escande D, Abriel H, Charpentier F. Variable na(v)1.5 protein expression from the wild-type allele correlates with the penetrance of cardiac conduction disease in the scn5a(+/-) mouse model. *PLoS One.* 2010;5:e9298
29. Stein M, van Veen TA, Hauer RN, de Bakker JM, van Rijen HV. A 50% reduction of excitability but not of intercellular coupling affects conduction velocity restitution and activation delay in the mouse heart. *PLoS One.* 2011;6:e20310
30. Jansen JA, Noorman M, Musa H, Stein M, de Jong S, van der Nagel R, Hund TJ, Mohler PJ, Vos MA, van Veen TA, de Bakker JM, Delmar M, van Rijen HV. Reduced heterogeneous expression of cx43 results in decreased nav1.5 expression and reduced sodium current that accounts for arrhythmia vulnerability in conditional cx43 knockout mice. *Heart Rhythm.* 2012;9:600-607
31. Oxford EM, Musa H, Maass K, Coombs W, Taffet SM, Delmar M. Connexin43 remodeling caused by inhibition of plakophilin-2 expression in cardiac cells. *Circ Res.* 2007;101:703-711
32. Cheng L, Yung A, Covarrubias M, Radice GL. Cortactin is required for n-cadherin regulation of kv1.5 channel function. *J Biol Chem.* 2011;286:20478-20489
33. Ramos E, O'Leary M E. State-dependent trapping of flecainide in the cardiac sodium channel. *J Physiol.* 2004;560:37-49
34. Remme CA, Verkerk AO, Hoogaars WM, Aanhaanen WT, Scicluna BP, Annink C, van den Hoff MJ, Wilde AA, van Veen TA, Veldkamp MW, de Bakker JM, Christoffels VM, Bezzina CR. The cardiac sodium channel displays differential distribution in the conduction system and transmural heterogeneity in the murine ventricular myocardium. *Basic Res Cardiol.* 2009;104:511-522
35. van Veen TA, Stein M, Royer A, Le Quang K, Charpentier F, Colledge WH, Huang CL, Wilders R, Grace AA, Escande D, de Bakker JM, van Rijen HV. Impaired impulse propagation in scn5a-knockout mice: Combined contribution of excitability, connexin expression, and tissue architecture in relation to aging. *Circulation.* 2005;112:1927-1935
36. Schalij MJ, Boersma L, Huijberts M, Allessie MA. Anisotropic reentry in a perfused 2-dimensional layer of rabbit ventricular myocardium. *Circulation.* 2000;102:2650-2658
37. Vetter FJ, Simons SB, Mironov S, Hyatt CJ, Pertsov AM. Epicardial fiber organization in swine right ventricle and its impact on propagation. *Circ Res.* 2005;96:244-251
38. Deo M, Sato PY, Musa H, Lin X, Pandit SV, Delmar M, Berenfeld

O. Relative contribution of changes in sodium current versus intercellular coupling on reentry initiation in 2-dimensional preparations of plakophilin-2-deficient cardiac cells. *Heart Rhythm*. 2011;8:1740-1748
39. Du CY, El Harchi A, Zhang YH, Orchard CH, Hancox JC. Pharmacological inhibition of the herg potassium channel is modulated by extracellular but not intracellular acidosis. *J Cardiovasc Electrophysiol*. 2011;22:1163-1170
40. Caballero R, Dolz-Gaiton P, Gomez R, Amoros I, Barana A, Gonzalez de la Fuente M, Osuna L, Duarte J, Lopez-Izquierdo A, Moraleda I, Galvez E, Sanchez-Chapula JA, Tamargo J, Delpon E. Flecainide increases kir2.1 currents by interacting with cysteine 311, decreasing the polyamine-induced rectification. *Proc Natl Acad Sci U S A*. 2010;107:-15631-15636
41. Radicke S, Vaquero M, Caballero R, Gomez R, Nunez L, Tamargo J, Ravens U, Wettwer E, Delpon E. Effects of mirp1 and dpp6 beta-subunits on the blockade induced by flecainide of kv4.3/kchip2 channels. *Br J Pharmacol*. 2008;154:774-786
42. Akar FG, Spragg DD, Tunin RS, Kass DA, Tomaselli GF. Mechanisms underlying conduction slowing and arrhythmogenesis in nonischemic dilated cardiomyopathy. *Circ Res*. 2004;95:717-725
43. Danik SB, Liu F, Zhang J, Suk HJ, Morley GE, Fishman GI, Gutstein DE. Modulation of cardiac gap junction expression and arrhythmic susceptibility. *Circ Res*. 2004;95:1035-1041
44. Gutstein DE, Morley GE, Tamaddon H, Vaidya D, Schneider MD, Chen J, Chien KR, Stuhlmann H, Fishman GI. Conduction slowing and sudden arrhythmic death in mice with cardiac-restricted inactivation of connexin43. *Circ Res*. 2001;88:333-339
45. van Tintelen JP, Entius MM, Bhuiyan ZA, Jongbloed R, Wiesfeld AC, Wilde AA, van der Smagt J, Boven LG, Mannens MM, van Langen IM, Hofstra RM, Otterspoor LC, Doevendans PA, Rodriguez LM, van Gelder IC, Hauer RN. Plakophilin-2 mutations are the major determinant of familial arrhythmogenic right ventricular dysplasia/cardiomyopathy. *Circulation*. 2006;113:1650-1658
46. van der Zwaag PA, Cox MG, van der Werf C, Wiesfeld AC, Jongbloed JD, Dooijes D, Bikker H, Jongbloed R, Suurmeijer AJ, van den Berg MP, Hofstra RM, Hauer RN, Wilde AA, van Tintelen JP. Recurrent and founder mutations in The Netherlands : Plakophilin-2 p.Arg79x mutation causing arrhythmogenic right ventricular cardiomyopathy/dysplasia. *Neth Heart J*. 2010;18:583-591
47. Asimaki A, Tandri H, Duffy ER, Winterfield JR, Mackey-Bojack S, Picken MM, Cooper LT, Wilber DJ, Marcus FI, Basso C, Thiene G, Tsatsopoulou A, Protonotarios N, Stevenson WG, McKenna WJ, Gautam S, Remick DG, Calkins H, Saffitz JE. Altered desmosomal proteins in granulomatous myocarditis and potential pathogenic links to arrhythmogenic right ventricular cardiomyopathy. *Circ Arrhythm Electrophysiol*. 2011;4:743-752

48. Grandy SA, Brouillette J, Fiset C. Reduction of ventricular sodium current in a mouse model of hiv. *J Cardiovasc Electrophysiol*. 2010;21:916-922
49. Lin X, Liu N, Lu J, Zhang J, Anumonwo JM, Isom LL, Fishman GI, Delmar M. Subcellular heterogeneity of sodium current properties in adult cardiac ventricular myocytes. *Heart Rhythm*. 2011;8:1923-1930
50. Gerull B, Heuser A, Wichter T, Paul M, Basson CT, McDermott DA, Lerman BB, Markowitz SM, Ellinor PT, MacRae CA, Peters S, Grossmann KS, Drenckhahn J, Michely B, Sasse-Klaassen S, Birchmeier W, Dietz R, Breithardt G, Schulze-Bahr E, Thierfelder L. Mutations in the desmosomal protein plakophilin-2 are common in arrhythmogenic right ventricular cardiomyopathy. *Nat Genet*. 2004;36:1162-1164
51. Gomes J, Finlay M, Ahmed AK, Ciaccio EJ, Asimaki A, Saffitz JE, Quarta G, Nobles M, Syrris P, Chaubey S, McKenna WJ, Tinker A, Lambiase PD. Electrophysiological abnormalities precede overt structural changes in arrhythmogenic right ventricular cardiomyopathy due to mutations in desmoplakin-a combined murine and human study. *Eur Heart J*. 2012

CHAPTER 9

General discussion

The research described in this thesis was set out to investigate the interaction of three important structures that are situated in the intercalated disk: 1) desmosomes, 2) sodium channels and 3) gap junctions. They exist together in the intercalated disk, which is located at the longitudinal ends of cardiomyocytes where they connect them to the neighboring cardiomyocyte. The desmosomes connect myocytes mechanically, while gap junctions facilitate electrical conductivity. Thirdly, the sodium channels ($Na_V1.5$), are the molecular substrate of myocyte excitability. Several studies have revealed a direct interaction between these three components of the intercalated disk (Figure 9.1). Cx43 has been found to coimmunoprecipitate with $Na_V1.5$,[1] and *in vitro* reduction of the desmosomal protein plakophilin2 (PKP2) causes both a reduction in Cx43 and in peak sodium current.[2, 3] Based on these findings we postulated the following central hypothesis of this thesis:

> *A large macromolecular complex is situated at the intercalated disk of the cardiomyocyte, consisting of gap junctions, sodium channels and desmosomes. Changes in expression or localization of one component will lead to changes in the others. These changes can create an arrhythmogenic substrate.*

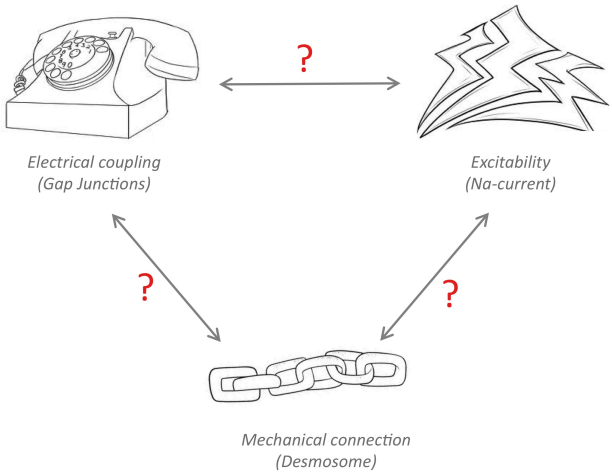

Figure 9.1 – *Model of determinants of conduction and their interactions.*

The disease that is associated with abnormal intercalated disk biology is Arrhythmogenic Cardiomyopathy (AC). In The Netherlands, this disease is in most cases associated with mutations in the desmosomal

protein Plakophilin-2 (PKP2). Patients with this mutation develop cardiac conduction abnormalities, which may ultimately lead to arrhythmias and sudden death. The approach of this thesis was 1) a basic approach focused on interaction of PKP2, Cx43 and $Na_V1.5$ using genetically modified mouse models and 2) to study the tissue from patients with AC. In the early stage of this disease, the concealed phase, no structural heart disease is observed. In this stage a large risk exists for sudden, possibly fatal arrhythmias. In the overt stage of the disease, major structural abnormalities are observed, leading to heart failure. To better understand the mechanism of this disease, especially in the concealed phase, it is essential to understand the cascade of events originating from changes in desmosomal composition that ultimately lead to electrical disturbances and arrhythmias.

Interaction of Cx43 and $Na_V1.5$

The first studies were focused on the interaction of the two electrical components, Cx43 and $Na_V1.5$ (Figure 9.1). In **chapter 3** we investigated the effect of abnormal Cx43 expression on $Na_V1.5$ expression and function. Tamoxifen-induced $Cx43^{CreER(T)/fl}$ mice, with a Cx43 protein level of about 5% as compared to the normal situation were tested for arrhythmia vulnerability. The study showed that animals in which we could induce arrhythmias (VT+) presented a larger reduction in Cx43 levels than animals without arrhythmias (VT-). Furthermore, heterogeneity of Cx43 was increased in these VT+ animals and, importantly, $Na_V1.5$ expression was lower in the VT+ mice. We showed that in regions of a strong Cx43 reduction, $Na_V1.5$ was absent as well. Interestingly, we found only low levels of fibrosis, comparable between VT+ and VT-, ruling this factor out as the primary cause of arrhythmogeneity in this model. In separate experiments on isolated rat ventricular cardiomyocytes that were completely silenced for Cx43 we showed that function of the sodium channel appeared also reduced. In conclusion regarding those experiments, we have shown in this chapter that there is an interaction between Cx43 and $Na_V1.5$ at the intercalated disk. Extreme reduction in Cx43 expression leads to reduction in $Na_V1.5$, eventually causing an arrhythmogenic substrate. Other studies with Cx43 knockout animal models have shown that a 50% reduction of Cx43 did not increase arrhythmia susceptibility, indicating that conduction reserve, which is defined as the extent to which conduction parameters may be altered before an effect on conduction

and arrhythmogeneity becomes evident, is not exceeded at a moderate reduction.[4, 5]

In **chapter 6** we tried to explore this connection further by studying post-mortem material and biopsies taken from several AC patients. As described in this chapter, a large majority of the AC patients showed a reduction in Cx43 and/or $Na_V1.5$. Whether the reduction of $Na_V1.5$ is caused by 1) a reduction in Cx43, or 2) the other way around, or 3) by a mutated desmosomal protein, or 4) by a currently still unresolved mechanism could not be concluded from this study. This has to be established in extensive future studies.

Since Cx43 and $Na_V1.5$ interact at the intercalated disk, extreme changes in one component can lead to an arrhythmogenic substrate by affecting the other. The connection between the components is not direct, but probably via scaffolding proteins, like for instance ZO-1,[6, 7] Ankyrin-G[8] or SAP97.[9] However, a mild reduction is not sufficient to tempt arrhythmogeneity because it will not exceed conduction reserve. This was already demonstrated earlier in our lab in a different study using mice with both a 50% reduction in Cx43 and $Na_V1.5$ or one of these factors separately, which did not lead to arrhythmias.[10]

In conclusion, we have established that combined severe reductions of Cx43 and $Na_V1.5$ are prerequisite for arrhythmias in mice. Typically, these reductions are found in patients with AC and presumably form the molecular substrate for the arrhythmias. The role of PKP2 in reduction of $Na_V1.5$ and Cx43 was subject of studies in **chapter 8**.

Interaction of desmosome (PKP2) and $Na_V1.5$

In The Netherlands, and also in the USA and Canada, a high prevalence of PKP2 mutations has been found in AC patients, compared to the other desmosomal proteins, as described in **chapter 4**. Therefore, we chose to study the function of PKP2 further in this thesis, to be able to search for disease mechanisms in patients with PKP2 associated AC.

As described before, total silencing of PKP2 leads to a reduced sodium current in isolated neonatal rat cardiomyocytes.[3] We studied mice with half the amount of PKP2 (PKP2-Hz) in **chapter 8**. Measurements in isolated cardiomyocytes from these mice indicated a decreased peak sodium current and changed activation and inactivation kinetics in PKP2-Hz at baseline. The conduction reserve for $Na_V1.5$ apparently is so high that this reduction in peak sodium current does not create an arrhythmogenic substrate in untreated mice; therefore,

the sodium channel blocker flecainide was used to unveil the sodium current deficit. Sodium channel blockers like flecainide or ajmaline are used commonly in clinical practice to unmask aberrant sodium channel function in patients.[11] Furthermore, previous studies conducted in mice haploinsufficient for $Na_V1.5$ showed that flecainide induced ventricular arrhythmias and conduction disturbances.[12] After addition of flecainide we observed conduction slowing and ventricular arrhythmias in our PKP2-Hz mice, but not in WT littermates. These findings are in favor of the hypothesis that changes in PKP2 have a negative effect on the function of $Na_V1.5$. Additional studies will be necessary to find the mechanism behind this interaction.

There is a striking difference in the results of **chapter 8**, where function of $Na_V1.5$ was altered in PKP2-Hz mice but no decrease in immunolabeling was found and the results of **chapter 6**, where in part of the AC patients a reduction in immunoreactive signal intensity was observed. In both cases $Na_V1.5$ is affected, but in a separate way. This could be due to the fact that the patients that we studied were not haploinsufficient for PKP2, but had, in a majority of cases, a mutation in PKP2 (Table 6.1). Previous studies already showed, albeit *in vitro,* that different mutations show different localizations in the cell.[13, 14] The effect of PKP2 mutations on protein structure and impact on the interaction with other proteins in the intercalated disk remains to be analyzed and could differ between mutations or mutation classes (i.e. truncating mutations, missense mutations).[15]

Furthermore, biopsies and HTX material from AC patients with a PKP2 mutation typically showed that PKP2 protein expression was not changed, both on immunohistochemistry and western blot. This has also been observed in other studies.[14, 16] Especially in patients with a truncation mutation in the first part of the protein, a haploinsufficient situation would have been expected.[17] However, also in these patients, a normal PKP2 expression level has been found. Possibly a feed-back mechanism at the transcriptional level results in up-regulation of the normal allele, which would explain the similar protein levels. In our patient-group, we had 3 real "haploinsufficient" patients, with a deletion of exon 1-4 or 1-14. In these patients we did observe reduced PKP2 levels (**chapter 6**).

In conclusion, we have shown that abnormal expression of PKP2 impairs sodium channel function, which may at least in part be responsible for electrical instability in patients.

Interaction of desmosome (PKP2) and Cx43

Total silencing of PKP2 in isolated neonatal rat ventricular cardiomyocytes leads to a decreased Cx43 expression as well as a changed localization of Cx43.[2] Furthermore, multiple studies have shown a reduction of Cx43 in AC patients, among which also patients with a mutation in *PKP2*.[18-20] These two observations both point towards an interaction between PKP2 and Cx43. In the patients described in **chapter 6** a subset of the patients with PKP2 mutation did not show Cx43 disturbances. Also, a reduction of PKP2 to 50% did not lead to a decrease in Cx43 as described in **chapter 8**, indicating that the remaining PKP2 is still able to retain normal Cx43. It seems that penetrance and possibly the type of mutations and the degree of PKP2 reduction is very important for development of the arrhythmogenic substrate.

Presumably, the interaction of PKP2 and Cx43 works only in one direction; reduction of PKP2 has a negative effect on the Cx43 expression levels, while reduction of Cx43 does not influence PKP2 expression. In a mouse model of cardiac specific conditional knockout of Cx43 it was shown that desmosomal proteins content was not changed as well as adherens junction proteins[21]. Unfortunately, PKP2 was not studied in this paper, so we cannot state that also expression of this desmosomal protein is not changed. We did not check PKP2 levels in our own $Cx43^{CreER(T)/fl}$ mice used in **chapter 3**.

From our experiments using genetically modified mouse models we can conclude that abnormal PKP2 expression does not necessarily lead to abnormal Cx43 expression. Conversely, abnormal Cx43 expression does not alter PKP2 expression.

AC mouse models

The complexity of the AC phenotype in patients makes it difficult to understand the mechanisms and identify leading components causing electrical and structural deterioration of the heart and development of arrhythmias. Several transgenic knockout mouse models for the desmosomal proteins have been developed to determine what the function of the particular proteins is and what the effect of their (partial) absence is on the heart. Furthermore, these mouse models can be used to further explore the interactions between desmosomes, Cx43 and $Na_V1.5$ (Figure 9.1). In **chapter 2** a part of these mouse models was already described. However, since this review was published in 2009, and a

fair amount of new studies have been published in the mean time, an update of the more recent studies can be found in the next paragraphs and in Table 9.1.

Plakoglobin mouse models

As described in **chapter 2**, mice with targeted deletion of plakoglobin (PKG) die from severe heart defects during embryogenesis.[22, 23] Heterozygous PKG-deficient mice display a typical right ventricular phenotype, including right ventricular dilatation, decreased right ventricular function and spontaneous ventricular ectopy. Left ventricular function was not altered. Endurance training in these animals accelerated development of the cardiac problems and also increased arrhythmia incidence. Remarkably, histology and electron microscopy did not show abnormalities in heterozygous mice: structure of desmosomal and adherens junctions was normal as well as Cx43 distribution and expression.[24] In a later study with the same mice it was shown that load-reducing therapy (furosemide and nitrates) could reduce the effect of training-induced cardiac dysfunction and arrhythmogenesis.[25] Conditional cardiac specific deletion of PKG caused extensive cardiac dysfunction, progressive loss of cardiomyocytes, inflammatory infiltration, and fibrous infiltration. Furthermore, this model showed reduced levels of PKG, DSG2, PKP2, DSP and also Cx43. Despite the reduction in Cx43, the mice did not have conduction abnormalities and arrhythmias were not inducible.[26] When these mice also received an inducible deletion of β-catenin however, spontaneous lethal ventricular arrhythmias occurred,[27] indicating that in the previous study probably β-catenin rescued the absence of PKG. In a cardiac specific PKG deletion mouse model generated by a different group extensive and progressive cardiac problems were described: ventricular dilatation, cardiac dysfunction and spontaneous arrhythmias. Furthermore, cardiac fibrosis, extensive cell death and absence of desmosomes were observed.[28] The reason as to why the cardiac problems in this model are so much more severe than the cardiac restricted model by Li et al. is probably because the second model is not a conditional model. In the conditional model, deletion was induced with Tamoxifen at age of 6-8 weeks old, implying a normal cardiac function up to that time point.[26] In the non-conditional model, PKG was knocked out at the onset of cardiac development, probably causing a much more pronounced effect.[28]

Table 9.1 – Murine models of AC

Protein	Model type	Phenotype	Histology	Reference
PKG	KO	Embryonic lethality, cardiac dysfunction.	Reduced desmosome number.	Bierkamp et al., 1996[16]
	KO	Embryonic lethality, cardiac dysfunction.	Desmosomes absent.	Ruiz et al., 1996[17]
	Hz-KO	RV dilatation, decreased RV function, spontaneous ventricular ectopy. Load-reducing therapy decreases training induced AC development.	No abnormalities on histology.	Kirchhof et al., 2006; Fabritz et al., 2011[18, 19]
	CS CKO	Cardiac dysfunction, no VT.	Cardiac fibrosis, desmosomal protein expression decreased, Cx43 expression decreased.	Li et al., 2011[20]
	CKO/DKO with β-cat	Cardiac dysfunction, conduction abnormalities, SCD.	Cardiac fibrosis, desmosomal protein expression decreased, Cx43 expression decreased.	Swope et al., 2012[21]
	CS KO	Ventricular dilatation, cardiac dysfunction, spontaneous VT.	Cardiac fibrosis, absence of desmosomes, normal Cx43	Li et al., 2011[22]
DSP	CS KO	Embryonic lethality, cardiac dysfunction, ventricular dilatation.	Fibrofatty infiltration.	Garcia-Gras et al., 2006[23]
	CS Hz-KO	Cardiac dysfunction, ventricular dilatation, spontaneous VT	Fibrofatty infiltration	
	CS Tg overexpression V30M / Q90R (N-terminus)	Ventricular dilatation, embryonic death		Yang et al., 2006[24]
	CS Tg overexpression R2834H (C-terminus)	Cardiac dysfunction, ventricular dilatation.	Fibrofatty infiltration, desmosomes absent, gap widening.	
	CS Hz-KO	Delayed conduction, inducible VT.	Cx43 expression reduced/changed localization	Gomes et al., 2012[25]
DSG2	Tg overexpression N271S	Cardiac dysfunction, ventricular dilatation, conduction slowing, spontaneous VT, SCD.	Cardiac fibrosis. Gap widening at desmosomal junctions. Cx43 expression normal.	Pilichou et al., 2009; Rizzo et al., 2012[26, 27]
	Tg deletion exon 4-6	LV dilatation, VT	Cardiac fibrosis	Krusche et al., 2011; Kant et al., 2012[28, 29]
PKP2	KO	Embryonic lethality, cardiac dysfunction.	Desmosomal protein expression reduced	Grossmann et al., 2004[30]
	Hz-KO	Conduction slowing, spontaneous VTs after sodium channel block.	Normal desmosomal/Cx43 protein expression. Gap widening	Chapter 8, this thesis

KO, knock-out; Hz-KO, Heterozygous knock-out; CS, cardiac specific; CKO, conditional knock-out; VT, ventricular tachycardia; DKO, double knock-out; SCD, sudden cardiac death; Tg, transgenic.

Desmoplakin mouse models

Cardiac-specific homozygous deletion of desmoplakin (DSP) induced high cardiac-related embryonic lethality. The DSP heterozygous mice from this same breed showed cardiac dysfunction, ventricular arrhythmias and fibrofatty replacement in the myocardium.[29] Cardiac specific overexpression of an N-terminal mutant of DSP, the site of binding to PKG and PKP2, caused severe ventricular dilatation, which resulted in embryonic lethality at E10-E12. Probably, the missing bindingsite for PKG and PKP2 resulted in unstable desmosomes, which were unable to cope with the mechanical load exerted on the developing heart.[30] Cardiac specific overexpression of a C-terminal mutant of DSP, the site of binding to the intermediate filaments, did result in viable offspring, though these mice had ventricular dilatation and bi-ventricular dysfunction, as well as fibrofatty infiltration. It was shown that these mice did not have desmosomes in their intercalated disk and gap widening was observed, whereas PKP2, PKG and Cx43 showed normal localization on immunohistochemistry.[30] A separate study showed that cardiac specific heterozygous deletion of DSP caused delayed activation and inducible arrhythmias. Furthermore, it was shown that Cx43 expression was reduced at the intercalated disk, but myocardial histology was normal. In this model, sodium current density was described as being normal in contrast to our findings in the PKP2-Hz mice (**chapter 8** of this thesis).[31]

Desmoglein-2 mouse models

A cardiac specific transgenic overexpression model for desmoglein-2 (DSG2) showed a dose-dependent severity of the phenotype. Mice with a higher overexpression of the mutation died at younger age than those with lower levels of the mutant. The transgenic mice showed spontaneous arrhythmias, cardiac dysfunction and dilatation of both ventricles, and also cardiac fibrosis was observed.[32] Furthermore, in a new study using the same mice[33] gap widening at the desmosomal junctions was observed, whereas Cx43 expression appeared to be normal. In a different transgenic model for DSG2, cardiac dilatation of especially the LV and sudden cardiac death was observed, as well as progressive cardiac fibrosis.[34, 35]

Table 9.2 – Electrophysiological parameters of wildtype versus PKP2-Hz

	3 months		6 months		Running	
	WT	**PKP2**	**WT**	**PKP2**	**WT**	**PKP2**
n	8	8	10	10	5	5
HW/BW (g/g)	0.62 ± 0.02	0.64 ± 0.03	0.52 ± 0.02	0.53 ± 0.03	0.64 ± 0.02	0.62 ± 0.02
RR (ms)	128.3 ± 4.9	135.9 ± 4.9	132.0 ± 5.6	130.0 ± 5.7	126.7 ± 6.5	118.6 ± 8.2
P (ms)	10.7 ± 0.5	10.7 ± 1.0	8.8 ± 0.6	8.6 ± 0.5	8.4 ± 0.3	8.3 ± 0.4
PR (ms)	41.1 ± 0.8	40.5 ± 1.3	40.7 ± 0.9	42.4 ± 1.2	39.2 ± 1.3	39.6 ± 1.2
QRS (ms)	11.4 ± 0.4	12.0 ± 0.5	9.3 ± 0.4	8.8 ± 0.2	9.4 ± 0.4	9.6 ± 0.4
QTc (ms)	138.0 ± 6.2	143.1 ± 6.0	132.4 ± 3.0	128.0 ± 2.0	123.0 ± 5.9	133.1 ± 6.6
FS (%)	-	-	-	-	45.7 ± 1.1	46.5 ± 0.3
Arrhythmia incidence	-	-	2 VT 2 AF	3 AF	1 VT	2 VT 1 AF
ERP LV (ms)	51.3 ± 4.4.	56.3 ± 5.0	52.5 ± 3.7	48.9 ± 2.6	68.0 ± 3.7	70.0 ± 8.4
ERP RV (ms)	43.8 ± 2.6	52.5 ± 4.5	42.0 ± 12.3	34.4 ± 2.9	46.0 ± 4.0	52.0 ± 2.0

	Sham		TAC		Sham		Shunt	
	WT	**PKP2**	**WT**	**PKP2**	**WT**	**PKP2**	**WT**	**PKP2**
n	5	9	8	9	5	3	5	4
HW/BW (g/g)	0.70 ± 0.11	0.58 ± 0.03	0.83 ± 0.06	0.87 ± 0.06	0.60 ± 0.03	0.66 ± 0.04	0.61 ± 0.05	0.74 ± 0.09
RR (ms)	118.6 ± 6.1	133.9 ± 5.3	122.5 ± 6.7	113.1 ± 3.2	123.9 ± 6.9	120.1 ± 12.2	125.5 ± 8.3	122.8 ± 2.4
P (ms)	9.4 ± 1.1	9.5 ± 0.5	10.0 ± 0.6	9.1 ±0.5	9.0 ± 0.5	8.6 ± 0.7	9.6 ± 0.7	9.2 ± 1.1
PR (ms)	39.9 ± 1.7	40.2 ± 0.6	40.8 ± 1.2	42.3 ± 0.6	42.4 ± 1.0	40.1 ± 0.4	42.6 ± 2.2	43.6 ± 1.6
QRS (ms)	9.2 ± 0.5	8.7 ± 0.4	11.0 ± 0.9	11.5 ± 0.6	9.4 ± 0.5	9.0 ± 0.2	9.9 ± 0.4	10.3 ± 0.6
QTc (ms)	140.1 ± 4.1	130.0 ± 2.9	141.6 ± 5.2	152.6 ± 4.7	136.4 ± 3.2	127.5 ± 5.1	134.0 ± 6.1	126.7 ± 4.8
FS (%)	46.3 ± 2.3	46.6 ± 1.2	37.7 ± 1.1	36.8 ± 2.2	48.7 ± 0.9	47.6 ± 1.7	41.5 ± 3.2	38.1 ± 3.6
Arrhythmia incidence	1 VT 1 AF	1 VT 3 AF	2 VT	2 VT	1 VT 1 AF	-	-	-
ERP LV (ms)	56.7 ± 5.6	50.0 ± 7.6	64.3 ± 4.8	56.3 ± 4.6	40.0 ± 0.0	56.7 ± 6.7	44.0 ± 2.4	53.3 ± 14.5
ERP RV (ms)	46.7 ± 6.7	42.9 ± 4.2	48.6 ± 2.6	46.3 ± 5.0	34.0 ± 2.4	46.7 ± 3.3	40.0 ± 3.2	56.7 ± 8.8

WT, Wildtype; PKP2, Plakophilin-2; HW/BW, heart weight/body weight ratio; FS, fractional shortening; ERP, effective refractory period; LV, left ventricle; RV, right ventricle.

Plakophilin-2 mouse models

Total knockout of plakophilin-2 (PKP2) is embryonically lethal.[36] However, heterozygous mice with the same background appeared fairly normal, as described in **chapter 8** of this thesis. Expression levels and localization of desmosomal proteins (other than PKP2), adherens junction protein, and gap junctional protein were not changed. Also, fibrotic infiltrations were absent. Furthermore, echocardiographic and ECG characteristics were not different between wildtype and PKP2-Hz mice under basic conditions (Table 9.2).

Since not all patients with a mutation in *PKP2* show symptoms of AC, there are additional factors that contribute to disease development. Such factors could be a volume- or pressure overload, viral infection, or inflammatory response. We tried to elucidate these factors in the PKP2-Hz mice using several approaches. We started by comparing young mice (3 months old) to older mice (6 months old), since it was described that arrhythmia incidence increases with age.[5, 37] Arrhythmia incidence was slightly increased in the 6 months old mice, although no differences were observed between WT and PKP2-Hz. Furthermore, electrophysiological parameters were unchanged. Increasing the age of our PKP2-HZ mice towards 18-22 months probably will lead to increased arrhythmia incidence, since it was described before that even WT mice become arrhythmogenic at high age.[37, 38] However, whether this extensive aging will discriminate between WT and PKP2-Hz remains to be determined.

Next, PKP2-Hz mice were subjected to voluntary running on a treadmill. It has been described that endurance training can decrease cardiac function and can provoke arrhythmias.[25, 39, 40] Therefore, patients with AC are often recommended to avoid endurance training.[41] Measurements were performed after 1 month of voluntary running. Arrhythmia incidence was again slightly increased, compared to sedentary 3 months old animals; however again, no difference between WT and PKP2-Hz was observed, although group numbers still have to be increased.

In a third series of experiments we performed Sham and transverse aortic constriction (TAC) surgery on PKP2-Hz and WT mice to induce pressure overload.[42] 8 weeks after surgery the mice were sacrificed. Previous studies from our group and others have shown that TAC surgery induces extensive electrical and structural remodeling of the heart and that arrhythmia vulnerability is largely increased.[42] As can be appreciated from Table 9.2 TAC surgery induced changes in the

QRS duration and in fractional shortening, which is a measurement for cardiac function. Fractional shortening was reduced after TAC surgery, however appeared not different between WT and PKP2-Hz. Also arrhythmia incidence increased slightly due to TAC surgery, but again WT and PKP2-Hz could not be separated.

Finally, we performed cardiac shunt surgery on the PKP2-Hz mice.[43] In this technique an aortocaval shunt is created to induce volume overload. This model did not seem to increase arrhythmia vulnerability of the mice nor introduction of any change in the electrophysiological parameters. However, although not statistically different due to low group numbers, fractional shortening seemed to decrease more in the PKP2-Hz mice than in WT.

The lack of an arrhythmogenic or structural phenotype after aging, voluntary running, TAC surgery and Shunt surgery in our PKP2-Hz mice is a negative result, but not unimportant. Apparently, a reduction of PKP2 towards 50% of normal levels is not enough, even after several precipitating factors, to discriminate between PKP2-Hz and WT mice. So possibly, extending it to the human situation, in AC patients it is not the reduction in normal PKP2 protein that causes the phenotype, but rather an external trigger (e.g. inflammation) or the presence of mutated PKP2 protein. Previous studies have shown that when mutant PKP2 DNA is transfected in isolated neonatal rat cardiomyocytes, endogenous Cx43 was reduced and also interaction with other desmosomal proteins was reduced.[13]

Table 9.3 – DNA constructs of PKP2 mutations

PKP2 mutant	**Protein weight**	**Localization in HEK293/COS7 cells**
PKP2wtAS	100 kD	Plasma membrane
PKP2Trp848X	95 kD	Protein synthesis and transport associated vesicles
PKP2Tyr807X	88 kD	Protein synthesis and transport associated vesicles / nucleus
PKP2Tyr616X	67 kD	Protein synthesis and transport associated vesicles / nucleus
PKP2Val406fsX4	49 kD	Protein synthesis and transport associated vesicles / nucleus
PKP2Gln133X	18 kD	Protein synthesis and transport associated vesicles
PKP2Arg79X	12 kD	Cytoplasm

To follow up on this study, we created WT and 6 progressively shorter DNA constructs encoding mutated PKP2 based on truncating mutations found in AC patients (Table 9.3). Localization of these DNA constructs in cellular systems was studied and we observed that none

of our constructs could mimic normal localization of wildtype PKP2, which is present on the plasma membrane. We found expression of the mutant constructs in the cytoplasm, in intracellular vesicles, and in the nucleus (Figure 9.2). Next, we made adenoviruses of these constructs. These viruses will facilitate in future studies to introduce a high expression level of mutated PKP2 in isolated cardiomyocytes or, after injection of the virus in the heart, in PKP2-Hz hearts to study the effect of mutated DNA on endogeneous PKP2 expression and other desmosomal/gap junctional proteins.

Synthesis and clinical relevance of this thesis

This thesis focuses on the interaction between desmosomes, gap junctions and sodium channels in the intercalated disk. We have used arrhythmogenic cardiomyopathy, a disease characterized by ventricular arrhythmias, syncope and sudden cardiac death, as a model for defective desmosomes. AC is also called "a disease of the desmosome", since a large subset of the patients has mutations in desmosomal proteins. The estimated prevalence of AC in the general population ranges from 1 in 2000 to 1 in 5000.[44] Prevalence could be higher since diagnosis of AC is difficult, especially in subjects in the concealed phase of the disease. Unfortunately, sudden death often is the first manifestation of the disease. In this thesis we aimed to get a better understanding of AC from a molecular level to a genetic/clinical level.

We have shown using mouse models that abnormal PKP2 expression leads to both reduced $Na_V1.5$ and Cx43 expression. This cascade of events may be present in the intercalated disk of AC patients: the mutation in a desmosomal protein alters the desmosome structure due to the expression of abnormal proteins or reduced expression of normal proteins.[14] This unstable desmosome is connected via scaffolding proteins to both the gap junction and the sodium channel and might impair expression of interaction of these [6-9] Apart from reduced expression levels, gap junction protein expression is also redistributed[16, 45, 46], causing a higher propensity for arrhythmias. Furthermore, the sodium channel expression and/or kinetics are altered, causing even larger electrical instability. Future studies are necessary to elucidate the exact molecular mechanisms behind these observations and to answer the question why some patients suffer from arrhythmias, and others having the same genetic predisposition don't.

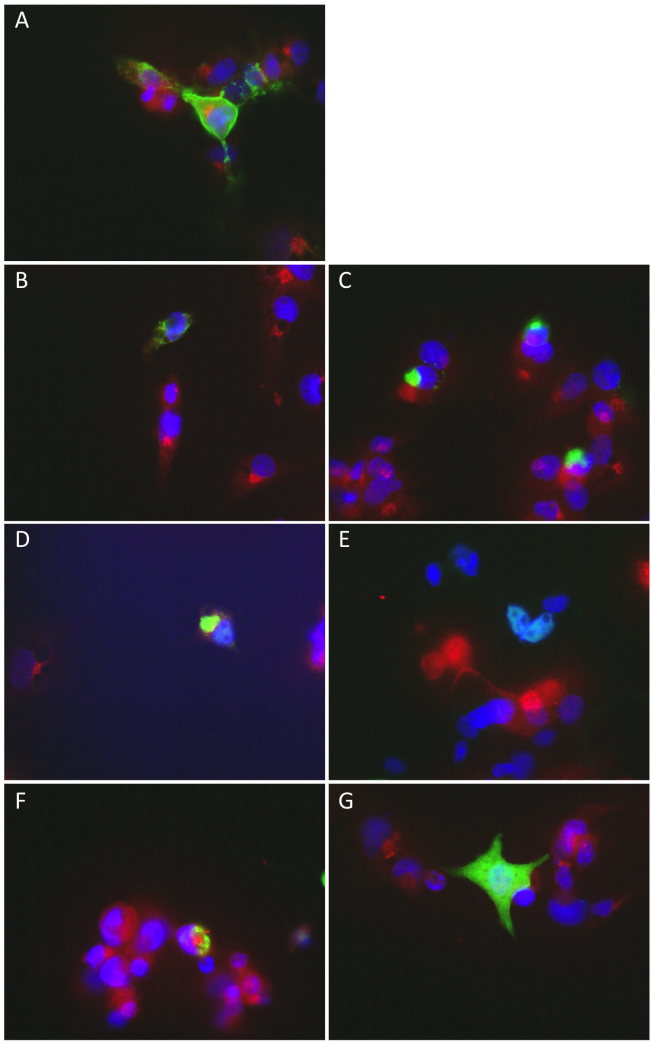

Figure 9.2 – *Expression pattern of mutant constructs in COS7 cells.* A. Wildtype PKP2 is expressed on the plasma membrane when expressed in COS7 cells. B. Pkp2Trp848X localizes close to the membrane. C. Pkp2Tyr 807X localizes in or just outside the nucleus D-E. Pkp2Tyr616X and Pkp2Val406fsX4 localize in the Golgi apparatus and in the nucleus. F. Pkp2Gln133X localizes in vesicles throughout the whole cell. G. Pkp2Arg79X localizes in the cytoplasm. Green: HA-tagged PKP2 construct; Red: Golgi apparatus; blue: nucleus.

Final goal of future studies is to be able to diagnose AC more accurate and earlier in the concealed phase of the disease development and

prevent sudden cardiac death in these patients.

Conclusion

In this thesis we have shown that our hypothesis

> *A large macromolecular complex is situated at the intercalated disk of the cardiomyocyte, consisting of gap junctions, sodium channels and desmosomes. Changes in expression or localization of one component will lead to changes in the others. These changes can create an arrhythmogenic substrate.*

is largely supported by our data. We can now fill in the gaps in Figure 9.1 and hence create Figure 9.3: Abnormal desmosome function leads to abnormal Cx43 and $Na_V1.5$ function and expression. This leads to electrical instability and high propensity for cardiac arrhythmias.

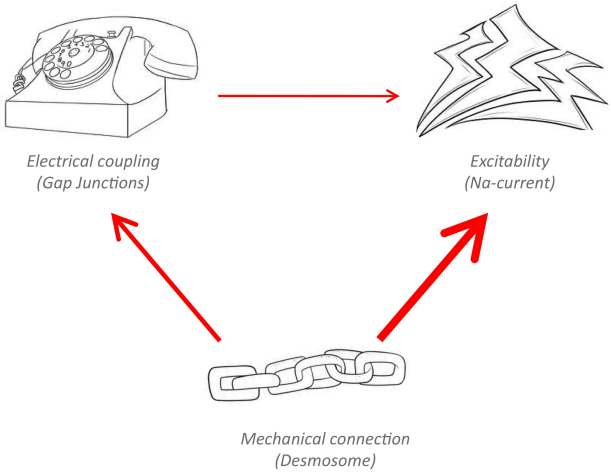

Figure 9.3 – *Model of determinants of conduction and their interactions.* Thickness of the arrow indicates the effect size.

References

1. Malhotra JD, Thyagarajan V, Chen C, Isom LL. Tyrosine-phosphorylated and nonphosphorylated sodium channel beta1 subunits are differentially localized in cardiac myocytes. *J Biol Chem.* 2004;279:40748-40754
2. Oxford EM, Musa H, Maass K, Coombs W, Taffet SM, Delmar M. Connexin43 remodeling caused by inhibition of plakophilin-2 expression in cardiac cells. *Circ Res.* 2007;101:703-711
3. Sato PY, Musa H, Coombs W, Guerrero-Serna G, Patino GA, Taffet SM, Isom LL, Delmar M. Loss of plakophilin-2 expression leads to decreased sodium current and slower conduction velocity in cultured cardiac myocytes. *Circ Res.* 2009;105:523-526
4. van Rijen HV, Eckardt D, Degen J, Theis M, Ott T, Willecke K, Jongsma HJ, Opthof T, de Bakker JM. Slow conduction and enhanced anisotropy increase the propensity for ventricular tachyarrhythmias in adult mice with induced deletion of connexin43. *Circulation.* 2004;-109:1048-1055
5. van Veen TA, Stein M, Royer A, Le Quang K, Charpentier F, Colledge WH, Huang CL, Wilders R, Grace AA, Escande D, de Bakker JM, van Rijen HV. Impaired impulse propagation in scn5a-knockout mice: Combined contribution of excitability, connexin expression, and tissue architecture in relation to aging. *Circulation.* 2005;112:1927-1935
6. Toyofuku T, Yabuki M, Otsu K, Kuzuya T, Hori M, Tada M. Direct association of the gap junction protein connexin-43 with zo-1 in cardiac myocytes. *J Biol Chem.* 1998;273:12725-12731
7. Laing JG, Saffitz JE, Steinberg TH, Yamada KA. Diminished zonula occludens-1 expression in the failing human heart. *Cardiovasc Pathol.* 2007;16:159-164
8. Sato PY, Coombs W, Lin X, Nekrasova O, Green KJ, Isom LL, Taffet SM, Delmar M. Interactions between ankyrin-g, plakophilin-2, and connexin43 at the cardiac intercalated disk. *Circ Res.* 2011;109:193-201
9. Petitprez S, Zmoos AF, Ogrodnik J, Balse E, Raad N, El-Haou S, Albesa M, Bittihn P, Luther S, Lehnart SE, Hatem SN, Coulombe A, Abriel H. Sap97 and dystrophin macromolecular complexes determine two pools of cardiac sodium channels $Na_V1.5$ in cardiomyocytes. *Circ Res.* 2011;108:294-304
10. Stein M, van Veen TA, Remme CA, Boulaksil M, Noorman M, van Stuijvenberg L, van der Nagel R, Bezzina CR, Hauer RN, de Bakker JM, van Rijen HV. Combined reduction of intercellular coupling and membrane excitability differentially affects transverse and longitudinal cardiac conduction. *Cardiovasc Res.* 2009;83:52-60
11. Brugada R, Brugada J, Antzelevitch C, Kirsch GE, Potenza D, Towbin JA, Brugada P. Sodium channel blockers identify risk for sudden death in patients with st-segment elevation and right bundle branch block but structurally normal hearts. *Circulation.* 2000;101:510-515

12. Martin CA, Zhang Y, Grace AA, Huang CL. In vivo studies of scn5a+/- mice modeling brugada syndrome demonstrate both conduction and repolarization abnormalities. *J Electrocardiol*. 2010;43:433-439
13. Joshi-Mukherjee R, Coombs W, Musa H, Oxford E, Taffet S, Delmar M. Characterization of the molecular phenotype of two arrhythmogenic right ventricular cardiomyopathy (arvc)-related plakophilin-2 (pkp2) mutations. *Heart Rhythm*. 2008;5:1715-1723
14. Kirchner F, Schuetz A, Boldt LH, Martens K, Dittmar G, Haverkamp W, Thierfelder L, Heinemann U, Gerull B. Molecular insights into arrhythmogenic right ventricular cardiomyopathy caused by plakophilin-2 missense mutations. *Circ Cardiovasc Genet*. 2012
15. Pilichou K, Thiene G, Basso C. Assessing the significance of pathogenic mutations and autopsy findings in the light of 2010 arrhythmogenic right ventricular cardiomyopathy diagnostic criteria: A clinical challenge. *Circ Cardiovasc Genet*. 2012;5:384-386
16. Fidler LM, Wilson GJ, Liu F, Cui X, Scherer SW, Taylor GP, Hamilton RM. Abnormal connexin43 in arrhythmogenic right ventricular cardiomyopathy caused by plakophilin-2 mutations. *J Cell Mol Med*. 2009;13:4219-4228
17. Chen X, Bonne S, Hatzfeld M, van Roy F, Green KJ. Protein binding and functional characterization of plakophilin 2. Evidence for its diverse roles in desmosomes and beta-catenin signaling. *J Biol Chem*. 2002;277:10512-10522
18. Kaplan SR, Gard JJ, Carvajal-Huerta L, Ruiz-Cabezas JC, Thiene G, Saffitz JE. Structural and molecular pathology of the heart in carvajal syndrome. *Cardiovasc Pathol*. 2004;13:26-32
19. Kaplan SR, Gard JJ, Protonotarios N, Tsatsopoulou A, Spiliopoulou C, Anastasakis A, Squarcioni CP, McKenna WJ, Thiene G, Basso C, Brousse N, Fontaine G, Saffitz JE. Remodeling of myocyte gap junctions in arrhythmogenic right ventricular cardiomyopathy due to a deletion in plakoglobin (naxos disease). *Heart Rhythm*. 2004;1:3-11
20. Asimaki A, Tandri H, Huang H, Halushka MK, Gautam S, Basso C, Thiene G, Tsatsopoulou A, Protonotarios N, McKenna WJ, Calkins H, Saffitz JE. A new diagnostic test for arrhythmogenic right ventricular cardiomyopathy. *N Engl J Med*. 2009;360:1075-1084
21. Antzelevitch C, Brugada P, Borggrefe M, Brugada J, Brugada R, Corrado D, Gussak I, LeMarec H, Nademanee K, Perez Riera AR, Shimizu W, Schulze-Bahr E, Tan H, Wilde A. Brugada syndrome: Report of the second consensus conference: Endorsed by the heart rhythm society and the european heart rhythm association. *Circulation*. 2005;111:659-670
22. Bierkamp C, McLaughlin KJ, Schwarz H, Huber O, Kemler R. Embryonic heart and skin defects in mice lacking plakoglobin. *Dev Biol*. 1996;180:780-785
23. Ruiz P, Brinkmann V, Ledermann B, Behrend M, Grund C, Thalhammer C, Vogel F, Birchmeier C, Gunthert U, Franke WW, Birchmeier W. Targeted mutation of plakoglobin in mice reveals essential functions

of desmosomes in the embryonic heart. *J Cell Biol*. 1996;135:215-225
24. Kirchhof P, Fabritz L, Zwiener M, Witt H, Schafers M, Zellerhoff S, Paul M, Athai T, Hiller KH, Baba HA, Breithardt G, Ruiz P, Wichter T, Levkau B. Age- and training-dependent development of arrhythmogenic right ventricular cardiomyopathy in heterozygous plakoglobin-deficient mice. *Circulation*. 2006;114:1799-1806
25. Fabritz L, Hoogendijk MG, Scicluna BP, van Amersfoorth SC, Fortmueller L, Wolf S, Laakmann S, Kreienkamp N, Piccini I, Breithardt G, Noppinger PR, Witt H, Ebnet K, Wichter T, Levkau B, Franke WW, Pieperhoff S, de Bakker JM, Coronel R, Kirchhof P. Load-reducing therapy prevents development of arrhythmogenic right ventricular cardiomyopathy in plakoglobin-deficient mice. *J Am Coll Cardiol*. 2011;-57:740-750
26. Li J, Swope D, Raess N, Cheng L, Muller EJ, Radice GL. Cardiac tissue-restricted deletion of plakoglobin results in progressive cardiomyopathy and activation of beta-catenin signaling. *Mol Cell Biol*. 2011;31:1134-1144
27. Swope D, Cheng L, Gao E, Li J, Radice GL. Loss of cadherin-binding proteins beta-catenin and plakoglobin in the heart leads to gap junction remodeling and arrhythmogenesis. *Mol Cell Biol*. 2012;32:1056-1067
28. Li D, Liu Y, Maruyama M, Zhu W, Chen H, Zhang W, Reuter S, Lin SF, Haneline LS, Field LJ, Chen PS, Shou W. Restrictive loss of plakoglobin in cardiomyocytes leads to arrhythmogenic cardiomyopathy. *Hum Mol Genet*. 2011;20:4582-4596
29. Garcia-Gras E, Lombardi R, Giocondo MJ, Willerson JT, Schneider MD, Khoury DS, Marian AJ. Suppression of canonical wnt/beta-catenin signaling by nuclear plakoglobin recapitulates phenotype of arrhythmogenic right ventricular cardiomyopathy. *J Clin Invest*. 2006;116:2012-2021
30. Yang Z, Bowles NE, Scherer SE, Taylor MD, Kearney DL, Ge S, Nadvoretskiy VV, DeFreitas G, Carabello B, Brandon LI, Godsel LM, Green KJ, Saffitz JE, Li H, Danieli GA, Calkins H, Marcus F, Towbin JA. Desmosomal dysfunction due to mutations in desmoplakin causes arrhythmogenic right ventricular dysplasia/cardiomyopathy. *Circ Res*. 2006;99:646-655
31. Gomes J, Finlay M, Ahmed AK, Ciaccio EJ, Asimaki A, Saffitz JE, Quarta G, Nobles M, Syrris P, Chaubey S, McKenna WJ, Tinker A, Lambiase PD. Electrophysiological abnormalities precede overt structural changes in arrhythmogenic right ventricular cardiomyopathy due to mutations in desmoplakin-a combined murine and human study. *Eur Heart J*. 2012
32. Pilichou K, Remme CA, Basso C, Campian ME, Rizzo S, Barnett P, Scicluna BP, Bauce B, van den Hoff MJ, de Bakker JM, Tan HL, Valente M, Nava A, Wilde AA, Moorman AF, Thiene G, Bezzina CR. Myocyte necrosis underlies progressive myocardial dystrophy in mouse dsg2-related arrhythmogenic right ventricular cardiomyopathy. *J Exp*

Med. 2009;206:1787-1802
33. Rizzo S, Lodder EM, Remme CA, Wolswinkel R, Pilichou K, Basso C, Thiene G, Bezzina CR. Intercalated disk abnormalities, conduction slowing and arrhythmogenesis in desmoglein-2 mutant mice prior to the development of cardiomyopathic changes. *Circulation*. 2011;Abstract
34. Krusche CA, Holthofer B, Hofe V, van de Sandt AM, Eshkind L, Bockamp E, Merx MW, Kant S, Windoffer R, Leube RE. Desmoglein 2 mutant mice develop cardiac fibrosis and dilation. *Basic Res Cardiol*. 2011;106:617-633
35. Kant S, Krull P, Eisner S, Leube RE, Krusche CA. Histological and ultrastructural abnormalities in murine desmoglein 2-mutant hearts. *Cell Tissue Res*. 2012
36. Grossmann KS, Grund C, Huelsken J, Behrend M, Erdmann B, Franke WW, Birchmeier W. Requirement of plakophilin 2 for heart morphogenesis and cardiac junction formation. *J Cell Biol*. 2004;167:149-160
37. Stein M, Noorman M, van Veen TA, Herold E, Engelen MA, Boulaksil M, Antoons G, Jansen JA, van Oosterhout MF, Hauer RN, de Bakker JM, van Rijen HV. Dominant arrhythmia vulnerability of the right ventricle in senescent mice. *Heart Rhythm*. 2008;5:438-448
38. Jansen JA, van Veen TA, de Jong S, van der Nagel R, van Stuijvenberg L, Driessen H, Labzowski R, Oefner CM, Bosch AA, Nguyen TQ, Goldschmeding R, Vos MA, de Bakker JM, van Rijen HV. Reduced cx43 expression triggers increased fibrosis due to enhanced fibroblast activity. *Circ Arrhythm Electrophysiol*. 2012
39. Benito B, Gay-Jordi G, Serrano-Mollar A, Guasch E, Shi Y, Tardif JC, Brugada J, Nattel S, Mont L. Cardiac arrhythmogenic remodeling in a rat model of long-term intensive exercise training. *Circulation*. 2011;123:13-22
40. Corrado D, Basso C, Schiavon M, Thiene G. Does sports activity enhance the risk of sudden cardiac death? *J Cardiovasc Med (Hagerstown)*. 2006;7:228-233
41. Maron BJ, Chaitman BR, Ackerman MJ, Bayes de Luna A, Corrado D, Crosson JE, Deal BJ, Driscoll DJ, Estes NA, 3rd, Araujo CG, Liang DH, Mitten MJ, Myerburg RJ, Pelliccia A, Thompson PD, Towbin JA, Van Camp SP. Recommendations for physical activity and recreational sports participation for young patients with genetic cardiovascular diseases. *Circulation*. 2004;109:2807-2816
42. Boulaksil M, Winckels SK, Engelen MA, Stein M, van Veen TA, Jansen JA, Linnenbank AC, Bierhuizen MF, Groenewegen WA, van Oosterhout MF, Kirkels JH, de Jonge N, Varro A, Vos MA, de Bakker JM, van Rijen HV. Heterogeneous connexin43 distribution in heart failure is associated with dispersed conduction and enhanced susceptibility to ventricular arrhythmias. *Eur J Heart Fail*. 2010;12:913-921
43. Toischer K, Rokita AG, Unsold B, Zhu W, Kararigas G, Sossalla S, Reuter SP, Becker A, Teucher N, Seidler T, Grebe C, Preuss L, Gupta SN, Schmidt K, Lehnart SE, Kruger M, Linke WA, Backs J, Regitz-

Zagrosek V, Schafer K, Field LJ, Maier LS, Hasenfuss G. Differential cardiac remodeling in preload versus afterload. *Circulation*. 2010;122:-993-1003

44. Thiene G, Corrado D, Basso C. Arrhythmogenic right ventricular cardiomyopathy/dysplasia. *Orphanet J Rare Dis*. 2007;2:45
45. Tandri H, Asimaki A, Dalal D, Saffitz JE, Halushka MK, Calkins H. Gap junction remodeling in a case of arrhythmogenic right ventricular dysplasia due to plakophilin-2 mutation. *J Cardiovasc Electrophysiol*. 2008
46. Oxford EM, Everitt M, Coombs W, Fox PR, Kraus M, Gelzer AR, Saffitz J, Taffet SM, Moise NS, Delmar M. Molecular composition of the intercalated disk in a spontaneous canine animal model of arrhythmogenic right ventricular dysplasia/cardiomyopathy. *Heart Rhythm*. 2007;4:1196-1205

CHAPTER 10

Summary

The cardiac conduction system

The heart is a pump, which continuously pumps the blood through the entire body. The cardiac conduction system ensures the coordinated depolarization and repolarization of the cardiomyocytes. Normal conduction through the heart starts at the sino-atrial node in the right atrium and spreads from there through the atria. After this, the activation front is collected and delayed in the atrioventricular node and continued through the His-bundle and the bundle branches towards the Purkinje fibers. From these fibers the ventricular myocardium is activated, followed by contraction. If the intra-ventricular impulse propagation is altered, ventricular arrhythmias can arise.

Several structures present in the intercalated disk at the longitudinal ends of the cardiomyocytes are important for the propagation of the electrical impulse. Gap junctions, of which Connexin43 (Cx43) is the most important protein in the ventricle, ensure electrical coupling between the cardiomyocytes. Mechanical connection between the cells at the site of the intercalated disk is maintained by desmosomes. Furthermore, the cardiac sodium channel ($Na_V1.5$) ensures excitability of the cells. Obviously, disturbances in expression or function of these structures can decrease cell-cell coupling and thereby smooth conduction, which can lead to severe cardiac arrhythmias.

Arrhythmogenic Cardiomyopathy

Arrhythmogenic Cardiomyopathy (AC) is a progressive cardiac disease characterized by electrical and structural degeneration, predominantly of the right ventricle, which may eventually also affect the left ventricle and interventricular septum. However, also predominantly left ventricular involvement may occur. Patients present with syncope, palpitations, and sudden cardiac death. 60% of the AC cases is associated with mutations in the genes encoding for desmosomal proteins: Plakophilin2 (PKP2), Plakoglobin (PKG), Desmoplakin (DSP), Desmocollin2 (DSC2) and/or Desmoglein2 (DSG2). Prevalence of the disease is 1:2000-1:5000, however (early) diagnosis of the disease is difficult, so many cases can be un- or misdiagnosed. Diagnosis is based on to the revised Task Force Criteria, which are based on global or regional dysfunction and structural alterations, tissue characterization of the ventricular wall, re- and depolarization or conduction abnormalities, arrhythmias, and family history.

This thesis

The aim of this thesis was to elucidate how $Na_V1.5$, Cx43, and desmosomal proteins (mainly PKP2), three components of the intercalated disk, interact with and influence each other and contribute to abnormal conduction and arrhythmias (**chapter 1**). This was studied using several mouse models and patient material. **Chapter 2** is an extensive literature overview describing structures in the intercalated disk and their function. Disease and animal models are described where one of the components of the intercalated disk is affected, causing disturbances in other structures. In **chapter 3** one of these animal models was used, where Cx43 expression was reduced towards 5% of its normal value. In 50% of the hearts of these mice we could induce arrhythmias. Arrhythmogenic hearts (VT+) were compared to non-arrhythmogenic hearts (VT-). Conduction slowing was more severe in VT+ as well as dispersion of conduction. Furthermore, a larger downregulation of Cx43 in VT+ was found and, more importantly, also $Na_V1.5$ was further decreased in VT+. Separate experiments on isolated neonatal cardiomyocytes showed that after silencing of Cx43, also peak sodium current was reduced. In summary, this chapter demonstrated interaction between Cx43 and $Na_V1.5$ in a situation of extreme Cx43 reduction, resulting in arrhythmias. Starting at **chapter 4** we focused on arrhythmogenic cardiomyopathy (AC), using this disease as a model of defective desmosomes. In this chapter an overview was given of the prevalence of mutations in desmosomal proteins in AC patients and the geographical distribution of these mutations. We found that in most populations that have been studied, mutations in the *pkp2* gene are most common, especially in The Netherlands, and Northern America. In **chapter 5** the clinical, histological, immunohistochemical and ultrastructural features of an AC patient that underwent a heart transplant was described. In the heart of this patient replacement fibrosis and fatty tissue were observed in the entire right ventricular wall and also in large parts of the left ventricle and interventricular septum. Surprisingly, gap junctions were only moderately affected in this patient, but areas of gap widening at the intercalated disk were observed on the ultrastructural level. Biopsies and autopsy material from AC patient hearts were used in **chapter 6** and **chapter 7**. In **chapter 6** the arrhythmogenic substrate of 20 AC patients on an immunohistological level was described. A downregulation of Cx43, $Na_V1.5$ and desmosomal protein PKG was observed in a large subset of the patients, which once again hints towards an interaction between the three

components. In **chapter 7** a more technical issue is addressed regarding tissue preservation and antibody dilutions, to prevent misdiagnosis of AC due to immunohistochemical errors based on tissue stainings. In **chapter 8** a mouse model is described with mice having half of the normal PKP2 expression. We found reduced sodium current in isolated cardiomyocytes from these mice, indicating an interaction between PKP2 and $Na_V1.5$. Furthermore, after addition of the sodium channel blocker flecainide, we saw, in the absence of structural disease, reduced conduction velocity in the longitudinal direction of the right ventricle, altered electrocardiographic characteristics and arrhythmias, emphasizing the pivotal role of $Na_V1.5$ in arrhythmias in AC. Finally in **chapter 9** all the preceding chapters are put into perspective.

Conclusion

In conclusion, in this thesis the interactions between gap junctions, the cardiac sodium channel and desmosomes are studied. It is shown that all of these structures are related and that disturbances of a component may lead to disturbances in the others. The desmosome is the most stable of the three: disturbances in Cx43 or $Na_V1.5$ do not lead to decreased desmosome function, whereas decreased desmosomal stability can lead to decreased electrical coupling and reduced excitability. Furthermore, gap junctional disturbances can affect excitability (in extreme situations). Remodeling of the three structures in the intercalated disk mentioned before leads tot development of an arrhythmogenic substrate and hence to an increased propensity for arrhythmias.

CHAPTER 11

Nederlandse samenvatting

Het geleidingssysteem

Het hart pompt voortdurend bloed door het hele lichaam. Het geleidingssysteem in het hart zorgt ervoor dat de hartspiercellen gecoördineerd depolariseren en repolariseren. Normale geleiding door het hart begint in de sinusknoop, welke gelegen is in de rechter boezem. Het elektrische signaal verspreidt zich vanuit daar door de beide boezems. Hierna komt het activatiefront samen in de AV-knoop (atrioventriculaire knoop), waar het signaal wordt opgevangen en vertraagd en vervolgens doorgestuurd wordt via de His-bundels en de bundeltakken naar de Purkinje vezels. Vanuit deze vezels worden de hartspiercellen in de kamers geactiveerd, gevolgd door hun samentrekking. Wanneer de geleiding door de hartkamers wordt verstoord, kunnen ritmestoornissen ontstaan in de kamer.

Verschillende structuren die aanwezig zijn in de intercalairschijf aan de longitudinale uiteinden van de hartspiercellen zijn belangrijk voor de voortgeleiding van het elektrische signaal. Gap junctions, waarvan Connexine43 (Cx43) de belangrijkste is in de kamers, zorgen voor de elektrische koppeling tussen de hartspiercellen. Mechanische koppeling tussen de cellen aan de kant van de intercalairschijf wordt verzorgd door desmosomen. Exciteerbaarheid van de cellen is afhankelijk van de natriumkanalen in het hart ($Na_V1.5$). Vanzelfsprekend kunnen verstoringen in expressie of functionaliteit van deze structuren de koppeling tussen de cellen verminderen en daarbij ook soepele voortgeleiding van de elektrische impuls. Dit kan leiden tot ernstige en soms fatale hartritmestoornissen.

Aritmogene Cardiomyopatie

Aritmogene cardiomyopatie (AC) is een progressieve hartziekte die wordt gekarakteriseerd door een degeneratie van voornamelijk de rechter kamer, en welke uiteindelijk ook de linker kamer en het septum kan aantasten. Er komen ook gevallen voor waarbij voornamelijk de linker kamer is aangetast. Patiënten presenteren zich met syncope (wegraken of flauwvallen), hartkloppingen en met plotselinge hartdood. Ongeveer 60% van de gevallen van AC wordt geassocieerd met mutaties in de genen die coderen voor de desmosomale eiwitten: Plakofiline2 (PKP2), Plakoglobine (PKG), Desmoplakine (DSP), Desmocolline2 (DSC2) en/of Desmogleine2 (DSG2). Prevalentie van de ziekte is 1:2000-1:5000. Echter, (vroege) diagnose van de ziekte is lastig, waardoor in veel

gevallen geen of een verkeerde diagnose gesteld kan worden. De diagnose wordt gesteld op basis van de gereviseerde Task Force Criteria, welke gebaseerd zijn op globale en regionale dysfunctie en structurele afwijkingen, weefselkarakterisatie van de kamerwand, afwijkingen in de re- en depolarisatie of voortgeleiding, ritmestoornissen en familiegeschiedenis.

Dit proefschrift

Het doel van dit proefschrift is om op te helderen of er interactie is tussen $Na_V1.5$, Cx43 en de desmosomale eiwitten (voornamelijk PKP2), drie componenten in de intercalairschijf; hoe ze elkaar beïnvloeden en bijdragen aan abnormale voortgeleiding en ritmestoornissen (**hoofdstuk 1**). Om dit te onderzoeken zijn verschillende muismodellen gebruikt, alsmede materiaal van patiënten. **Hoofdstuk 2** is een uitgebreide literatuurstudie waarin de structuren in de intercalairschijf en hun functie worden beschreven. Ziekte- en diermodellen worden genoemd waarin één van de componenten van de intercalairschijf is aangetast en waardoor andere structuren worden verstoord. In **hoofdstuk 3** wordt gebruik gemaakt van één van deze diermodellen, waarin Cx43 expressie is teruggebracht naar 5% van de normale hoeveelheid. In de helft van de harten van deze muizen konden ritmestoornissen worden geïnduceerd. Harten met ritmestoornissen (VT+) werden vergeleken met harten zonder ritmestoornissen (VT-). De geleidingsvertraging en dispersie van de voortgeleiding waren ernstiger in VT+. Verder was de expressie van Cx43 lager in VT+ en, heel belangrijk, ook de expressie van $Na_V1.5$ was verder verlaagd in deze harten. Aparte experimenten laten zien dat in geïsoleerde neonatale hartspiercellen waarin Cx43 volledig is gesilenced ook de natriumstroom is verminderd. Samenvattend heeft dit hoofdstuk de interactie tussen Cx43 en $Na_V1.5$ aangetoond in het geval van extreme Cx43 afname, wat resulteerde in ritmestoornissen. Vanaf **hoofdstuk 4** richten we ons op aritmogene cardiomyopatie (AC), waarbij we deze ziekte als een model voor defecte desmosomen hebben gebruikt. In dit hoofdstuk wordt een overzicht gegeven van de prevalentie van mutaties in desmosomale eiwitten in patiënten met AC en de geografische distributie van deze mutaties. We hebben gevonden dat in de meeste studiepopulaties mutaties in het *pkp2* gen het meest frequent voorkomen, vooral in Nederland en in Noord Amerika. In **hoofdstuk 5** worden de klinische, histologische, immunohistologische en ultrastructurele kenmerken beschreven

van een patiënt met AC die een harttransplantatie heeft ondergaan. In het hart van deze patiënt werden bind- en vetweefsel gevonden in de volledige rechter vrije wand en ook in grote delen van de linker kamer en het septum. Verrassend genoeg waren de gap junctions slechts matig aangetast in deze patiënt, hoewel er wel plekken werden gevonden waar de ruimte tussen de hartspiercellen in de intercalairschijven was verwijd op het ultrastructurele niveau. Biopten en autopsie materiaal van patiënten met AC werden gebruikt in **hoofdstuk 6** en **hoofdstuk 7**. In **hoofdstuk 6** wordt het aritmogene substraat van 20 AC patiënten op immunohistologisch niveau beschreven. Een afname van Cx43, $Na_V1.5$ en PKG expressie werd gezien in een groot deel van de patiënten, wat wederom duidt op een interactie tussen de verschillende componenten. In **hoofdstuk 7** wordt een technisch punt besproken betreffende weefsel preservatie en antilichaam verdunningen, om misdiagnose door fouten in de procedure van immunohistochemie te voorkomen. In **hoofdstuk 8** wordt een muismodel beschreven, waarin de muizen slechts de helft van de normale PKP2 expressie hebben. We hebben een afname van de natriumstroom gevonden in geïsoleerde hartspiercellen van deze muizen, wat wijst op een interactie tussen PKP2 en $Na_V1.5$. Na toevoeging van de natriumkanaalblokker flecainide zagen we, bij afwezigheid van structurele afwijkingen, een afname in de longitudinale geleidingssnelheid in de rechter kamer, veranderingen op het ECG en ritmestoornissen. Dit alles demonstreert de belangrijke rol die $Na_V1.5$ speelt in ritmestoornissen bij AC. Tenslotte worden alle voorgaande hoofdstukken bediscussieerd in **hoofdstuk 9**.

Conclusie

In dit proefschrift worden de interacties tussen gap junctions, natrium kanalen en desmosomen bestudeerd. Al deze structuren vertonen interactie met elkaar en verstoring in een van de componenten kan leiden tot verstoringen in de anderen. De desmosoom is de meest stabiele van de drie: verstoringen in Cx43 of $Na_V1.5$ leiden niet tot verminderd functioneren van de desmosoom, terwijl verminderde stabiliteit van de desmosoom kan leiden tot verminderde elektrische koppeling en verminderde exciteerbaarheid. Verder kunnen verstoringen in de gap junctions de exciteerbaarheid beïnvloeden (in extreme situaties). Remodelering van de drie genoemde componenten van de intercalairschijf leidt tot de ontwikkeling van een aritmogeen substraat en daardoor tot een verhoogd risico op ritmestoornissen.

CHAPTER 12

Acknowledgements

Een proefschrift schrijven doe je niet alleen (gelukkig!). Daarom ben ik aan veel mensen veel dank verschuldigd voor het tot stand komen van dit boekje.

Natuurlijk te beginnen met mijn directe begeleiders: mijn promotors en copromotors. Met een flinke club begeleiders was er altijd wel iemand bij wie ik kon aankloppen voor advies en waren er altijd nieuwe ideeën om mee aan de slag te gaan. Mijn eerste promotor professor Hauer, **Richard**, dank voor je grote kennis op het klinische vlak en enorme interesse en enthousiasme voor het basale onderzoek, ik heb veel van je geleerd. Juist de combinatie van klinisch en basaal onderzoek maakte het AC-onderzoek zo boeiend. Kersverse professor van Rijen, **Harold**, al vanaf het eerste moment dat ik binnenstapte bij de Medische Fysiologie voor mijn Masterstage was je mijn begeleider. Dank voor je eeuwige enthousiasme, je openheid, het regelen van water in een vastzittende lift, het Apple-virus en je goede raad. Ik ben er supertrots op dat ik de eerste promovenda ben waarbij jij fungeert als promotor. En ik ben natuurlijk heel benieuwd hoe die jurk je zal staan op de 23e! Copromotor **Marcel**, dank voor het overbrengen van al je kennis van de moleculaire biologie. Ik geloof dat ik in totaal welgeteld 1 PCR heb laten lukken en kloneren ben ik zelfs nooit aan begonnen, maar de theoretische achtergrond ken ik nu in ieder geval! Copromotor **Toon**, dank voor al je goede raad, zowel op wetenschappelijk als op persoonlijk vlak. En natuurlijk voor alle hilarische momenten op de diverse congressen. Ik ben heel blij dat je op de valreep toch nog mijn copromotor bent geworden. Is voor jou natuurlijk weer eens goede gelegenheid om je favoriete stropdas weer eens om te doen ;). **Jacques**, eigenlijk ook nog steeds een beetje mijn promotor. Ik heb enorm respect voor je bescheidenheid, het plezier dat je uitstraalt als je het over de wetenschap hebt en voor je enorme kennis over de mechanismen van ritmestoornissen. **Marc**, ik heb veel geleerd van jouw politieke inzicht in de wetenschap. Ik heb met heel veel plezier de afgelopen jaren op jouw afdeling gewerkt, dank daarvoor. Dank ook voor het accepteren van het voorzitterschap van mijn beoordelingscommissie. Ook veel dank aan de overige leden van de beoordelingscommissie voor het kritisch lezen en beoordelen van mijn proefschrift.

Het kiezen van mijn paranimfen was het makkelijkste van dit hele promotietraject. **Jasminka**, al mijn vriendinnetje vanaf de middelbare school. Dank voor je gezelligheid en vriendschap! Ik blijf het bijzonder vinden dat we al zo lang vriendinnen zijn en hoop dat dat nog heel lang zo blijft. **Judith**, mijn AC-maatje, het was geweldig om samen

te werken! Er zijn diverse nagels in onze doodskisten geslagen tijdens het werk, maar gelukkig kunnen we ook samen lachen en het naïeve blondje uithangen. Succes met de rest van jouw promotie; je hebt m'n nummer voor als er stoom afgeblazen moet worden, hè ;).

Vervolgens de conduction group, een apart cluppie binnen de medische fysiologie. De vergaderingen duurden altijd veel te lang, maar dat kwam dan vooral door de gezelligheid! **Mera**, mijn stage begeleidster, het was leuk! Ik heb veel van je geleerd in het muizenlab en de fietsdates waren gezellig. **Mohamed**, altijd de rust zelve. Niemand kan zo goed moeilijke dingen uitleggen als jij. **John**, Tielenaar in hart en nieren, met jou viel er altijd wel wat te lachen. Het zal nooit saai zijn met jou in de buurt. Ik heb ontzettend veel geleerd van jullie als mijn voorgangers in de conduction club, eerst als student en daarna als AIO, niet alleen over mappen, electrofysiologie en meer wetenschappelijk verantwoorde zaken, maar ook over plezier in onderzoek doen; ik vond het super om met jullie te werken! Nu zijn **Sanne** en **Magda** (you understand Dutch now, don't you?) de vertegenwoordigers van de conduction club: succes met alle operaties en het afronden van jullie onderzoek! **Roel**, dank voor alle gezellige dagen op het muizenlab! Ik heb een hoop van je geleerd en zal nooit meer de verkeerde hoeveelheid Calcium in de buffer doen (mocht ik dat überhaupt ooit nog eens doen...). We moeten snel maar weer eens een fietsdate plannen met John en Sanne!

Dank ook aan alle andere collega's van de Medische Fysiologie (in volstrekt willekeurige volgorde). **Leonie**(tje), dank voor alle proeven die je voor me hebt gedaan; op een gegeven moment vond ik het wel lastig om het lab nog te vinden. En dank natuurlijk voor je gezelligheid (we moeten maar goed contact blijven houden over slechte tv-programma's en shopsessies). **Bart**, het was altijd leuk om met jou op het lab te staan, slechte muziek en slechte grappen te maken en weg te dromen bij jouw fantastische vakantiefoto's. **Jet**, we hebben nooit samengewerkt, maar ik vond het heel gezellig met jou als kamergenoot. Ook met **Vincent** was het gezellig op de kamer; nog bedankt voor de Toblerone en de mooie limericks. **Malin**, zoals jij al zei in je dankwoord: het was inderdaad jammer dat we niet meer samenzaten op de AIOkamer, samen met Sanne. Maar het was wel goed voor de productiviteit ;). Hoop dat de etentjes met jullie en de mannen nog lang door zullen gaan (ik zal de volgende weer eens plannen). **Peter**, wat is het liedje van de dag? Het was gezellig om je buuf te zijn lang lang geleden. (Dexter begint in september weer trouwens!) **Lukas**, thanks for organizing the magnificent trip to Prague, it was great. **Tamara**, het was super in

Orlando, vooral onze cheesecakelunch in de shopping mall ;). Veel succes in Canada. **Rosanne, Christian, Rianne, Thom, Siddarth** en **Sofieke**, het was gezellig met jullie! Heel veel succes allemaal met de rest van jullie promotie. **Linda**, voor jou is het ook bijna zover: ik ben heel benieuwd naar je boekje! **Marien**, ondanks je slechte muzieksmaak ;) was het toch altijd gezellig om met jou op het lab te staan. **Marti**, dank voor al je hulp met de virussen. **Teun**, dank voor je hulp als ik de microscoop even niet snapte of ruzie had met m'n Mac. **Maria** en **Martin**, dat jullie toch niet vaker zijn komen klagen over het geluidsniveau van jullie buurkamer verbaast me nog steeds! En tenslotte natuurlijk **Tonny**, mama van de afdeling, zonder jou zou de afdeling niet meer draaien, zowel op praktisch als op sociaal vlak!
Er is in de 4 jaar van mijn promotietraject een hele schare aan studenten de revue gepasseerd: **Johan**, **Kainat**, **Maartje P**, **Janine**, **Sarah**, **Jerome** en **Kirolos**. Dank allemaal voor jullie harde werken aan het AC-project en het aan mij leren hoe je studenten moet begeleiden. Een speciaal woord van dank aan **Sara** en **Elise** die ook na afloop van hun stage hard door zijn blijven gaan met mooie immunoplaatjes maken voor het bioptenstuk.

Mario, thanks for the hospitality with which you welcomed me in your lab. I enjoyed working at NYU and living in NY very much. I admire your intelligence and am honored that you are part of my reading committee. I also want to thank **Marina**, for the nice hours in the mouse lab, lessons on mouse ECGs, and good advice on where to go in NY. Finally, I'd especially like to thank, next to the rest of the Delmar-lab, **Halina**, **Esperanza** and **Ronald** for their help in the lab, but also for the good lunches every day!

Moniek Cox, de eerste twee jaar mijn AC- (toen nog ARVC) maatje. Het was fijn met je samen te werken. Misschien moeten we binnenkort toch nog eens dat afgesproken ijsje gaan halen! UMC Utrecht collega's van de Cardiologie, Genetica en Pathologie: **Nicolaas de Jonge, Aryan Vink, Dennis Dooijes** en **Jasper van der Smagt**: dank allemaal voor de prettige samenwerking tijdens het AC-project.
Oud-collega's (maar huidige vriendinnetjes) **Wendy** en **Kanita**, we zijn alle drie gestart als AIO bij de medische fysiologie, maar helaas gingen onze wegen als onderzoeksters al snel uit elkaar. De vriendschap is gebleven gelukkig!
Lieve vriendinnetjes (+aanhang) van de **Anticie** en vriendjes en vriendinnetjes van het **USKO**; weer een proefschrift om toe te voegen aan de rij boekjes van deze clubs die al in de kast stonden (en er zullen

er nog wel een paar volgen). Dank voor jullie steun en belangstelling voor mijn onderzoek dat voor sommigen waarschijnlijk wat beter te begrijpen is dan voor anderen.
Henny en **Riet**, dank voor jullie belangstelling voor mijn onderzoek. En natuurlijk voor het feit dat jullie me zo gastvrij hebben verwelkomd in jullie familie.

Alles is te doen als je weet dat het thuisfront altijd achter je staat. **Mama**, dank voor het altijd luisteren en goede raad geven als het nodig is. **Papa**, dank voor je altijd praktische oplossingen op mijn problemen en voor het supermooi layouten van mijn proefschrift. Jullie zijn de liefste ouders van de wereld.
Lieve **Sander** en **Nils** en natuurlijk ook jullie lieve **vriendinnetjes**: ik ben blij met jullie als mijn broers! Dit is het dan waar ik de afgelopen jaren druk mee ben geweest. Dank voor jullie steun en belangstelling.

Jules. Dank voor het jij-zijn. Voor het steunen als het even tegenzit en voor het opentrekken van de champagne als er iets te vieren is (en ook als er niets te vieren is). Dank voor het samen genieten van het leven en van elkaar. Dit proefschrift is voor jou.

CHAPTER 13

Curriculum vitae

Curriculum Vitae

Maartje Noorman was born on the 13th of December 1983 in Veldhoven, The Netherlands. She graduated in 2002 from the Gymnasium at Pleincollege van Maerlant in Eindhoven (secondary school with Latin). In September 2002 she started at Utrecht University with the Bachelor program Biomedical Sciences. After receiving her BSc in February 2006, she continued her academic study at Utrecht University with the Master Biology of Disease. During this Master she did a 9-month research project at the department of Medical Physiology in the UMC Utrecht, working on arrhythmias in the aged mouse heart. Her second internship was at L'Institut du Thorax at the University of Nantes, France where she studied the genetic profile of mice having a cardiac pressure overload. After writing her Masters' thesis about the function and regulation of cell-cell junctions in the heart at the department of Medical Physiology, she obtained her MSc in February 2008 with the qualification "Cum Laude". She started as a PhD-student in March 2008 on the project "Arrhythmogenic Right Ventricular Dysplasia/Cardiomyopathy. From Bedside to Intercellular Coupling" under the supervision of prof.dr. Richard Hauer, prof.dr.ir. Jacques de Bakker, prof.dr. Harold van Rijen, dr. Marcel van der Heyden and dr. Toon van Veen. During her PhD-project, Maartje went to New York to perform research at the division of Cardiology at New York University, NY, USA for 2 months.

Maartje will defend her thesis called "Arrhythmogenic remodeling of the intercalated disk" on the 23rd of October 2012. She started working as a staff member at the research office of the executive board of the UMC Utrecht on the 1st of June 2012.

CHAPTER 14

List of publications

Cerrone M, **Noorman M**, Lin X, Chkourko H, Liang FX, van der Nagel R, Hund T, Birchmeier W, Mohler P, van Veen TA, van Rijen HV, Delmar M. Sodium current deficit and arrhythmogenesis in a murine model of plakophilin-2 haploinsufficiency. *Cardiovasc Res.* 2012;95:460-468

Jacob KA, **Noorman M**, Cox MGPJ, Groeneweg JA, Hauer RNW, van der Heyden MAG. Geographical distribution of plakophilin-2 mutation prevalence in patients with arrhythmogenic cardiomyopathy. *Neth Heart J.* 2012;20:234-9

Jansen JA, **Noorman M**, Musa H, Stein M, de Jong S, van der Nagel R, Hund TJ, Mohler PJ, Vos MA, van Veen TA, de Bakker JM, Delmar M, van Rijen HV. Reduced heterogeneous expression of cx43 results in decreased nav1.5 expression and reduced sodium current that accounts for arrhythmia vulnerability in conditional cx43 knockout mice. *Heart Rhythm.* 2012;9:600-7

Cox MG, van der Zwaag PA, van der Werf C, van der Smagt JJ, **Noorman M**, Bhuiyan ZA, Wiesfeld AC, Volders PG, van Langen IM, Atsma DE, Dooijes D, van den Wijngaard A, Houweling AC, Jongbloed JD, Jordaens L, Cramer MJ, Doevendans PA, de Bakker JM, Wilde AA, van Tintelen JP, Hauer RN. Arrhythmogenic right ventricular dysplasia/cardiomyopathy: Pathogenic desmosome mutations in index-patients predict outcome of family screening: Dutch arrhythmogenic right ventricular dysplasia/cardiomyopathy genotype-phenotype follow-up study. *Circulation.* 2011;123:2690-2700

Cox MG, van der Smagt JJ, **Noorman M**, Wiesfeld AC, Volders PG, van Langen IM, Atsma DE, Dooijes D, Houweling AC, Loh P, Jordaens L, Arens Y, Cramer MJ, Doevendans PA, van Tintelen JP, Wilde AA, Hauer RN. Arrhythmogenic right ventricular dysplasia/cardiomyopathy diagnostic task force criteria: Impact of new task force criteria. *Circ Arrhythm Electrophysiol.* 2010;3:126-133

Boulaksil M, **Noorman M**, Engelen MA, van Veen TA, Vos MA, de Bakker JM, van Rijen HV. Longitudinal arrhythmogenic remodelling in a mouse model of longstanding pressure overload. *Neth Heart J.* 2010;18:509-515

Stein M, Boulaksil M, Jansen JA, Herold E, **Noorman M**, Joles JA, van Veen TA, Houtman MJ, Engelen MA, Hauer RN, de Bakker JM, van Rijen HV. Reduction of fibrosis-related arrhythmias by chronic renin-angiotensin-aldosterone system inhibitors in an aged mouse model. *Am J Physiol Heart Circ Physiol.* 2010;299:H310-321

Noorman M, van der Heyden MA, van Veen TA, Cox MG, Hauer RN, de Bakker JM, van Rijen HV. Cardiac cell-cell junctions in health and disease: Electrical versus mechanical coupling. *J Mol Cell Cardiol.* 2009;47:23-31

Stein M, van Veen TA, Remme CA, Boulaksil M, **Noorman M**, van Stuijvenberg L, van der Nagel R, Bezzina CR, Hauer RN, de Bakker JM, van Rijen HV. Combined reduction of intercellular coupling and membrane excitability differentially affects transverse and longitudinal cardiac conduction. *Cardiovasc Res.* 2009;83:52-60

Noorman M, van Rijen HV, van Veen TA, de Bakker JM, Stein M. Differences in distribution of fibrosis in the ventricles underlie dominant arrhythmia vulnerability of the right ventricle in senescent mice. *Neth Heart J.* 2008;16:356-358

Stein M, **Noorman M**, van Veen TA, Herold E, Engelen MA, Boulaksil M, Antoons G, Jansen JA, van Oosterhout MF, Hauer RN, de Bakker JM, van Rijen HV. Dominant arrhythmia vulnerability of the right ventricle in senescent mice. *Heart Rhythm.* 2008;5:438-448

Wiegerinck RF, van Veen TA, Belterman CN, Schumacher CA, **Noorman M**, de Bakker JM, Coronel R. Transmural dispersion of refractoriness and conduction velocity is associated with heterogeneously reduced connexin43 in a rabbit model of heart failure. *Heart Rhythm.* 2008;5:1178-1185